Hamiltonian Formalism of Spin–Orbit Jahn–Teller and Pseudo-Jahn–Teller Problems in Trigonal and Tetragonal Symmetries

Kun Wang

A THESIS SUBMITTED TO

THE FACULTY OF GRADUATE STUDIES

IN PARTIAL FULFILLMENT OF THE REQUIREMENTS FOR THE DEGREE

OF

MASTER OF SCIENCE

GRADUATE PROGRAM IN CHEMISTRY

YORK UNIVERSITY

TORONTO, ONTARIO

July 2020

Abstract

A formalism for expansions of all bimodal spin–orbit Jahn–Teller and pseudo-Jahn–Teller Hamiltonian operators in trigonal and tetragonal symmetries is presented. With the formalism, we can easily obtain expansion formulas of the Hamiltonian matrix elements in symmetry-adapted vibrational coordinates up to arbitrary order. The formalism is presented as a set of generic matrices and lookup tables, which are convenient to use even without understanding the derivation of the formalism. Three examples are used to demonstrate the correctness, completeness, and conciseness of the formalism. One of the examples is also used to demonstrate how to obtain expansion formulas in more than two vibrational modes by using the bimodal formalism. This work lays a foundation for deriving a unified formalism for spin–orbit and non-spin–orbit (pseudo-)Jahn–Teller Hamiltonians in general axial symmetries.

Acknowledgements

First, I thank my supervisor, Dr. Tao Zeng, for his support and guidance. There is no proper word to express my gratitude and respect to him. Without his help, I cannot finish my research and thesis. I would appreciate Dr. René Fournier and Dr. Christopher Caputo for taking their time to be my committee members and providing their suggestions and advice to my research and thesis. I also thank York University and the Department of Chemistry for offering me this opportunity to finish my master's study. I would like to thank Carleton University and the Department of Chemistry for giving me the chance to begin my master's study. I deeply thank my parents, Yandong Wang and Xuemei Bu, for their support throughout my life.

Table of Contents

List of Tables

List of Figures

List of Publications

K. Wang and T. Zeng* "Hamiltonian Formalisms of Spin-Orbit Jahn-Teller and Pseudo-Jahn-Teller Problems in Trigonal and Tetragonal Symmetries." *Phys. Chem. Chem. Phys*. **2019**, 21, 18939-18957. (Highlighted as one of the **2019 PCCP HOT Articles**)

Chapter 1 Introduction

The Jahn–Teller (JT) effect was proposed about 80 years ago.[1] Nonlinear polyatomic systems with a principal axis $\geqslant$3-fold can have orbital degeneracy. Paradoxically, the orbital degeneracy forces the systems to distort to lower symmetries and lose the degeneracy. The distortion arises from the fact that electronic Hamiltonian matrix elements of the degenerate states depend on non-totally-symmetric vibrations.[2,3,4] Such a vibronic coupling also occurs between non-degenerate states and leads to the pseudo-Jahn–Teller (pJT) distortion of systems.[5] JT and pJT interactions are ubiquitous in chemistry and physics, leading to numerous phenomena in spectroscopy, structural chemistry, solid-state physics, and materials science.[6,7,8,9,10,11,12] The JT and pJT interactions are important as they provide the only source of spontaneous symmetry breaking in polyatomic systems.[13]

Section 1.1 Illustration of Jahn-Teller effects using H_3^+ and H_3 as examples.

The JT effect is exemplified using H_3^+ and H_3 systems in Figure 1.1. This homonuclear triatomic system must be one of the simplest cases of JT effect, since only systems with symmetry axis $\geqslant$3-fold can undergo JT distortion. We assume that H_3 adopts an equilateral D_{3h} structure shown in Figure 1.1(a). There can only be three vibrational mode for the triatomic equilateral, the nondegenerate a_1' breathing mode in Figure 1.1(b) and the degenerate e' modes in Figure 1.1(b) and (c). Mulliken symbols in lower case are used to label symmetry-adapted vibrational modes and molecular orbitals. The two e' components are denoted using the x and y subscripts according to their evenness and oddness with respect to the C_2' axis shown in Figure 1.1(a). Evidently, any distortion of the equilateral triangle must be via the e' modes.

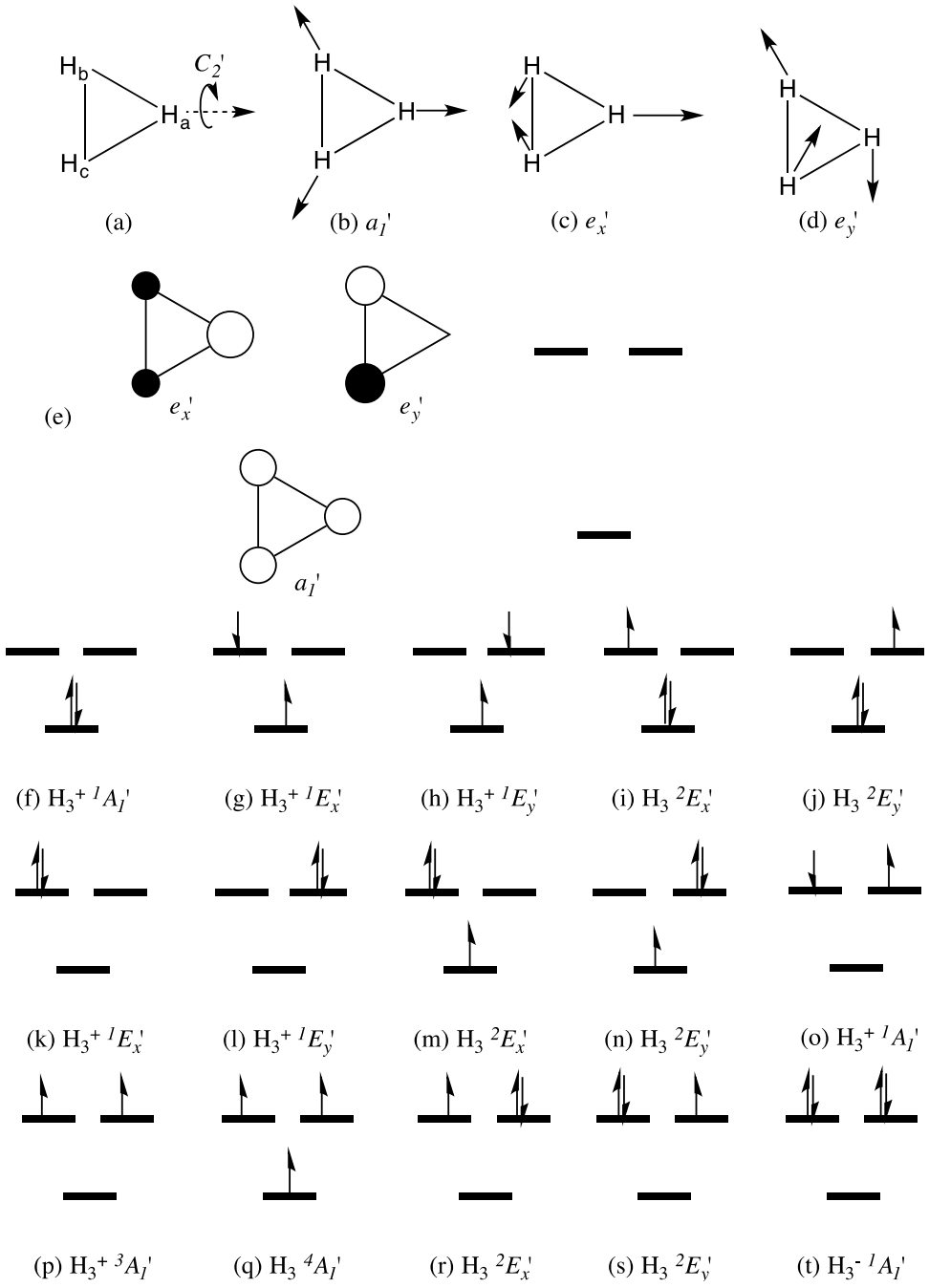

Figure 1.1. Illustration of Jahn-Teller effect using H_3 as an example: (a) equilateral triangular arrangement of H_3; (b) the a_1' vibrational mode of H_3; (c) and (d) the e' degenerate vibrational mode of H_3; (e) the valence a_1' and e' molecular orbitals of H_3; (f)-(t) occupation schemes of some representative H_3^+ and H_3 states. The three atoms are labeled using subscripts a-c to facilitate discussion. The white and black lobes in (e) represent + and – phases of the atomic orbitals.

The valence molecular orbitals (MOs) formed by the 1s atomic orbitals of the H atoms are shown in Figure 1.1(e). Their forms and mathematical expressions are solely determined by symmetry, just like the three vibrational modes. The a_1' orbital features completely bonding character among the three H atoms and is hence of the lowest energy. The e' orbitals have antibonding character and are of higher energy. The H_a-H_b and H_a-H_c antibonding characters in e_x' and the H_b-H_c bonding character favor the distortion to an isosceles triangle through the e_x' mode Figure 1.1(e), which results in a shorter H_b-H_c distance and longer H_a-H_b and H_a-H_c distances. The H_b-H_c antibonding character in e_y' favors the distortion along the opposite direction of the e_x' mode, which results in a longer H_b-H_c distance.

It is generally true that symmetry-determined degenerate orbitals are not of totally symmetry in terms of interatomic interaction. The interaction can be of bonding/antibonding nature, *e.g.*, in the present example, or of electrostatic nature. No matter how, the occupation of one of the degenerate orbitals results in non-totally symmetric forces onto the nuclear framework. The framework thus tends to distort to a structure with lower symmetry, *e.g.*, from D_{3h} to C_{2v} in the present example. Electronic states in Figure 1.1(g)-(j) of H_3 and H_3^+ all have the single occupation of one electron in one e' orbital. They all suffer the D_{3h} to C_{2v} JT distortion. When one of the degenerate orbitals is occupied by two electrons while the other is empty, *e.g.*, Figure 1.1(k)-(n), the tendency of distortion is even stronger.

Now let's consider the occupation of each of the e' orbitals by one electron, *e.g.*, the states in Figure 1.1(o)-(q). The equal occupation of the two e' orbitals favors the e_x' mode distortion in the positive and negative direction **equally**. The D_{3h} symmetry remains, and JT distortion does not occur. When one of the degenerate orbitals is occupied by two electrons and the other by one, *e.g.*, in Figure 1.1(r)-(s), there is a stronger tendency to distort towards one direction of the e_x' mode,

the JT distortion to C_{2v} occurs. When the *e'* shell is fully occupied, *e.g.*, in Figure 1.1(t), the distortion tendencies are cancelled again. The JT distortion does not occur.

In the examples of these occupation schemes, we see that whenever degenerate orbitals are not equally occupied, there is a preference towards the distortion favored by the orbital that is occupied by more electrons, and there is JT distortion. On the contrary, when the occupancies of the degenerate orbitals are identical, there is a cancellation of the distortion tendencies. No JT distortion occurs. In the language of molecular spectroscopy, the unequal occupation of the degenerate orbitals must generate a degenerate electronic state with a degenerate state term symbol. This is because there is more than one way to populate the degenerate orbitals, and because of the degeneracy of the orbitals, the different options result in states of the same energy. Consequently, JT distortion occurs for all degenerate states induced by symmetry. All effects associated with such distortions-induced-by-high-symmetry are included in the concept of JT effects. The JT effects are ubiquitous for high symmetry systems. Even if there is no distortion for the ground state, *e.g.*, the ground state of H_3^+ in Figure 1.1(f), there can be distortions for excited states.

Before we move on to more discussion on JT effects, we should note the exception of linear molecules, whose degenerate states do not lead to distortion. This is exemplified by the degenerate π^* orbitals of CO_2 (Figure 1.2). Each of the orbitals does not favor any distortion. Taking the π_x^* orbital for example, the antibonding interactions of the two CO atomic pairs above the molecule are cancelled by the same magnitude of antibonding interactions of the same atomic pairs. The antibonding interactions thus cannot bend (distort) the linear molecule. A Similar argument can be made of any degenerate orbitals of any linear molecules. The ultimate reason is because those degenerate orbitals are non-totally-symmetric **only** with respect to the rotation about the molecular axis. In other words, they are not cylindrically symmetric like σ-type orbitals. However, for linear

molecules, there are no bond lengths or bond angles around the molecular axis. The non-totally-symmetric occupation of electrons in the degenerate orbitals, hence, have no structural parameters to change.

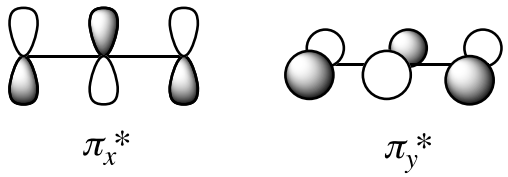

Figure 1.2. The degenerate π^* orbitals of CO_2.

Section 1.2 Potential energy surfaces of Jahn-Teller distorted system

The JT problem exemplified above using H_3^+ and H_3 as examples involve degenerate *E* type electronic states and degenerate *e* type vibrational modes. It belongs to the $E \otimes e$ class problems. We follow the convention of using upper case Mulliken symbols to label electronic states. Generically, the $E \otimes e$ problem for D_{3h} symmetry features the potential energy surfaces (PESs) of the two states along the two vibrational coordinates which are shown in Figure 1.3(a). Similar topology of the PESs apply regardless of actual systems. The surfaces form a conical intersection at the undistorted D_{3h} structure with the vibrational coordinates *x* and *y* of the *e* type modes being zero. This corresponds to the degeneracy of *E* type states at D_{3h} symmetry. The cone near where the two PESs intersect demonstrates the lack of a stationary point at the D_{3h} high symmetry, which implies the lack of stationary high symmetry structure, and hence the necessity of JT distortion. The 1-D cut of the PESs in Figure 1.3(b) shows the distortion of the structure along the positive and negative e_x direction. In the H_3^+/H_3 example, the positive and negative *x* directions correspond to distortion along the positive and negative directions of the e_x' mode in Figure 1.1(c), *i.e.*, distorting to acute and obtuse isosceles triangles, respectively. At $x = 0$, the forces for the ground state towards the positive and negative *x*, *i.e.*, the first derivative of the purple

curve in Figure 1.3(b) at $x = 0^+$ and 0^-, must be identical due to symmetry. However, as the distortion magnitude increases, the energy lowering becomes different in the two directions. In this example, we assign the positive direction to the one giving a lower energy. Correspondingly, the acute isosceles triangle is a stable distorted C_{2v} structure.

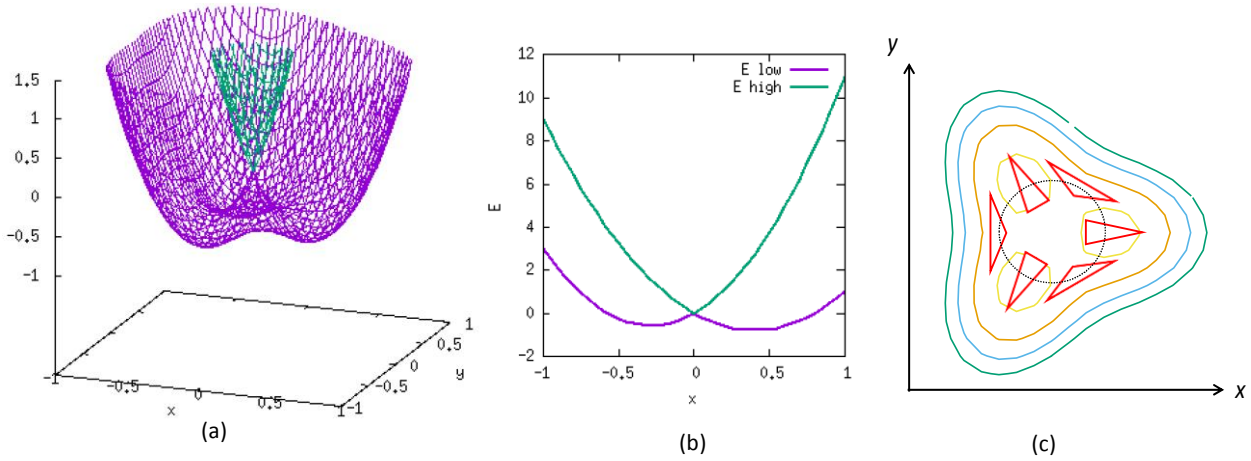

Figure 1.3. (a) Generic potential energy surfaces of $E \otimes e$ problems in D_{3h} symmetry; (b) the 1-D cut of the surfaces along x with $y = 0$; (c) the contours of the low-lying potential energy surface. x and y are vibrational coordinates for e_x and e_y modes.

The potential energy surfaces must satisfy the same D_{3h} symmetry as the undistorted structure. This is a result of the molecular symmetry group. In plain language, the three H atoms are symmetrically equivalent. The three isosceles triangles with the tips at H_a, H_b, and H_c, respectively, must have the same energy. Consequently, the ground state PES in Figure 1.3(a) (the purple surface) has three equivalent minima, corresponding to the three acute isosceles triangles. The three minima and the orientations of the three acute isosceles triangles are clearly shown in the contour map of the ground state PES in Figure 1.3(c). The obtuse triangle is a minimum on the negative x of Figure 1.3(b). However, it is a transition state structure connecting two acute triangles. In Figure 1.3(c), all six isosceles triangles are shown at their corresponding locations on the

potential energy surfaces. The lowest energy trough of the PES connects the six triangles. This low energy trough is represented by the dashed circle in Figure 1.3(c). Along the low energy trough, the triangle distorts alternatively between acute and obtuse, **without molecular rotation**. "Without molecular rotation" means, for our H_3 example, in all the six triangles, H_a is always the rightmost vertex, H_b is always the top-left vertex, and H_c is always the bottom-right vertex. Although the molecule does not rotate, people call the deformation along the trough "pseudo-rotation", as the triangle appears (but only appears) to rotate, and the trough passes around the undistorted origin on the PES.

Section 1.3 Static and dynamical Jahn-Teller effects.

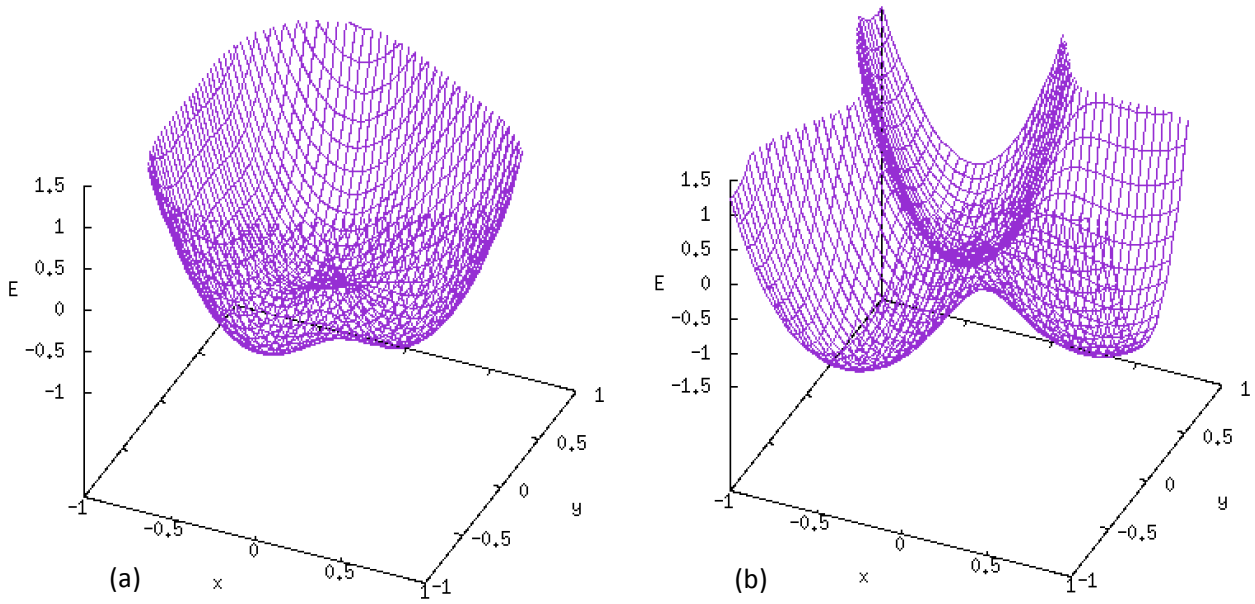

Figure 1.4. Comparison of $E\otimes e$ ground state potential energy surfaces with (a) shallow minima and (b) deep minima.

In Figure 1.4, we compare the ground state potential energy surfaces of $E\otimes e$ Jahn-Teller problems with shallow and deep minima. The "depth" has two meanings: (1) the energy lowering along the distortion is large; (2) the barriers on the low energy trough that separate the minima are

large. The large energy lowering and large barriers are clearly shown in Figure 1.4(b). The depth of the energy lowering is determined by actual systems. Here, we are just making a generic comparison. For $E \otimes e$ systems with deep ground state PES, the distorted structure is trapped in one of the minima, and never convert to the other minima, *e.g.*, when the equilateral triangle distorts to one acute triangle in Figure 1.3(c), it can never convert to the other acute triangles. This type of Jahn-Teller distortions are called static JT distortions. The associated static JT effects are all related to the pure structural change. For instance, the system gains a permanent electric dipole moment in this distortion, the NMR shieldings for the three nuclei become different, *etc.* The pseudo-rotation mentioned above is quenched by the large barriers. It may, however, occur at high enough temperature. Please note that in most of undergraduate textbooks, the discussion of JT effects is concentrated on the static JT effects. In these textbooks, "Jahn-Teller" is limited to structural change from high to low symmetry induced by inequal electron occupations on symmetry-induced degenerate orbitals.

When the ground state PES is shallow as exemplified in Figure 1.4(a), then the molecule can have high enough nuclear kinetic energy to sample all the minima. The pseudo-rotation can hence occur. The JT distortion is dynamical. An obvious result of the pseudo-rotation is that the properties of the different distorted structures are dynamically averaged out. For instance, while each of the acute triangles in Figure 1.3(c) have permanent dipole moments, the pseudo-rotation averages their dipoles to zero. In terms of similar properties, there seem to be no JT distortion in the dynamical case. However, the JT effects for the shallow dynamical cases are still observable? They are called dynamical JT effects. For instance, there is a geometric phase effect, that the vibrational wave function of the e_x and e_y modes must change its sign on one round of the pseudo-

rotation. This effect deeply influences the selection rules for vibronic spectrum, reaction dynamics for pathway around the conical intersection, and excited state dynamics.

The studies of static JT effects are relatively easy. All we need is to optimize the structure of a JT-active system with the appropriate distorted symmetry, and analyze the properties of the distorted structure. The studies of dynamical JT effects are much more difficult. In general, we need to simulate the dynamics of the system using vibronic Hamiltonian operator of the JT system. Please note that whether the JT problem is static or dynamic is not solely determined by the shape of the energy landscape. The masses of the nuclei matter. The lighter the nuclei, the higher their vibrational zero point energy, the more likely they are to overcome the barriers between the minima, even when the barriers are fairly high. Also, the lighter nuclei would have higher probability to tunnel through the barriers. In general, lighter nuclei favor dynamical JT effects.

Section 1.4 Vibronic coupling.

"Vibronic" stands for vibrational + electronic. Vibrational motion and electronic motion in a polyatomic system are always coupled. Here, vibrational motion means general nuclear motion. But the coupling strength varies in different systems. Even for the same system, the coupling strength varies significantly as the structure of the system changes. Here, we borrow the energy diagrams for electron transfer in Marcus Theorem to demonstrate weak and strong vibronic coupling.

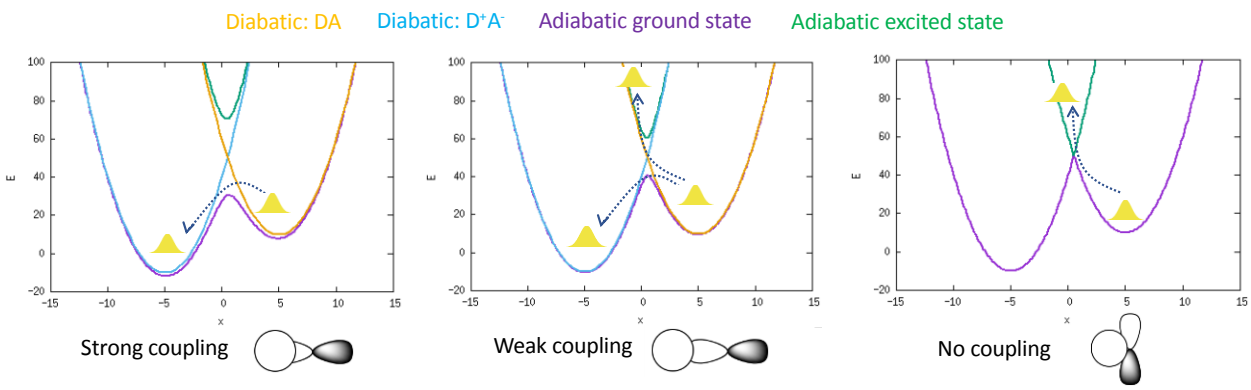

Figure 1.5. Energy diagrams for electron transfer in Marcus Theorem, with strong to weak electronic coupling. Note that strong (weak) electronic coupling implies weak (strong) vibronic coupling. E and *x* are in arbitrary units as the diagrams are only for illustration. The yellow gaussian symbolically represents vibrational wave packet.

Let's assume that there is an electron donor (D) approaching an electron acceptor (A). There is a tendency for the donor to lose an electron to the acceptor, converting the DA pair to the D^+A^- pair. The energies of the DA and D^+A^- pairs in general depend on the configuration of the dimer of D and A, and also the solvents around. All the dimer and solvent configurations are abstractly represented by a 1-D coordinate, *x*, as in the Marcus Theorem. The DA and D^+A^- energies are represented as the orange and cyan parabolas in Figure 1.5. The D^+A^- curve has a lower minimum than the DA curve, representing the energy tendency for the electron transfer. The DA and D^+A^- states are called diabatic states. Diabatic states mean electronic states that preserve their characters at different nuclear configurations. The DA and D^+A^- states keep their pre- and post-charge-transfer characters regardless of the *x* value. They are hence diabatic states.

In addition to the minimum-to-minimum energy gap between the two parabolas (*i.e.*, the thermodynamics tendency for the charge transfer), another factor that determines the efficiency of the transfer is the coupling strength between the two diabatic states. This coupling, labeled as *V*,

in plain language, is determined by orbital overlap. We may just simplify the charge transfer as from a Na atom to a Cl atom, which serve as D and A, respectively. In the three panels of Figure 1.5, the three situations of large, small, and strictly no overlap of the Na 3s and Cl 3p orbitals are shown. The diabatic energies and the coupling strength V together form a 2×2 electronic Hamiltonian matrix:

$$\underline{\underline{H}} = \begin{pmatrix} H_{DA} & V \\ V & H_{D^+A^-} \end{pmatrix} \qquad \text{Eqn 1.1}$$

We can find eigenvectors and eigenvalues that satisfy the eigenvalue equation of the Hamiltonian matrix:

$$\underline{\underline{H}} \begin{pmatrix} c_g^{DA} & c_e^{DA} \\ c_g^{D^+A^-} & c_e^{D^+A^-} \end{pmatrix} = \begin{pmatrix} c_g^{DA} & c_e^{DA} \\ c_g^{D^+A^-} & c_e^{D^+A^-} \end{pmatrix} \begin{pmatrix} E_g & 0 \\ 0 & E_e \end{pmatrix} \qquad \text{Eqn 1.2}$$

where each column of the $\underline{\underline{c}}$ matrix is an eigenvector, labeled by "*g*" and "*e*" for ground and excited states, and the E_g and E_e are the corresponding eigenvalues, the ground and excited state energies. The ground and excited state energies are represented by purple and green curves in Figure 1.5.The ground and excited states are called adiabatic states, they are linear combinations of the DA and D^+A^- diabatic states using the eigenvector elements as coefficients. Different from diabatic states, their characters vary as the structure of the system changes. In Figure 1.5, at $x < 0$, the ground state is dominated by the D^+A^- state, while at $x > 0$, it is dominated by the DA state. The excited state features the opposite character. As the system structure approaches the x value where the two diabatic curves crosses, each of the adiabatic states changes its character.

Figure 1.5(a) shows the energy diagram when V is large. When V is large, the adiabatic energy curves are smooth. The smoothness reflects the gradual change of the characters of the adiabatic states along the nuclear motion on x, *i.e.*, weak coupling between electronic motion and

vibrational motion, *i.e.*, weak vibronic coupling. Please note that a strong electronic coupling (V) between diabatic states speak for a weak vibronic coupling of adiabatic states. With the large V case, if the nuclear wave function is initially situated in the ground state, it will only evolve on the ground state. It may switch back and forth between the two minima of pre- and post-charge-transfer. The excited state does not affect the nuclear dynamics. This single-electronic-state picture of nuclear dynamics is just a manifestation of the concept that underlies the famous Born-Oppenheimer Approximation, that nuclear motion is much slower than electronic motion and we can assume that nuclear motion occurs on separate potential energy surface of one adiabatic electronic state. This is represented by the yellow gaussian that moves only on the ground state potential energy curve in Figure 1.5(a). The yellow gaussian symbolically represents a nuclear motion wave packet.

As the magnitude of V decreases, the change of characters of the adiabatic states at the crossing region of the diabatic curves becomes less and less gradual. Correspondingly, the maximum of the ground state and the minimum of the excited state become less smooth, and the minimum gap between the adiabatic states decreases. At the limit of $V = 0$ in Figure 1.5(c), the adiabatic states change their character abruptly at the crossing point. The degeneracy of the adiabatic states at the crossing point also implies the sharp turn of the adiabatic energy curves. The quick change of character of the adiabatic states with respect to nuclear structure at the crossing point indicates a strong vibronic coupling. Please note that a weak electronic coupling (V) between diabatic states leads to a strong vibronic coupling for adiabatic states.

Suppose that for the $V = 0$ situation, we have an initial nuclear wave function situated at the ground state minimum at $x > 0$, with a large momentum moving towards the negative x direction. When the nuclear wave packet reaches the crossing point, it will simply remain on the

DA diabatic curve, *i.e.*, it will transit to the excited state (track the yellow gaussian in Figure 1.5(c)). Two adiabatic states are involved in the nuclear dynamics, in striking contrast to the situation of large *V*. The nuclear motion that propagates on more than one adiabatic potential energy surface is called non-adiabatic molecular dynamics. The Born-Oppenheimer Approximation becomes invalid in the strong vibronic coupling case. We have to consider electronic and nuclear motions on the same footing, instead of the first being fast and the latter being slow. JT problems feature strong non-adiabatic vibronic coupling. Please compare Figure 1.3(b) and Figure 1.5(c), especially their abrupt turn-over of the adiabatic energy curves. Whenever there is electronic degeneracy, with the exceptions of linear molecules, the nuclear motion and electronic motion are non-adiabatic. Consequently, JT problems are all intrinsically non-adiabatic problems. The reason that we can ignore the non-adiabaticity in introducing JT effects to undergraduate students is because the textbook writers have implicitly confined their discussions on the realm of static JT distortion, and the nuclear motion only rattles around one of the minima, with no possibility to sample the degenerate structure.

The weak *V* situation in Figure 1.5(b) is in-between of Figure 1.5(a) and (c). The change of adiabatic state characters at the crossing region is faster than the states in the large *V* case, while not infinitely fast as in the $V = 0$ case. When a nuclear wave packet reaches the crossing region, it would not just evolve on the ground state (as in Figure 1.5(a)) or fully transits to the excited state (as in Figure 1.5(c)). Instead, the wave packet would bifurcate into two packets, one each of the adiabatic states (track the yellow gaussian(s) in Figure 1.5(b)). The dynamics is evidently of non-adiabatic nature. Please note that $V = 0$ is a strict requirement, which only a small subspace in nuclear coordinates can satisfy. Small *V* is more common. Actually, in the vicinity of the nuclear

structure with $V = 0$, there must be a region of small V. In Figure 1.5(c), if we slightly move the Na 3s orbital upwards or downwards, the situation is immediately converted to the small V case.

Section 1.5 Vibronic Hamiltonian operator

Like for any quantum mechanics problems, to describe a Jahn-Teller problem accurately, we need an accurate vibronic Hamiltonian operator. The Hamiltonian of a polyatomic system looks like this:

$$\hat{H} = \hat{T}_n + \hat{T}_{el} + \hat{V} = \hat{T}_n + \hat{H}_{el};\ \hat{V} = \hat{V}_{nn} + \hat{V}_{ee} + \hat{V}_{ne} \qquad \text{Eqn 1.3}$$

The detailed forms of the three composite operators are not shown. The three composite operators are the nuclear kinetic operator $\hat{T}_n$, the electronic kinetic operator $\hat{T}_{el}$, and potential operator $\hat{V}$ that contain all possible interactions between the charged particles. The three components of nucleus-nucleus repulsion, nucleus-electron attraction, and electron-electron repulsion are explicitly given in the equation above. While the kinetic operators involve differential operators with respect to the particles' coordinates, the potential operators involve the coordinates themselves only. $\hat{T}_{el}$ and $\hat{V}$ are grouped together to form the electronic Hamiltonian $\hat{H}_{el}$. Note that the $\hat{V}_{nn}$ term of nucleus-nucleus repulsion is also absorbed into $\hat{H}_{el}$, although it contains nuclear coordinates only. By including $\hat{V}_{nn}$, the eigenvalues of $\hat{H}_{el}$ provide adiabatic potential energy surfaces for nuclear motions. The purple and green curves in Figure 1.5 are obtained by solving eigenvalue problem of $\hat{H}_{el}$. Since $\hat{H}_{el}$ parametrically depend on nuclear position through $\hat{V}_{ne}$ and $\hat{V}_{nn}$, the eigenvalues and eigenfunctions of $\hat{H}_{el}$ are functions of nuclear position. That is why the purple and green curves and the ground and excited states in Figure 1.5 depend on x.

Let's say that we have found *all* electronic eigenstates of $\hat{H}_{el}$ at *one* nuclear structure (*e.g.*, at the crossing point of the diabatic potential energy curves in Figure 1.5), $\{|\Phi^d\rangle\}$. These electronic

states form a complete basis set. We can then use $\{|\Phi^d\rangle\}$ to construct an identity operator in the space of electronic coordinates, $\hat{I} = \sum_n |\Phi_n^d\rangle\langle\Phi_n^d| = |\Phi_n^d\rangle\langle\Phi_n^d|$. The superscript *d* indicates that these are diabatic states: they are eigenstates of one structure only, and are not allowed to change as the structure change. The subscript *n* is used to number the states. In principle, the summation over *n* is an infinite summation, since there must be an infinite number of eigenstates for one nuclear structure. In the second equal sign, Einstein's convention is used to simplify the summation expression: duplicate numbering indices imply a summation over the index. The same convention of summation expression is followed throughout this thesis. Please recall that *d* is not a numbering index here. The bra-ket notation is used. We can understand the ket state $|\Phi_n^d\rangle$ as the wave function $\Phi_n^d(\{r\})$ for all electrons' coordinates $\{r\}$, and the bra state $\langle\Phi_n^d|$ as the integral operator $\int \Phi_n^d(\{r\})^*$ ... $\{dr\}$. When the … is replaced by a function, the integral returns a value. The asterisk indicates taking the complex conjugate of the denoted function. We can then use $\hat{I}$ to resolve the total Hamiltonian $\widehat{H}$:

$$\begin{aligned}\widehat{H} = \hat{I}\widehat{H}\hat{I} &= |\Phi_n^d\rangle\langle\Phi_n^d|\widehat{H}|\Phi_m^d\rangle\langle\Phi_m^d| = |\Phi_n^d\rangle\langle\Phi_n^d|\hat{T}_n + \widehat{H}_{el}|\Phi_m^d\rangle\langle\Phi_m^d| \\ &= |\Phi_n^d\rangle\langle\Phi_n^d|\hat{T}_n|\Phi_m^d\rangle\langle\Phi_m^d| + |\Phi_n^d\rangle\langle\Phi_n^d|\widehat{H}_{el}|\Phi_m^d\rangle\langle\Phi_m^d| \\ &= \hat{T}_n + |\Phi_n^d\rangle H_{el,nm}^d\langle\Phi_m^d|\end{aligned} \qquad \text{Eqn 1.4}$$

Subscripts *n* and *m* are used to number the states when two summations are present. Please note that they are dummy summation indices. Since $\{|\Phi^d\rangle\}$ do not vary with respect to nuclear structure, the differential operator $\hat{T}_n$ with respect to nuclear coordinates does not act on $\{|\Phi^d\rangle\}$. Consequently, $\hat{T}_n$ remains itself after this resolving. What has been changed is $\widehat{H}_{el}$. $H_{el,nm}^d = \langle\Phi_n^d|\widehat{H}_{el}|\Phi_m^d\rangle$ is an integral of $\int \Phi_n^d(\{r\})^* \widehat{H}_{el}\Phi_m^d(\{r\})\{dr\}$. $\{r\}$ is used to label all electronic coordinates of a polyatomic system. The integral is a matrix element with the row index *n* and

column index m. $|\Phi_n^d\rangle H_{el,nm}^d \langle\Phi_m^d|$ is a matrix multiplication form of $\widehat{H}_{el}$, with a row of ket states $\{|\Phi^d\rangle\}$, multiplied by a square matrix $\underline{\underline{H_{el}^d}}$, and a column of bra states $\{\langle\Phi^d|\}$.

The advantage of resolving $\widehat{H}$ using the identity operator $\hat{I}$ is to convert the differential eigenvalue problem of solving the Schrödinger equation for $\widehat{H}$ to a linear eigenvalue problem. It comes with a cost. The row and column dimensions of the $\underline{\underline{H_{el}^d}}$ square and Hermitian matrix are infinite. The resolving itself is not an approximation. Now, an approximation is made. We approximate the infinite summation in $\hat{I} = \sum_n |\Phi_n^d\rangle\langle\Phi_n^d|$ by a finite summation. So, $\hat{I} \approx \sum_{n=1}^N |\Phi_n^d\rangle\langle\Phi_n^d|$ is used. The larger the dimension N, the better the approximation. Let's draw an analogy. The use of the true $\hat{I}$ to resolve an operator is like taking a photo using a conventional film camera. The photo must be made of continuous shapes and color patterns, no matter how much we magnify the photo. The use of the approximate $\hat{I}$ with a finite dimension of electronic states is like taking a photo using a digital camera with a finite number of pixels. The shapes and color patterns in the photo are discretized. However, as the number of "pixels" N is large, the digital photo delivers the same information as the film photo. And the digital photo is easier to process and transmit. Indeed, it is way easier to use a modern computer to handle large dimension matrices than a differential equation. This is one of the most (if not the most) obvious motivations to resolve $\widehat{H}$ using an approximate $\hat{I}$.

A further approximation is to use only a small number of electronic states to construct $\hat{I}$. Let's say we are only interested in a finite space of nuclear structure of a molecule. This is usually the case. For instance, in reaction dynamics, we are interested in a few reaction coordinates, and each of them vary in finite regions. Within the interesting ranges of the interesting nuclear coordinates, only a small number of electronic states become degenerate at some structures in this

space, then we are allowed to select only this small number of electronic states to construct $\hat{I}$. This is because these states are uncoupled from the others. One example is in Figure 1.5 again. The charge transfer process involves only two electronic states, DA and D^+A^-. Only these two states cross at the interesting range of nuclear coordinate *x*. Then, we may just set $N = 2$ in constructing $\hat{I}$, *i.e.*, $\hat{I} = |DA\rangle\langle DA| + |D^+A^-\rangle\langle D^+A^-|$. This approximation of using a small number of non-adiabatically coupled electronic states to resolve $\widehat{H}$ is called the Group-Born-Oppenheimer approximation. The small number of states are adiabatically separable from the other states, while they are non-adiabatically coupled among themselves.

For dynamical JT problems, degenerate states at high symmetry configuration must be included in constructing $\hat{I}$. If they become degenerate or pseudo-degenerate with other states, then $\hat{I}$ has to be expanded to include those "intruder" states.

Now let's take a look at the matrix elements, $H^d_{el,nm} = \langle \Phi^d_n | \widehat{H}_{el} | \Phi^d_m \rangle$. Φ^d_n and Φ^d_m are functions of electronic coordinates only. $\widehat{H}_{el}$ consists of differential operator of electrons' coordinates, and potential operators that are smooth functions of electrons' and nuclei' position coordinates. The integration $\langle \Phi^d_n | \widehat{H}_{el} | \Phi^d_m \rangle$ is over all electronic coordinates. Consequently, $H^d_{el,nm}$ is a function of nuclear coordinates only, $H^d_{el,nm}(\{R\})$. $\{R\}$ is used to label all nuclear coordinates of a polyatomic system. Φ^d_n and Φ^d_m are not functions of $\{R\}$, $\widehat{H}_{el}$ smoothly varies in the $\{R\}$ space. Consequently, $\langle \Phi^d_n | \widehat{H}_{el} | \Phi^d_m \rangle$ must be a smooth function in the $\{R\}$ space. Matrix elements $\left\{H^d_{el,nm}\right\}$ must all be differentiable functions in the whole $\{R\}$ space. Therefore, they can be expanded as Taylor series of the nuclear coordinates. At what order shall we truncate the potentially infinite Taylor series?[3,4] It is determined by the balance of accuracy and cost, and also the specific problem at hand. The higher the order, the higher the accuracy of the vibronic Hamiltonian, yet the higher the cost of using the vibronic Hamiltonian to simulate the system.

High order expansions matter. This is exemplified in Figure 1.6, where the simulated photo-detachment spectra of AlH_4^- using 2^{nd} and 4^{th} order vibronic Hamiltonian operators are compared with experimental data. The conventional 2^{nd} order expansion formulas generated a spectrum with features that are too sharp. Only when the expansion was raised to 4^{th} order the simulated spectrum is more comparable to the experiment.

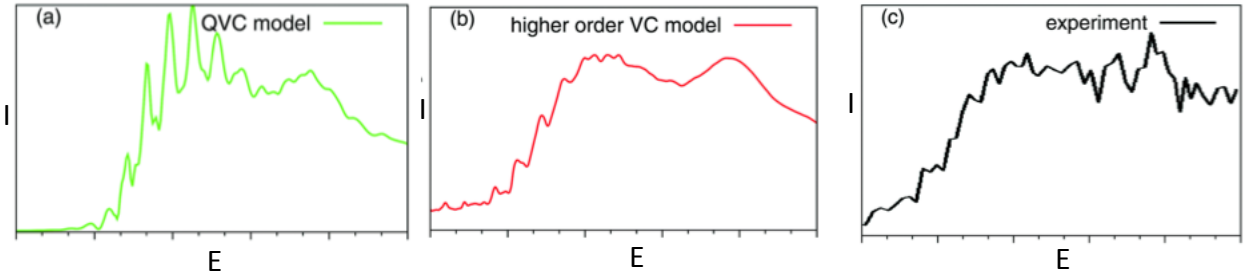

Figure 1.6. Comparison of simulated photo-detachment spectra for AlH_4^-: (a) simulation using vibronic Hamiltonian expanded up to 2^{nd} order series of vibrational coordinates; (b) up to 4^{th} order; (c) experimental spectrum. The figures are taken from Ref.14.

No matter how, we need to know the expansion formulas for the matrix elements in nuclear coordinates up to infinite order, so that they are available when they are needed. One focus of this research group is to derive the infinite order expansion formulas for the vibronic Hamiltonian matrix elements of JT problems. And this thesis is dedicated to deriving expansion formulas for JT problems with spin-orbit coupling.

Section 1.6 Spin-orbit coupling

Each electron possesses an intrinsic angular momentum called spin. There is an associated spin magnetic dipole moment. When an electron moves around a nucleus, in the view of the electron, it is the nucleus that is moving around itself. The rotation of the positively charged nucleus creates a magnetic field. The interaction between this orbital-motion-induced magnetic field and the spin magnetic dipole is called spin-orbit coupling (SOC).[15,16,17,18,19,20,21,22] The

rotational motions between two electrons also generate spin-orbit coupling. The total spin orbit coupling in a polyatomic system consists of both the electron-nucleus and electron-electron components. Because of the opposite charges of electrons and nuclei, the electron-electron SOC can be considered as a screening (or shielding) for the electron-nucleus SOC. SOC is responsible for splitting of lines in electronic and vibronic spectra, and in general any processes that are spin-forbidden. This is because SOC mixes electronic states of different electronic spins. Two examples are intersystem crossing and phosphorescence. In general, any elementary chemical reactions that involve reactants and products of different electronic spins are facilitated by SOC. SOC only occurs for open-shell systems. Paired electrons have opposite spins, so that any difference induced by the SOC of the spin-up electron will be cancelled by the SOC of the spin-down electron.

SOC is important, especially for heavy elements compounds.[15,16, 17, 22,23,24,25,26] The high positive charges of heavy nuclei create large magnetic fields to interact with electronic spin. This is why phosphorescence and intersystem crossing are more pronounced for heavy element compounds. It is necessary to consider SOC to study heave element compounds. Even for light element compounds, the inclusion of SOC is also desired for studying their electronic and vibronic spectra, as the spectroscopic precision has been significantly improved in the past few decades. Naturally, we should include SOC in studying Jahn-Teller systems.

SOC is intimately connected to the JT effects.[23,27,28,29,30,31,32,33,34,35,36,37,38,39,40] They are both related to degeneracy of electronic states. As we will see later, the SOC operator involves a dot product of electronic orbital angular momentum operator and electronic spin operator. In atomic physics, we have seen the connection between orbital degeneracy and angular momentum. s orbitals are non-degenerate and have 0 angular momentum. p orbitals are 3-fold degenerate and have angular quantum number l = 1, with the square of angular momentum $2\hbar^2$. The $2l$+1-fold

degeneracy and $\sqrt{l(l+1)}\hbar$ magnitude of angular momentum of each *nl* subshell in atoms clearly show that there is no angular momentum for non-degenerate orbitals. Most chemists like to view atoms and molecules using real-valued orbitals, such as p_x, p_y, and p_z, instead of the complex-valued counterparts p_{+1}, p_0, and p_{-1}. We hence focus our discussion of angular momentum using real-valued orbitals. Shown in Figure 1.7(a) are a set of degenerate *e* bonding orbitals for a hypothetical molecule MH_3, M is a heavy metal. Please feel free to hypothesize it as Tl or Bi. Let's assume that there is only one electron occupying the *e* set. This can be realized by ionizing the molecule. SOC is mainly induced by the heavy central atom. If the electron is occupying any of the e_x or e_y orbitals, it has no angular momentum, *i.e.*, it is not rotating. Consequently, there is no SOC. The angular momentum operator actually couples the two orbitals, *i.e.*, the electron rotation around the central atom is realized by the electron jumping from the e_x to the e_y orbitals. Pictorially, a rotation by 90 degrees is finished in this jumping. With consecutive jumping between the two orbitals as shown in Figure 1.7(b), the electron continuously rotates about the central atom. SOC ensues. The electron can freely jump between the two orbitals, because the orbitals are degenerate. It does not cost any energy to jump between them. Now, let's assume that the electron is initially in the e_x orbital, and induces a JT distortion shown by the arrows in Figure 1.7(a). The bending leads to larger overlaps between the p_x orbital at the centre and the two s orbitals. The stabilization of e_x comes with the destabilization of e_y, since the bonding overlaps between the p_y and the two s orbitals are reduced along the bending. The energy splitting along the JT distortion results in a gap that hinders the jumping of the electron from e_x to e_y, as shown in Figure 1.7(c). The electron rotation is hence quenched, and so is the SOC.

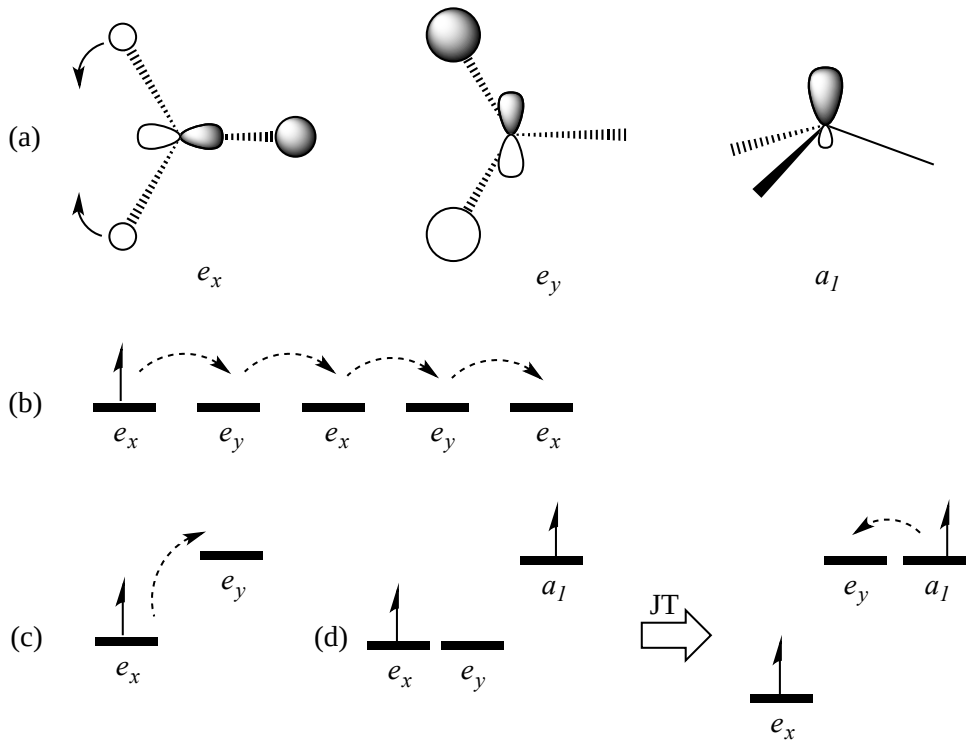

Figure 1.7. Examples of JT and SOC quenching each other and enhancing each other. (a) Valence orbitals of an MH_3 hypothetical molecule that are discussed in the text. (b) Consecutive electron jumping between the two *e* orbitals. (c) Hindered electron jumping between the *e* orbitals after their degeneracy is lifted by JT distortion. (d) Energy alignment of the *e* and a_1 orbitals before and after the JT distortion, and the free electron jumping between the a_1 and e_y orbitals when they become degenerate.

We have just demonstrated how JT may quench SOC. Now, we are to demonstrate that SOC can reversely quench JT. This time, we have to rely on complex-valued orbitals. The angular momentum eigenstates that represent the electron rotation by jumping consecutively between the two *e* orbitals are $e_{\pm} = \frac{1}{\sqrt{2}}(e_x \pm ie_y)$, with i being the imaginary unit. The + and – states correspond to the counterclockwise and clockwise rotations. Those are the orbitals used in constructing eigenstates of SOC. Please note that each of the $e_{\pm}$ orbitals has equal contributions

of e_x and e_y. Since e_x and e_y favor opposite JT distortion directions, the equal contributions exactly cancel the opposite tendencies of distortion. The JT distortion is hence quenched.

So, in the example above JT and SOC quench each other. Now, one more example is given to show that JT and SOC can enhance each other. Shown in Figure 1.7 (a) is also the a_1 lone pair orbital. By "lone pair", we are making analogy to NH_3. Now, we assume that the "lone pair" orbital contains only one electron. It is of higher energy than the *e* shell since it has no bonding character. It can be understood as a hybrid between s and p_z orbital of the central atom. The energy alignment of the a_1 and the *e* orbitals before JT distortion is shown in Figure 1.7(d), where the occupation scheme corresponds to a ${}^3E_x$ state. As the electron in the e_x orbital drives the JT distortion to occur, the e_y orbital energy increases. The a_1 orbital energy is unchanged along the distortion because of its nonbonding character. Eventually, the e_y orbital gets close to the a_1 orbital and the two may become degenerate. Degenerate or not, the hindrance for the consecutive electron jumping between a_1 and e_y is reduced. Electron rotation occurs. SOC ensues. Please note that the s component in the a_1 orbital does not participate in the SOC. It is the p_z component that participates. And the jumping between the p_y component in e_y and p_z component in a_1 corresponds to a rotation about the *x* axis. This SOC is turned on purely by JT. Reversely, the extra energy lowering of the SOC provides extra driving force for the JT distortion. In short, in this example, SOC and JT enhance each other.

Section 1.7 Vibronic Hamiltonian operators for problems with both SOC and JT effects.

The intimate relation between SOC and JT has been shown in the previous section. We need to consider them on the same footing, at least for heavy element compounds. SOC enters $\widehat{H}$ as an additional term:

$$\hat{H} = \hat{T}_n + \hat{T}_{el} + \hat{V} + \hat{V}_{SOC} = \hat{T}_n + \hat{H}_{el} \quad \text{Eqn 1.5}$$

SOC is also included in the electronic Hamiltonian $\hat{H}_{el}$, and it modifies the matrix elements $H^d_{el,nm} = \langle \Phi^d_n | \hat{H}_{el} | \Phi^d_m \rangle$, and also their expansion formulas in nuclear coordinates. The objective of this research is to derive expansion formulas for those matrix elements, including SOC and JT effects together.

Section 1.8 Pseudo-Jahn-Teller effects.

Distortion and symmetry-lowering may also occur for non-degenerate states.[5] The associated effects are called pseudo-Jahn-Teller (pJT) effects. The origin of pJT distortion is exemplified in Figure 1.8. We come back to the trigonal planar structure, but this time with a central atom. We can picture it as NH_3. At the planar D_{3h} structure, the central p_z orbital is of a_2'' irreducible representation, while the symmetrized peripheral *s* orbitals are of a_1' irreducible representation. They do not mix, since one is symmetric while the other is antisymmetric with respect to the molecular plane. Neither of them exhibits any tendency for out of plane distortion. So, putting 1 or 2 electron in either of these orbitals does not distort the D_{3h} structure, *i.e.*, there is no force for out of plane distortion. However, if the out of plane distortion (also called umbrella mode, umbrella inversion, *etc*.) does occur and the symmetry is lowered to C_{3v}, the two orbitals are of the same a_1 irreducible representation. They can mix, forming a bonding and an antibonding orbital. Shown in Figure 1.8(a) is the formation of the bonding orbital. The antibonding orbital takes an opposite phase for the p_z orbital. Let's say that there are less than four electrons occupying the two orbitals, then there must be more electron(s) occupying the lower-lying bonding orbital than the higher-lying antibonding orbital. The distortion hence lowers the ground state energy of the system. Conversely, the excited state with more electron(s) occupying the antibonding orbital

must have its energy increased along the distortion. The energy diagram of such a ground and an excited state is shown in Figure 1.8(b). It should be compared with Figure 1.5(b). The smaller the energy gap between the undistorted structure, the more non-adiabatic the vibrational dynamics. Non-adiabatic vibronic coupling is hence needed.

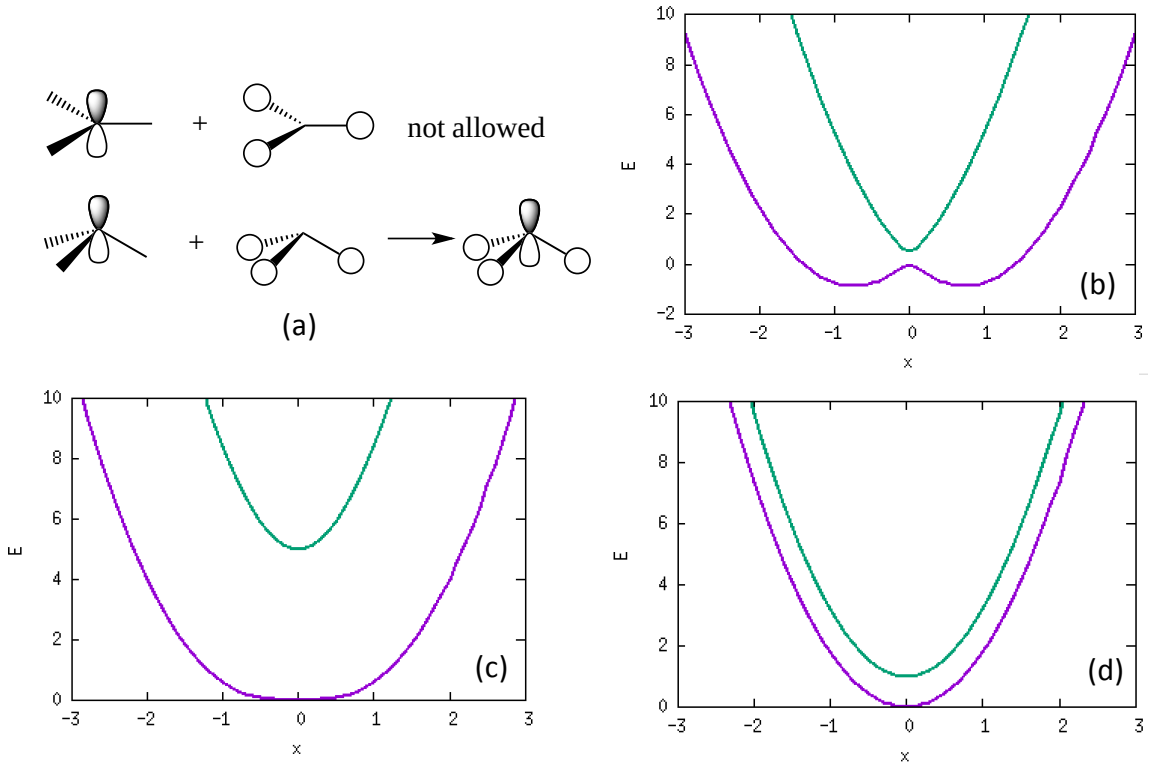

Figure 1.8. An example of pseudo-Jahn-Teller distortion from D_{3h} to C_{3v} structure of a trigonal planar molecule: (a) mixing of the p_z orbital at the central atom and the symmetrized *s* orbitals of the surrounding atoms; energy diagrams of (b) strong and (c), (d) weak pseudo-Jahn-Teller interaction. The distortion coordinate and energy are in arbitrary unit for this hypothetical example.

Whether the distortion occurs solely depends on whether the bonding interaction is substantial enough to lower the energy of the bonding orbital. In undergraduate chemistry textbooks, we have learned that two factors besides the symmetry-matching determine the strength of the bonding interaction, *i.e.*, the strength of the pJT distortion: the gap between the orbitals and

their overlap. Mathematically, it is the F^2/Δ ratio that determines whether pJT distortion occurs, with F being the interaction strength (overlap) between the orbitals and Δ is the orbital energy gap. While Figure 1.8(b) shows the strong pJT case with small orbital energy gap and large overlap, Figure 1.8(c) and (d) show the weak pJT cases with a large gap and a small overlap, respectively.

SOC is also closely related to pJT. Two examples are shown in Figure 1.9. It is the same D_{3h}-to-C_{3v} hypothetical system. Now, we also consider the e_x and e_y bonding orbitals and the corresponding antibonding orbitals. All the orbitals are shown in Figure 1.9(a). We first consider the situation where there is only one electron occupying the *e* shell. There is SOC for the rotation of the electron within the e shell, which is a rotation about the *z* axis. The axes frame is given in the Figure 1.9(a). As long as the energy gap between the e shell and the a_1^* antibonding orbital is accessible at the D_{3h} structure, the electron can undergo a hindered rotation by jumping from the *e* shell to the a_1^* orbital. This rotation about the *x* and/or *y* axes results in further SOC. This extra SOC disfavors the pJT distortion, as the distortion enlarges the *e*-a_1^* gap and further hinders the rotation, and then SOC. This situation of SOC and pJT quenching each other is shown in Figure 1.9(b). But the *e* and a_1^* orbitals have higher energies along the distortion, as the former lose bonding character and the later gains antibonding character. However, the energy raising due to increased antibonding character is in general quicker than that due to reduced bonding character. This is the reason for the *e*-a_1^* gap enlargement along the distortion, and the mutual quenching of SOC and pJT.

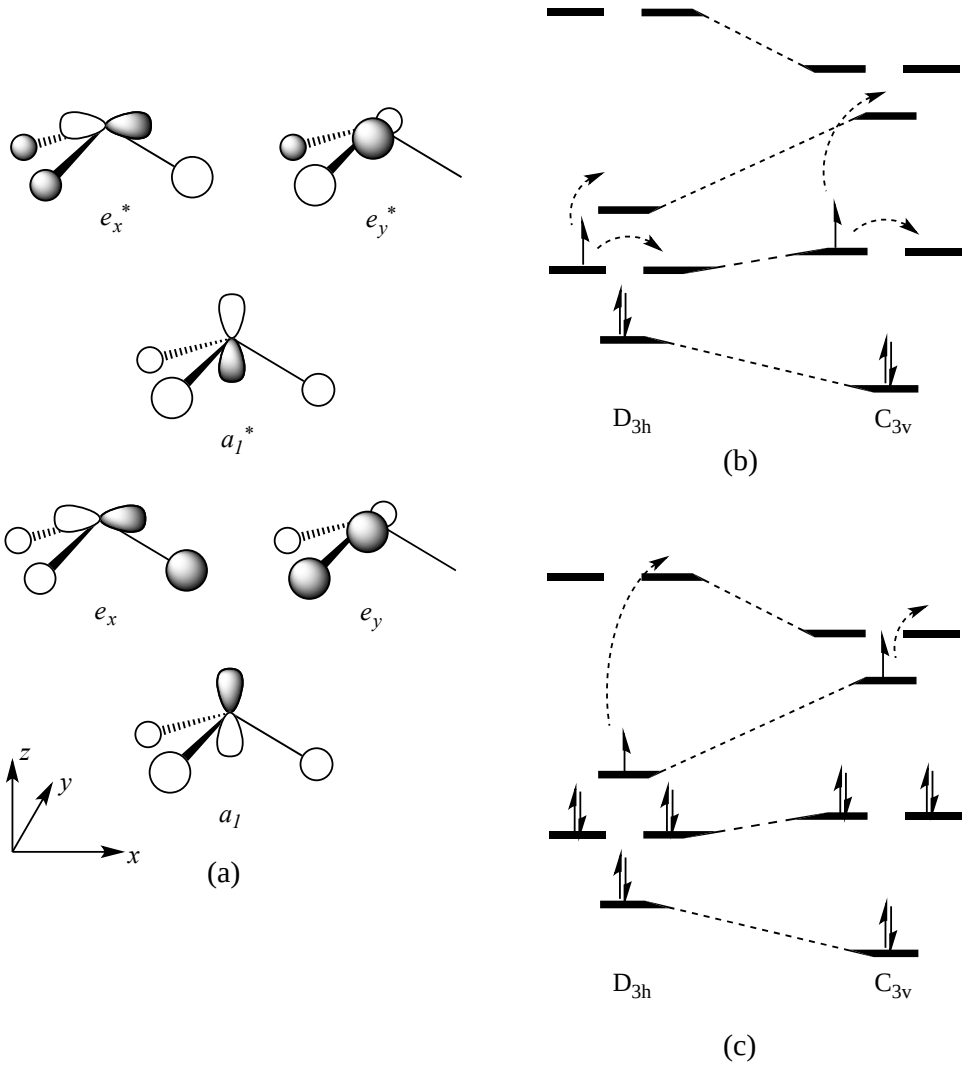

Figure 1.9. Two examples that show the interplay between spin-orbit coupling and pseudo-Jahn-Teller distortion. All relevant orbitals are shown in (a), the situation of SOC and pJT quench each other is shown in (b), and the mutual enhancing situation is shown in (c).

We then consider the situation in Figure 1.9(c). The *e* shell is fully occupied by four electrons. The a_1^* electron cannot jump to the *e* shell to realize its rotation around the *x* and *y* axes, due to the Pauli exclusion principle. It may, if allowed, jump to the e^* shell to have SOC. This SOC is hindered at the undistorted structure, due to the large a_1^*-e^* gap. However, along the distortion, the e^* orbitals lose antibonding character and have their energy decreased. Along with

the increased a_1^* energy, the a_1^*-e^* gap is reduced, the electron jump becomes possible, and the SOC is enhanced. This is the situation of SOC and pJT enhancing each other.

Given the close interplay between SOC and pJT, we also consider vibronic problems with the two effects in our derivation. The Hamiltonian operator $\hat{H}$ takes the same form as in the SOC-JT cases, except that the diabatic states that are used to construct the $\hat{I}$ operator are non-degenerate.

Section 1.9 Generalization.

While in most textbooks, JT effects are introduced in the context of transition metals, here we use hypothetical trigonal planar systems as examples to explain the relevant concepts. This is because trigonal symmetry is the lowest symmetry that gives degenerate irreducible representation (*E*-type), and is hence the lowest symmetry that gives JT effects. Again, in undergraduate education, only the knowledge of static JT effects is delivered. And structural distortions are more often seen for transition metal compounds, which feature higher symmetries. However, we are more interested in dynamical JT effects, which are ubiquitous for excited states and ionic states for all kinds of systems. NH_3 is the most commonly seen trigonal system. Its photoelectron spectrum shows strong JT effects, once an electron is removed from its *e* shell.

However, our discussions of JT, pJT, SOC, and their interplays are applicable for all symmetries. The degeneracy may increase from 2-fold for the trigonal systems to 3-fold for cubic systems, and even 4- and 5-fold for icosahedral systems. Still, the picture of electrons freely jumping between degenerate orbitals to realize their rotations, and hence SOC is applicable. The picture of unequal occupancies on degenerate orbitals leading to non-totally-symmetric bonding/electrostatic interaction, and hence JT distortion is still applicable. The picture of symmetry-lowering inducing orbital mixing, and hence pJT distortion is still applicable. The

picture of orbital energies varying along JT/pJT distortion, resulting in weaker or stronger SOC is still applicable.

Section 1.10 Current state of knowledge.

Our work is focused on deriving expansion formulas for spin-orbit Jahn-Teller/pseudo-Jahn-Teller (SO JT/pJT) vibronic Hamiltonian operators. The first attempt to include linear dependence of SOC on vibrational coordinate was made by Moffitt and Thorson in their study of SO JT effect in octahedral complexes.[41] Half a century later, Poluyanov and Domcke and their coworkers carried out a series of studies on SO JT/pJT interactions in trigonal, tetragonal, and cubic systems using SO Hamiltonian expanded to the first order in vibrational coordinates.[37,42,43,44] They pointed out the relativistic origins of some JT interactions in tetragonal and cubic systems.

In the past 15 years, more and more studies on electrostatic (*i.e.*, non-SO) JT/pJT systems showed the inadequacy of the standard second order model Hamiltonians,[45,46,47,48,49,50,51,52,53] especially in simulating vibronic spectra. The main source of the inadequacy is the anharmonicity in the potential energy surfaces of the diabatic states, which is often induced by large amplitude motion of nuclei.[48] There is no reason to assume exemption from this inadequacy in SO JT/pJT problems that involve heavy elements. Therefore, high-order expansion formulas of SO JT/pJT Hamiltonian matrix elements in vibrational coordinates are highly desired, as much as the high-order formulas of non-SO JT/pJT Hamiltonians.

The first attempts to derive high-order expansion formulas for SO JT/pJT Hamiltonians were made in 2016 by the Domcke group[54] and the Eisfeld group.[55] Domcke and coworkers derived expansion formulas for a set of p orbitals in the tetrahedral and trigonal environments. They derived the relations between SO and non-SO JT/pJT Hamiltonian matrix elements of the p orbitals. One can then adapt non-SO JT/pJT expansion formulas to express SO JT/pJT expansions.

Weike and Eisfeld derived expansion formulas for the $(E + A_1) \otimes (e + a_1)$ and $(E + A_1) \otimes (3e + 3a_1)$ JT/pJT problems in C_{3v} symmetry, with the purpose to study the SO JT/pJT interactions in CH_3I^+.

Section 1.11 What we did in this thesis research

All the aforementioned pioneering and enlightening works motivate us to perform the present study to derive general expansion formulas for SO JT/pJT Hamiltonians in trigonal and tetragonal symmetries. The two classes of symmetries are chosen because: (1) trigonal symmetries are the lowest symmetries that allow for orbital degeneracy and thus JT effect; (2) tetragonal symmetries are the lowest symmetries that possess all three types of irreducible representations (irreps) of axial symmetries (*i.e.*, symmetries with only one principal symmetry axis), A-, B-, and E-type; (3) tetragonal symmetries are the lowest symmetries that feature purely SO-induced JT effect. Our objective is to obtain bimodal expansion formulas up to arbitrary order for all SO JT/pJT problems in all 6 trigonal symmetries (C_3, $C_{3v}, D_3, C_{3h}, D_{3h}$, and D_{3d}) and all 7 (C_4, S_4, C_{4v}, C_{4h}, D_{2d}, D_4, and D_{4h}) tetragonal symmetries. This objective is attained by our efficient derivation, which is based on the idea of "descent in symmetry",[56] the root-branch approach, and the modularized approach. The idea and approaches have been employed in our recent derivations of arbitrarily high order expansion formulas for non-SO JT/pJT problems in trigonal, tetragonal, and cubic symmetries.[57,58,59,60,61] They can be equally employed in deriving SO JT/pJT formulas, and the resultant formulas can be similarly summarized in a set of look-up tables. Each independent Hamiltonian matrix element of a SO JT/pJT problem carries a set of symmetry eigenvalues, which guide us to retrieve the element's expansion formulas in the tables. We focus on bimodal problems because: (1) it is usually adequate to consider up to two vibrational modes; (2) problems involving more than two modes can be approximated as composites of

bimodal sub-problems; (3) it is straightforward to extend the bimodal expansions to formulas for more vibrational modes. One example of the extension is given in **Section 4.3**.

Chapter 2 Methodology

Section 2.1 Setting, symbols, and terminologies

Following the tradition in the JT community, we use upper case Mulliken symbols to label electronic states and lower-case symbols to label vibrations. As shown later, only one-electron states (*i.e.*, orbitals) need to be considered in the derivation. We label the two real-valued components of an E state as $|X\rangle$ and $|Y\rangle$, and the two components of an e vibrational mode as e_x and e_y. The component states are so oriented that they transform under $\hat{C}_n$ ($n = 3, 4$) as:

$$\hat{C}_n|X\rangle = \cos\frac{2\pi}{n}\,|X\rangle + \sin\frac{2\pi}{n}\,|Y\rangle;\ \hat{C}_n|Y\rangle = \cos\frac{2\pi}{n}\,|Y\rangle - \sin\frac{2\pi}{n}\,|X\rangle \qquad \text{Eqn 2.1}$$

and the component modes transform similarly. The component states are combined to form eigenstates of $\hat{C}_n$,

$$\begin{gathered}(|+\rangle|-\rangle) = (|X\rangle|Y\rangle)\frac{1}{\sqrt{2}}\begin{pmatrix}1 & 1\\ i & -i\end{pmatrix};\\ \hat{C}_3|\pm\rangle = e^{\mp i\frac{2}{3}\pi}|\pm\rangle;\ \hat{C}_4|\pm\rangle = \mp i|\pm\rangle.\end{gathered} \qquad \text{Eqn 2.2}$$

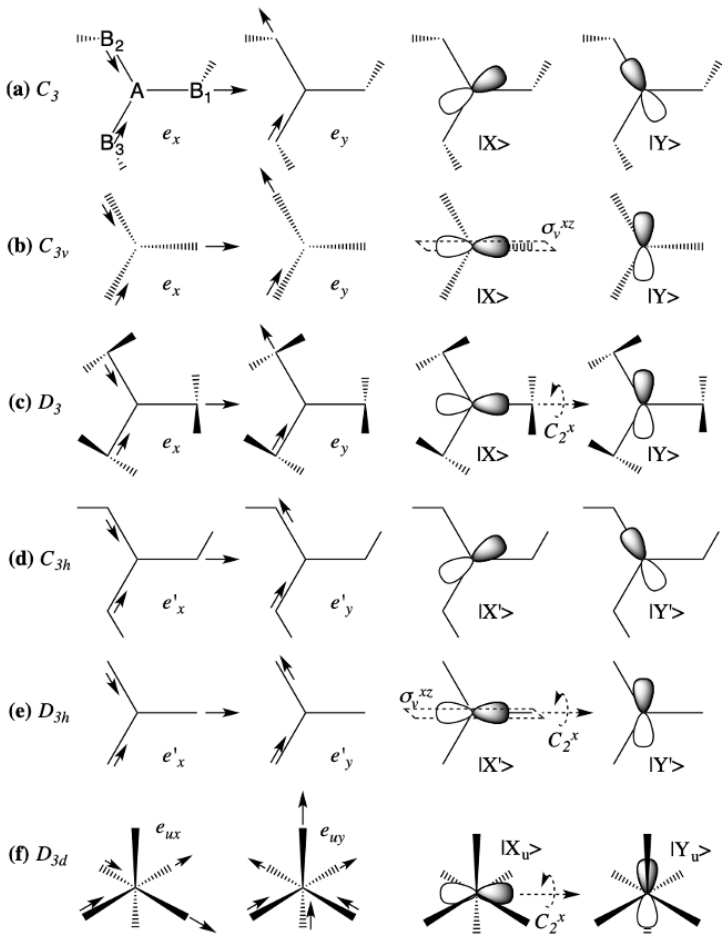

Figure 2.1 . Examples of orientations of e and E components in trigonal symmetries, on which the derivations are based. Atomic motions in the modes are represented by solid arrows. With the atom labelling in panel(a),$e_x = \frac{1}{\sqrt{6}}\left(2\Delta r_{AB_1} - \Delta r_{AB_2} - \Delta r_{AB_3}\right)$, and $e_y = \frac{1}{\sqrt{2}}\left(\Delta r_{AB_1} - \Delta r_{AB_3}\right)$ The e_x expressions means the combination of changing two equivalences of the AB_1 bond length and changing one equivalence of the AB_2 and AB_3 bond lengths in the opposite direction. Similar definitions apply to the displayed e modes in the other panels.

In D_3, D_{3h}, D_{3d}, D_4, D_{4h}, and D_{2d} symmetries, $|X\rangle$ and $|Y\rangle$ are further defined so that the former is symmetric with respect to one $\hat{C}_2'$, while the latter is antisymmetric. In C_{nv} symmetry, the

component states follow the same transformation but with $\hat{C}_2{}'$ being replaced by $\hat{\sigma}_v$. The two e component modes transform similarly under $\hat{C}_2{}'$ and $\hat{\sigma}_v$ in the respective symmetries. Such a setting of the E component states and e component modes is exemplified in Figure 2.1 and Figure 2.2 for trigonal and tetragonal symmetries, respectively. A consequence of such an orientation setting of the real-valued E component states is:

$$\hat{C}_2'|\pm\rangle = |\mp\rangle = (|\pm\rangle)^*;\ \ \hat{\sigma}_v|\pm\rangle = |\mp\rangle = (|\pm\rangle)^* \qquad \text{Eqn 2.3}$$

For these complex-valued states, the actions for the two symmetry operators give the same results as the time-reversal operator (vide infra).

x and y and their polar counterparts ρ and ϕ ($x = \rho\, cos\, \phi$; $y = \rho\, sin\, \phi$) are used to label vibrational coordinates of the e_x and e_y component modes, z for a mode, and w for b mode. SOC and JT interaction between states arising from the same term symbol are called intra-term couplings. They are labelled as $\Gamma \otimes (\gamma_{(1)} + \gamma_{(2)})$ and correspond to SO JT interactions. The interactions between states from different term symbols are called inter-term couplings. They are labelled as $(\Gamma_I + \Gamma_{II}) \otimes (\gamma_{(1)} + \gamma_{(2)})$ and correspond to SO pJT interactions. As the multi-electronic states reduce to one-electron orbitals in the following derivation, the terminologies of "intra-shell coupling" and "inter-shell coupling" are used instead.

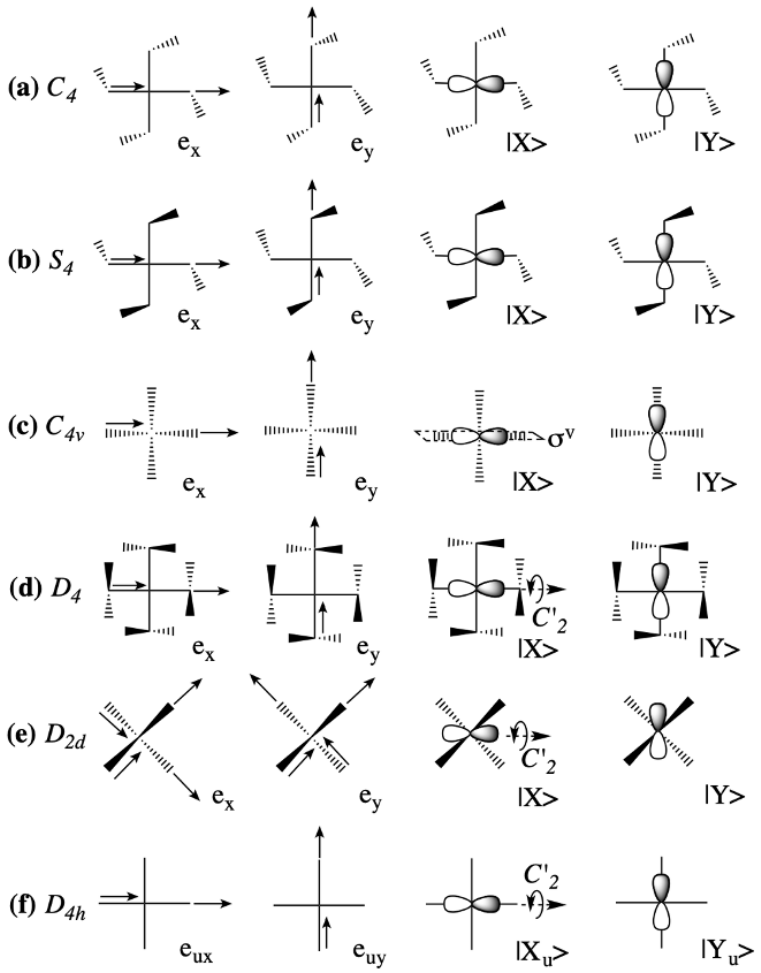

Figure 2.2:Examples of orientations of e and E components in tetragonal symmetries, on which the derivations are based. Atomic motions in the modes are represented by solid arrows. The orientations in C_{4h} symmetry are not shown. They are similar to those in C_4 symmetry.

α and β are used to label the two electronic spin functions with spin-up and -down. The z axis for spin quantization is chosen to be the principal C_n axis. This setting leads to the transformation:

$$\hat{C}_3 \left|\pm\frac{1}{2}\right\rangle = e^{\mp i\frac{\pi}{3}} \left|\pm\frac{1}{2}\right\rangle; \hat{C}_4 \left|\pm\frac{1}{2}\right\rangle = e^{\mp i\frac{\pi}{4}} \left|\pm\frac{1}{2}\right\rangle. \qquad \text{Eqn 2.4}$$

Here, $\left|\frac{1}{2}\right\rangle$ and $\left|-\frac{1}{2}\right\rangle$ are used to represent the α and β spin functions. In D_3, D_{3h}, D_{3d}, D_4, D_{2d}, and D_{4h}(C_{3v} and C_{4v}) symmetries, we need to consider the transformations of the spin functions under the actions of $\hat{C}_2'(\hat{\sigma}_v)$. Therefore, we also need to consider spin quantizations along directions perpendicular to the z axis. The most convenient setting is that the $\hat{C}_2'$ axis in D_3, D_{3h}, D_{3d}, D_4, D_{2d}, and D_{4h}symmetries is chosen to be the x axis, along which the Pauli matrix

$$\sigma_x = \begin{pmatrix} 0 & 1 \\ 1 & 0 \end{pmatrix} \qquad \text{Eqn 2.5}$$

is used to represent the $\hat{\vec{s}}_x$ component of the spin operator $\hat{\vec{s}}$. "$\hat{C}_2'$" and "$\hat{C}_2^x$" are used interchangeably in the text below. In C_{3v} and C_{4v} symmetries, the x axis is defined to be perpendicular to the principal axis and contained by the σ_v plane. The y axis is obtained by the cross product $\vec{y} = \vec{z} \times \vec{x}$. Such a setting of the spin quantization axes is exemplified in Figure 2.3. With this setting, the spin functions transform under $\hat{\sigma}_v$ and $\hat{C}_2'$ as

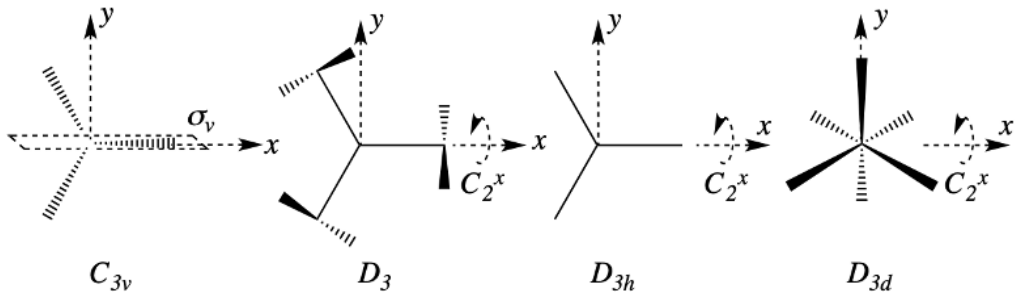

Figure 2.3:Examples of x and y axes for spin quantizations in C_{3v}, D_3, D_{3h}, and D_{3d} symmetries. The z axis is the C_3 axis pointing out of the paper. The x and y axes follow similar definitions in C_{4v}, D_4, D_{2d}, and D_{4h} symmetries.

$$\hat{\sigma}_v(\alpha,\beta) = \hat{I}\hat{C}_2^y(\alpha,\beta) = \hat{C}_2^y(\alpha,\beta) = (\alpha,\beta)\begin{pmatrix} 0 & -1 \\ 1 & 0 \end{pmatrix}; \qquad \text{Eqn 2.6}$$

$$\hat{C}_2'(\alpha,\beta) = \hat{C}_2^x(\alpha,\beta) = (\alpha,\beta)\begin{pmatrix} 0 & -i \\ -i & 0 \end{pmatrix}. \quad \text{Eqn 2.7}$$

$\hat{I}$ is the inversion operation, and should not be misunderstood as the identity operator in Eqn 1.4. It only acts on spatial functions, but not on spin functions. That is why it disappears after the second equal sign in Eqn 2.6. The σ_h plane in C_{3h}, D_{3h}, C_{4h}, and D_{4h} symmetries is the xy plane. Under $\hat{\sigma}_h$, the spin functions transform as

$$\hat{\sigma}_h(\alpha,\beta) = \hat{I}\hat{C}_2^z(\alpha,\beta) = \hat{C}_2^z(\alpha,\beta) = (\alpha,\beta)\begin{pmatrix} -i & 0 \\ 0 & i \end{pmatrix}. \quad \text{Eqn 2.8}$$

Again, the $\hat{I}$ operator does not act on the spin functions.

Section 2.2 Spin-orbit Hamiltonian and its approximation as an effective one-electron operator

Under the Breit–Pauli approximation,[17] SOC operator in atomic unit reads

$$\begin{aligned} \hat{H}_{SO} &= \frac{1}{2c^2}\left[\sum_i \sum_A \frac{Z_A}{r_{i,A}^3}\hat{\vec{l}}_{iA}\cdot\hat{\vec{s}}_i - \sum_{i\neq j}\frac{1}{r_{ij}^3}\hat{\vec{l}}_{ij}\cdot\left(\hat{\vec{s}}_i + 2\hat{\vec{s}}_j\right)\right] \\ &= \sum_i \hat{\vec{z}}_i^{(1)}\cdot\hat{\vec{s}}_i + \sum_{i\neq j}\hat{\vec{z}}_{ij}^{(2)}\cdot\left(\hat{\vec{s}}_i + 2\hat{\vec{s}}_j\right) \\ &= \sum_i \hat{h}_{SO}^{1e}(i) + \sum_{i\neq j}\hat{h}_{SO}^{2e}(i,j), \end{aligned} \quad \text{Eqn 2.9}$$

Summation indices *i* and *A* run over electrons and nuclei, respectively, Z_A is the nuclear charge, $r_{i,A}$ is the distance between electron *i* and nucleus *A*, $\hat{\vec{l}}_{iA}$ is the angular momentum operator of electron *i* around nucleus *A*, $\hat{\vec{s}}_i$ is the spin operator of electron *i*, r_{ij} and $\hat{\vec{l}}_{ij}$ are the inter-electron analogues of $r_{i,A}$ and $\hat{\vec{l}}_{iA}$, and *c* is the speed of light. Definitions of the symbols in the second and third rows become clear when the rows are compared with the first row. $\hat{H}_{SO}$ contains both one-

and two-electron components, corresponding to the electronic orbital motions around nuclei and other electrons, *i.e.*, $\hat{\vec{l}}_{iA}$ and $\hat{\vec{l}}_{ij}$, respectively. $\widehat{H}_{SO}$ under other approximations, *e.g.*, Douglas–Kroll–Hess, [62, 63] infinite-order two-component, [64] and relativistic elimination of small components,[65,66] carry the same symmetry properties. Since only these symmetry properties matter in the following derivation, the resultant formalism is applicable regardless of the approximation in obtaining $\widehat{H}_{SO}$.

The main part of the two-electron SO interaction can be viewed as the screening of the one-electron SO interaction. Consequently, the matrix element between two multi-electronic states $|\Psi_I\rangle$ and $|\Psi_J\rangle$ can be safely approximated as a summation of integrals of the mean-field one-electron SO operator $\hat{h}_{SO}^{1e}$.[67,68,69,70,71]

$$H_{IJ}^{SO} = \langle \Psi_I | \widehat{H}_{SO} | \Psi_J \rangle \approx \sum_i \sum_j P_{ij}^{IJ} \langle \psi_i | \hat{h}_{eff}^{1e} | \psi_j \rangle$$
$$= \sum_i \sum_j P_{ij}^{IJ} \left\langle \phi_i \middle| \hat{\vec{z}}_{eff}^{(1)} \middle| \phi_j \right\rangle \cdot \langle \sigma_i | \hat{\vec{s}} | \sigma_j \rangle \qquad \text{Eqn 2.10}$$

where i and j loop over all molecular spin orbitals ψ_i, ψ_j, and P^{IJ} stands for the one-electron transition density matrix between the two states. The spin orbitals are products of spatial orbitals ϕ_i, ϕ_j and spin functions σ_i, σ_j.

Eqn 2.10 represents an important simplification. Any multi-electronic SO matrix element can be eventually expressed using one-electron SO matrix elements. It is for this reason that the expansion formulas obtained in ref. 54 and 55, in which the derivations were based on the one-electron Pauli SOC operator and spin orbitals, are also applicable in expanding SO matrix elements of multi-electronic states. The procedure is as follows. Given a pair of diabatic states $|\Psi_I\rangle$ and $|\Psi_J\rangle$ that are built using a common set of diabatic spin orbitals $\{\psi\}$, one first calculates its transition

density matrix P^{IJ}. A few pairs of ψ_i and ψ_j that correspond to P_{ij}^{IJ} elements with large magnitude are selected. The expansions of the one-electron elements $\langle\psi_i|\hat{h}_{eff}^{1e}|\psi_j\rangle$s in vibrational coordinates are then linearly combined with the P_{ij}^{IJ} coefficients to give the expansion of H_{IJ}^{SO}. Clearly, the derivation of H_{IJ}^{SO} expansion formulas has been reduced to deriving expansion formulas for $\langle\psi_i|\hat{h}_{eff}^{1e}|\psi_j\rangle$s, which are the focus of this work. Henceforth, the term "matrix element" is reserved for $\langle\psi_i|\hat{h}_{eff}^{1e}|\psi_j\rangle$. The actual forms of $\hat{h}_{eff}^{1e}$and $\hat{\tilde{z}}_{eff}^{(1)}$ are not of importance. We only need to know that they share the same structures and symmetries with the $\hat{h}_{SO}^{1e}$ and $\sum_A \frac{Z_A}{r_{i,A}^3}\hat{\tilde{l}}_{iA}$ operators in Eqn 2.9, respectively.

Section 2.3 Symmetry

Symmetry properties of $\widehat{H}_{SO}$ have been thoroughly discussed in ref. 15 and 72. In short, the operator is invariant with respect to the time-reversal operator and all symmetry operators of a system. Furthermore, the Wigner–Eckart theorem (WET) allows us to obtain a set of $\langle\Psi_I(M_S)|\widehat{H}_{SO}|\Psi_J(M_S')\rangle$s with a constant $\Delta M_S = M_S - M_S'$, from one element of the set. In this set of elements, all bra states only differ in the projection of total spin (*i.e.*, the M_S quantum number), and so do all the ket states. Also, an element is nonzero only for $\Delta M_S = 0, \pm 1$. All these symmetry properties are transferrable to $\hat{h}_{eff}^{1e}$, which is just a one-electron special case of $\widehat{H}_{SO}$. In the following sections, we will discuss how the time-reversal symmetry and WET simplify the structure of the $\langle\psi_i|\hat{h}_{eff}^{1e}|\psi_j\rangle$ matrix.

Section 2.3.1 Time-reversal symmetry

General aspects of time-reversal symmetry and the time-reversal operator $\hat{\mathcal{T}}$, especially those that are relevant to our derivation, are detailed in ref. 73. They are recapitulated here:

1. $\hat{\mathcal{T}}$ converts all imaginary unit i in its operand to $-i$, α to β, and β to $-\alpha$;

2. each state $|X\rangle$ has its time-reversal counterpart $|X'\rangle = \hat{\mathcal{T}}|X\rangle$. $|X'\rangle$ may be equal to $|X\rangle$ when it is a state of an even number of electrons. In this situation, we may multiply i to the $|X\rangle$. The resultant $|Y\rangle = i|X\rangle$ satisfies $\hat{\mathcal{T}}\ |Y\rangle = -\ |Y\rangle$. Within this section, $|X\rangle$and $|Y\rangle$indicate generic electronic states, not the E component states as defined in **Section 2.1**;

3. for a Hamiltonian operator $\hat{H}$ that is time-reversal symmetric, its matrix elements between states of even numbers of electrons satisfy $\langle X_i|\hat{H}|X_j\rangle = \langle X_j'|\hat{H}|X_i'\rangle$ and $\langle X_i|\hat{H}|X_j'\rangle = \langle X_j|\hat{H}|X_i'\rangle$;

4. its matrix elements between states of odd numbers of electrons satisfy $\langle X_i|\hat{H}|X_j\rangle = \langle X_j'|\hat{H}|X_i'\rangle$ and $\langle X_i|\hat{H}|X_j'\rangle = -\langle X_j|\hat{H}|X_i'\rangle$.

Point 3 determines that a Hamiltonian matrix of a set of time-reversal-adapted states of an even number of electrons adopt the block structure shown in Figure 2.4(a). The states are ordered so that the first $2k$ states are k pairs of $|X_i\rangle$s and $|X_i'\rangle$s, the k $|X_i\rangle$s first, followed by the k $|X_i'\rangle$s; then n $|Y_i\rangle$s that are invariant under the action of $\hat{\mathcal{T}}$; then m $|Z_i\rangle$s that change their signs under the action of $\hat{\mathcal{T}}$. The whole set of the adapted states can be transformed to all $|Y_i\rangle$-type or all $|Z_i\rangle$-type states. We keep the form of Figure 2.4(a) to maintain generality.

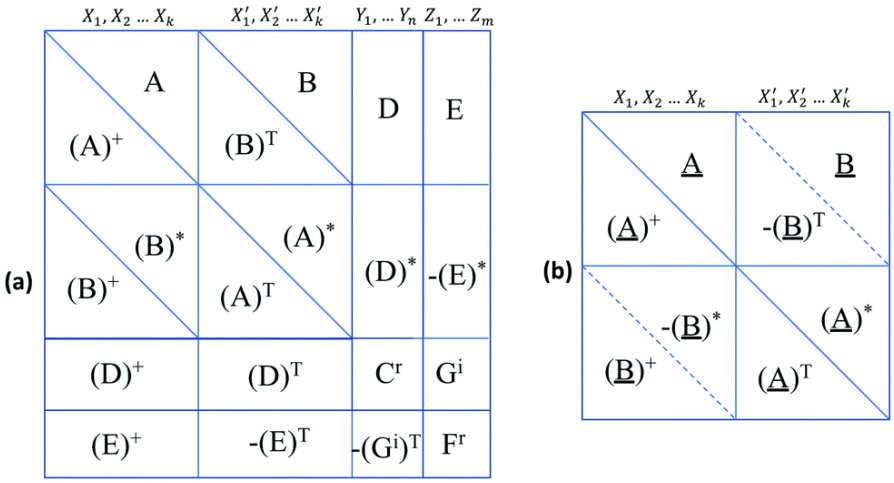

Figure 2.4. Block structures of general matrices of a time-reversal symmetric Hamiltonian in a set of time-reversal-adapted states with (a) an even number and (b) an odd number of electrons. Superscripted asterisk, T and dagger indicate taking the complex conjugate, the transpose, and both for the denoted block of matrix. Superscripted i indicates that the denoted block is purely imaginary. Superscripted r indicates that that the denoted square block is real and symmetric. The two dashed lines in (b) indicate that the "diagonal" elements of the two off-diagonal blocks are zero.

Point 4 determines that a Hamiltonian matrix of a set of time-reversal-adapted states of an odd number of electrons adopt the block structure in Figure 2.4(b). For a system with an odd number of electrons, the $|Y_i\rangle$-type and $|Z_i\rangle$-type states do not exist. All states in the set must be paired into the $|X_i\rangle$-type and $|X'_i\rangle$-type states, underlying the Kramers doublet degeneracy.[74] Putting $i = j$ in the second equality in Point 4, we immediately see $\langle X'_i|\hat{H}|X'_i\rangle = 0$, which gives the dashed lines in Figure 2.4(b), which indicate zero "diagonal" elements on the off-diagonal blocks. The block structure in Figure 2.4(b) is most relevant to our derivation. We are deriving expansion formulas for $\langle\psi_i|\hat{h}^{1e}_{eff}|\psi_j\rangle$s, with $|\psi_i\rangle$ and $|\psi_j\rangle$ being one-electron states (*i.e.*, spin orbitals or spinors). Clearly, given a time-reversal-adapted set of $2k$ spin orbitals, we only need to

consider the $\frac{k(k+1)}{2}$ elements in the A triangle block and the $\frac{k(k-1)}{2}$elements in the B triangle block. Henceforth, all matrices discussed adopt the form of Figure 2.4(b). And there are only k^2 independent matrix elements. Compared to the $\frac{2k(2k+1)}{2}$ independent matrix elements in a $2k \times 2k$ hermitian matrix, the time-reversal symmetry has reduced the number of independent matrix elements by more than one half. The terms "A block" and "B block" are frequently used below. We emphasize that they denote the different triangle blocks in Figure 2.4(b), and one shall not associate the A and B in the terms to A- and B-type irreps.

The connections between $\hat{\mathcal{T}}$, $\hat{\sigma}_v$, and $\hat{C}_2'$ are important. It has been pointed out under Eqn 2.3 that for the complex-valued E component states, the operations of $\hat{\sigma}_v$ and $\hat{C}_2'$ give the same result as acting $\hat{\mathcal{T}}$. The comparison of Point 1, Eqn 2.6 and Eqn 2.7 clearly shows that for the spin functions, the operation of $\hat{\sigma}_v$ is equivalent to $\hat{\mathcal{T}}$. $\hat{C}_2'$ is also closely related to $\hat{\mathcal{T}}$ by swapping the two functions. The three operators all reverse the direction of the angular momentum along the principal axis, and that is why they are connected. As shown below, the close connections between $\hat{\mathcal{T}}$, $\hat{\sigma}_v$,and $\hat{C}_2'$ allow us to derive the expansion formulas without resorting to constructing eigenfunctions of $\hat{\sigma}_v$ and $\hat{C}_2'$. This is one technical difference between the present work and ref. 55.

Section 2.3.2 Symmetry relation dictated by the Wigner–Eckart theorem

Now, we order a time-reversal-adapted set of spin orbitals so that the $|X_i\rangle$-type states all have α spin functions, and the $|X_i{}'\rangle$-type states all have β spin functions, *i.e.*,

$$\phi_1\alpha, \phi_2\alpha, \dots, \phi_k\alpha, \phi_1^*\beta, \phi_2^*\beta, \dots, \phi_k^*\beta \qquad \text{Eqn 2.11}$$

ϕ_i indicates the spatial part of a spin orbital. According to WET, the matrix element $\langle\psi_i|\hat{h}_{eff}^{1e}|\psi_j\rangle$ can be written as[72]

$$\langle X_i|\hat{h}_{eff}^{1e}|X_j\rangle = \langle \phi_i\alpha|\hat{h}_{eff}^{1e}|\phi_j\alpha\rangle = \langle \phi_i\|\hat{z}_{eff,0}^{1e}\hat{\vec{s}}\|\phi_j\rangle \left(\frac{1}{2},1,\frac{1}{2},0\middle|\frac{1}{2},\frac{1}{2}\right) \quad \text{Eqn 2.12}$$

where $\left(\frac{1}{2},1,\frac{1}{2},0\middle|\frac{1}{2},\frac{1}{2}\right)$ is the Clebsch–Gordan coefficient with the format $(j_1,j_2,m_1,m_2|j,m)$, and $\langle \phi_i\|\hat{z}_{eff,0}^{1e}\hat{\vec{s}}\|\phi_j\rangle$ the reduced matrix element of the one-electron spin operator $\hat{\vec{s}}$, along with the 0 spherical component of the rank-1 tensor operator $\hat{z}_{eff}^{1e}$. Since $\left(\frac{1}{2},1,\frac{1}{2},0\middle|\frac{1}{2},\frac{1}{2}\right) = -\left(\frac{1}{2},1,-\frac{1}{2},0\middle|\frac{1}{2},-\frac{1}{2}\right)$,

$$\langle X_i|\hat{h}_{eff}^{1e}|X_j\rangle = -\langle \phi_i\|\hat{z}_{eff,0}^{1e}\hat{\vec{s}}\|\phi_j\rangle \left(\frac{1}{2},1,-\frac{1}{2},0\middle|\frac{1}{2},-\frac{1}{2}\right) = -\langle \phi_i\beta|\hat{h}_{eff}^{1e}|\phi_j\beta\rangle \quad \text{Eqn 2.13}$$

If $\phi_i\beta$ and $\phi_j\beta$ happen to be in the set of $|X_i'\rangle$-type states, *i.e.*, $\phi_i\beta = X_m'$ and $\phi_j\beta = X_m'$ (or equivalently, $\phi_i = \phi_m^*$and $\phi_j = \phi_l^*$), then

$$\langle X_i|\hat{h}_{eff}^{1e}|X_j\rangle = -\langle X_m'|\hat{h}_{eff}^{1e}|X_l'\rangle \quad \text{Eqn 2.14}$$

and this equality reduces the number of independent matrix elements in the A block in Figure 2.4(b). Eqn 2.14 is used in all considered cases below to further simplify the derivation.

For one-electron spin orbitals, WET can only be used through Eqn 2.13 and Eqn 2.14, *i.e.*, to connect the $\langle \phi_i\alpha|\hat{h}_{eff}^{1e}|\phi_j\alpha\rangle$ and $\langle \phi_i\beta|\hat{h}_{eff}^{1e}|\phi_j\beta\rangle$ elements by a sign change. In plain language, this sign change can be associated to the spin flipping from α to β. Given the same magnetic field generated by the electron rotation hopping between ϕ_i and ϕ_j, the flipping of the spin magnetic moment changes the sign of its magnetic interaction with the field. Given two spatial orbitals ϕ_i and ϕ_j, there are two more $\hat{h}_{eff}^{1e}$ matrix elements:

$$\begin{aligned}\langle \phi_i\alpha|\hat{h}_{eff}^{1e}|\phi_j\beta\rangle &= \langle \phi_i\|\hat{z}_{eff,-1}^{1e}\hat{\vec{s}}\|\phi_j\rangle \left(\frac{1}{2},1,-\frac{1}{2},1\middle|\frac{1}{2},\frac{1}{2}\right);\\ \langle \phi_i\beta|\hat{h}_{eff}^{1e}|\phi_j\alpha\rangle &= \langle \phi_i\|\hat{z}_{eff,+1}^{1e}\hat{\vec{s}}\|\phi_j\rangle \left(\frac{1}{2},1,\frac{1}{2},-1\middle|\frac{1}{2},-\frac{1}{2}\right).\end{aligned} \quad \text{Eqn 2.15}$$

The reduced matrix elements of the 0, +1 and −1 spherical component of $\hat{z}_{eff}^{1e}$ are in general independent of each other. Therefore, we can only associate $\langle\phi_i\alpha|\hat{h}_{eff}^{1e}|\phi_j\alpha\rangle$ and $\langle\phi_i\beta|\hat{h}_{eff}^{1e}|\phi_j\beta\rangle$, which share a reduced matrix element. The spatial symmetry of a polyatomic system may impose relations between the reduced matrix elements $\langle\phi_i\|\hat{z}_{eff,0,\pm1}^{1e}\hat{\vec{s}}\|\phi_j\rangle$ or nullify some of them. However, the symmetry lowering due to JT/pJT distortion in general alleviates such constraints. We hence do not consider any symmetry relations between the reduced matrix elements.

Before ending this section, we note that with the spin orbitals ordering convention in Eqn 2.11, SOC matrix elements of the $\hat{z}_{eff,z}^{(1)}\hat{s}_z$ component in the dot product in Eqn 2.10 are in the A block, while those of the $\hat{z}_{eff,x}^{(1)}\hat{s}_x$and $\hat{z}_{eff,y}^{(1)}\hat{s}_y$components are in the B block.

Section 2.3.3 Spatial symmetry of $\widehat{H}_{SO}$

Spatial symmetry means the actual symmetry of the system under consideration. While the system's symmetry is fully represented by a point group, it in general requires us to consider the associated double group in discussing $\widehat{H}_{SO}$, since spin is involved. Here, we show that we only need to consider the point group symmetry in deriving expansion formulas of the matrix elements of $\widehat{H}_{SO}$. The double group symmetry can be left aside.

The two spin functions α and β gain a minus sign under any 2π rotation (labelled as $\hat{R}$), instead of returning to themselves like usual objects do. Only when they are rotated by 4π they return to themselves.[24] The pair of spin functions hence form a new irreducible representation, and correspondingly, the number of symmetry elements is doubled. Any product of $\hat{S}\hat{R}$, with $\hat{S}$ being a symmetry operation of the original point group, is a new symmetry operation. The extended

group is the double group of the original point group. In general, any electronic states with an even number of electrons return to themselves under the action of $\hat{R}$, and those with an odd number of electrons change their signs. The former belong to Boson irreps while the latter belong to Fermion irreps of the relevant double groups.[15]

Resolving $\hat{H}_{SO}$ in a set of electronic states $\{|\Psi_I\rangle\}$, the Hamiltonian becomes

$$\hat{H}_{SO} = |\Psi_I\rangle H_{IJ}^{SO} \langle\Psi_J| \qquad \text{Eqn 2.16}$$

Please recall that Einstein's convention of summing over all duplicate indices in a mathematical expression is followed. Under the symmetry operation $\hat{R}$, the Hamiltonian becomes

$$\hat{R}\hat{H}_{SO}\hat{R}^{-1} = \left|\hat{R}\Psi_I\right\rangle\left(\hat{R}H_{IJ}^{SO}\right)\left\langle\hat{R}\Psi_J\right| = p_I p_J \langle\Psi_I|\left(\hat{R}H_{IJ}^{SO}\right)|\Psi_J\rangle = |\Psi_I\rangle\left(\hat{R}H_{IJ}^{SO}\right)\langle\Psi_J| \qquad \text{Eqn 2.17}$$

p_I and p_J stand for the $+1$ or -1 phases that the Ψ_I and Ψ_J gain under the action of $\hat{R}$. Since $\hat{H}_{SO}$ conserves the number of electrons, Ψ_I and Ψ_J must have the same number of electrons, p_I and p_J must be equal, giving $p_I p_J = 1$ and the last equality in Eqn 2.17. The Hamiltonian belongs to the totally symmetric irrep, which is a Boson irrep. It thus must return to itself under the action of $\hat{R}$. To satisfy this symmetry requirement of $\hat{R}\hat{H}_{SO}\hat{R}^{-1}$, we must have $\hat{R}H_{IJ}^{SO} = H_{IJ}^{SO}$ for the matrix elements, which are in general functions of vibrational coordinates. Therefore, all the matrix elements must belong to Boson irreps, and we only need to consider symmetry operations of normal point groups in deriving expansion formulas for the matrix elements. This conclusion is tenable for the one-electron matrix elements $\langle\psi_i|\hat{h}_{eff}^{1e}|\psi_j\rangle$s, which are special cases of H_{IJ}^{SO}s. With all these understandings of symmetry properties of SOC matrix elements, we commence deriving their expansion formulas.

Section 2.3.4 Modularized approach

The electronic diabatic states that we use to resolve a Hamiltonian operator are always symmetry-adapted, *i.e.*, the bra and ket states in the resolved operator $|\Phi_n^d\rangle H_{el,nm}^d \langle\Phi_m^d|$ transform as irreps of the relevant point group. Consequently, the matrix elements $\{H_{el,nm}^d\}$ need to transform as certain irreps so that the operator is invariant with respect to all symmetry operators. In other words, each $H_{el,nm}^d$, which is a function of vibrational coordinates, needs to feature certain symmetry eigenvalues of a desired irrep. The main part of our work in **Chapter 3** below is to find symmetry eigenvalues of the matrix elements. Different symmetry elements may feature the same set of symmetry eigenvalues.

Once we know the desired symmetry eigenvalues for a matrix element, we need to construct an expansion in vibrational coordinates that has the same set of symmetry eigenvalues. Let's use the simplest example in one dimensional coordinate *x*. If the matrix element $H_{nm}(x)$ needs to be an odd function under an operation that changes *x* to *-x*, then only odd power terms of the polynomial expansion in *x* shall be kept in the expansion formula of the matrix element. If the matrix element needs to be an even function, then only the even terms are kept. Now, if we have another matrix element, which features the same parity as H_{nm}, the same even or odd expansion formula of *x* can be reused. The odd and even expansions in *x*, for which the expansion coefficients are yet to be determined, are **modules**. They are selected based on the symmetry of matrix elements.

The problems have more complicated symmetries and require multidimensional expansions. However, the similar idea of modularized approach applies. A set of expansion formulas in multidimensional vibrational coordinates are prepared to feature all possible symmetry eigenvalues. They are selected based on the desired symmetry eigenvalues of matrix elements.

Section 2.3.5 Root-branch approach

It is not surprising that matrix elements of problems in a higher symmetry need to feature more symmetry eigenvalues than those in a lower symmetry. A simple example is C_{2v} vs. C_2. Matrix elements in C_{2v} symmetry need to feature symmetry eigenvalues of E, C_2, σ_v, and σ_v', while those in C_2 symmetry only need to feature eigenvalues of E and C_2. Here, E means the identity symmetry operator, following the convention of most textbooks. The more symmetry eigenvalues, the more restrictive on the matrix elements' expansions. Actually, expansion formulas for higher symmetry matrix elements can be obtained by imposing constraints on lower symmetry matrix elements, *i.e.*, dropping some terms.

We hence first derived expansion formulas for the lowest symmetry in a class of symmetries. For instance, C_3 is the lowest symmetry in all trigonal symmetries. The expansion formulas for all matrix elements in C_3 symmetry are called **root** formulas. We then impose constraints on the root formulas to obtain expansion formulas for the other, higher trigonal symmetries, C_{3v}, D_3, D_{3d}, *etc*. These higher symmetry expansions are called **branch** formulas.

The modularized approach and the root-branch approach are the two keys that allow us to derive expansion formulas for all problems in a whole class of symmetries within one thesis. How many problems are there in one class of symmetries? Hundreds, or even up to thousands! The importance of the two approaches can never be overemphasized.

In the next chapter, we first present detailed derivation and discussion for the trigonal formalism in **Section 3.1**. Many of the results are transferrable to the tetragonal formalism that is derived in **Section 3.2**. This transferability lays a foundation for future efficient derivation of general n-gonal formalism.

Chapter 3 Derivation and results

Section 3.1 Hamiltonian structures and symmetry eigenvalues for trigonal systems

There are A- and E-type irreps in trigonal symmetries, giving the two types of intra-shell coupling and the $(E + E)$, $(E + A)$, and $(A + A)$ three types of inter-shell coupling. It has been well known that angular momentum operator matrix element between identical real-valued functions is zero due to the purely imaginary nature and hermiticity of the operator. Since the A-type spatial orbitals can always be taken real-valued, the A-type intra-shell SOC is null. We only need to consider the other four types of SOC. The essence of the modularized approach[57,58,59,60] to obtain expansion formulas for Hamiltonian matrix elements is to first derive the symmetry eigenvalues of the matrix elements. Expansions in vibrational coordinates that feature these symmetry eigenvalues are modules. They are selected by matching their eigenvalues with those of the matrix elements. This efficient approach allows us to derive expansion formulas for thousands of non-SO JT/pJT problems in one work.[58] In this section, we set out the first step to identify independent matrix elements in each of the four types of SOC, and also derive their symmetry eigenvalues.

Section 3.1.1 E-Type Hamiltonian

We start with the intra-shell SOC of a set of E-type orbitals. It is the most common type of SOC in trigonal symmetries. There are in total four spin orbitals, $|X\alpha\rangle$, $|Y\alpha\rangle$, $|X\beta\rangle$, and $|Y\beta\rangle$ with the real-valued X and Y spatial orbitals, or those with complex-valued spatial orbitals obtained using the transformation in Eqn 2.2. Our derivation is based on the complex-valued orbitals: $|+\alpha\rangle$, $|-\alpha\rangle$, $|+\beta\rangle$, and $|-\beta\rangle$. $|+\alpha\rangle$ and $|-\beta\rangle$ together transform as $E_{3/2}$-type irreps in any trigonal and tetragonal double groups except S_4^2, while the other two transforms as $E_{1/2}$-type irreps. In the

S_4^2 double group, the former transform as the $E_{1/2}$ irrep, while the latter as the $E_{3/2}$irrep. The SOC matrix of these spinors is shown in Figure 3.1(a). Clearly, it takes the structure in Figure 2.4(b), as the spinors are properly ordered. Henceforth, we just use $\widehat{H}$ to label the one-electron effective SOC operator and H_{ij} to label its matrix elements between spin orbitals. There is only one element in the B block, $H_{+\alpha+\beta}$. For the A block, $H^r_{+\beta+\beta} = -H^r_{+\alpha+\alpha}$ due to WET. Consequently, the four real-valued (denoted by the superscript r) diagonal elements are all connected to $H^r_{+\alpha+\alpha}$. WET also determines $H_{+\beta-\beta} = -H_{+\alpha-\alpha}$. The block structure in Figure 2.4(b) (*i.e.*, time-reversal symmetry) determines $H_{+\beta-\beta} = H_{+\alpha-\alpha}$. The last two equalities together determine $H_{+\alpha-\alpha} = 0$. Therefore, $H^r_{+\alpha+\alpha}$ is the only independent matrix element in the A block.

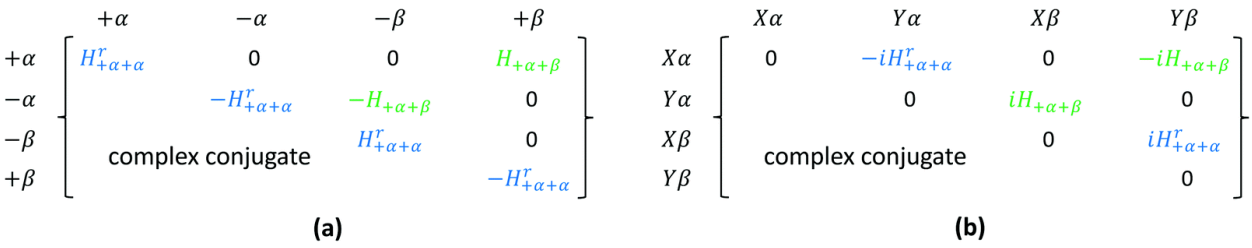

Figure 3.1:Structures of the intra-shell spin–orbit coupling matrices within a set of E-type orbitals in (a) the complex-valued and (b) the real-valued bases. Only the elements in the upper triangle of each matrix are given. The lower triangle is just the complex conjugate of the upper triangle. Matrix elements that are derived from one independent matrix element by time-reversal symmetry and WET are given in the same color.

Expressed using the two independent matrix elements, the intra-shell SO Hamiltonian reads

$$\begin{aligned}\widehat{H} = (|+\alpha\rangle\langle+\alpha| + |-\beta\rangle\langle-\beta| - |-\alpha\rangle\langle-\alpha| - |+\beta\rangle\langle+\beta|)H^r_{+\alpha+\alpha} \\ + (|+\alpha\rangle\langle+\beta| - |-\alpha\rangle\langle-\beta|)H_{+\alpha+\beta} \\ + (|+\beta\rangle\langle+\alpha| - |-\beta\rangle\langle-\alpha|)H^*_{+\alpha+\beta}\end{aligned} \quad \text{Eqn 3.1}$$

We start with the lowest symmetry in the trigonal class, C_3 symmetry. This is the essence of the root-branch approach. There is only one representative symmetry operator in this point group, which is $\hat{C}_3$. With the $\hat{C}_3$-transformations in Eqn 2.2 and Eqn 2.4, we easily obtain the $\hat{C}_3$-transformed Hamiltonian:

$$\begin{aligned}\hat{C}_3\widehat{H}\hat{C}_3^{-1} = (|+\alpha\rangle\langle+\alpha| + |-\beta\rangle\langle-\beta| - |-\alpha\rangle\langle-\alpha| - |+\beta\rangle\langle+\beta|)\hat{C}_3H^r_{+\alpha+\alpha} \\ + (|+\alpha\rangle\langle+\beta| - |-\alpha\rangle\langle-\beta|)e^{-i\frac{2\pi}{3}}\hat{C}_3H_{+\alpha+\beta} \\ + (|+\beta\rangle\langle+\alpha| - |-\beta\rangle\langle-\alpha|)e^{i\frac{2\pi}{3}}\hat{C}_3H^*_{+\alpha+\beta}\end{aligned} \quad \text{Eqn 3.2}$$

In order to let $\hat{C}_3\widehat{H}\hat{C}_3^{-1} = \widehat{H}$, $H^r_{+\alpha+\alpha}$ and $H_{+\alpha+\beta}$ need to be eigenfunctions with $\hat{C}_3$, with eigenvalue $\chi^{C_3} = 1$ and $e^{i\frac{2\pi}{3}}$, respectively.

In C_{3v} symmetry, we need to consider the action of σ_v. The $\hat{\sigma}_v$-transformations in Eqn 2.3 and Eqn 2.6 leads to the $\hat{\sigma}_v$-transformed $\widehat{H}$:

$$\begin{aligned}\hat{\sigma}_v\widehat{H}\hat{\sigma}_v^{-1} = (|+\alpha\rangle\langle+\alpha| + |-\beta\rangle\langle-\beta| - |-\alpha\rangle\langle-\alpha| - |+\beta\rangle\langle+\beta|)\hat{\sigma}_vH^r_{+\alpha+\alpha} \\ + (|+\beta\rangle\langle+\alpha| - |-\beta\rangle\langle-\alpha|)\hat{\sigma}_vH_{+\alpha+\beta} \\ + (|+\alpha\rangle\langle+\beta| - |-\alpha\rangle\langle-\beta|)\hat{\sigma}_vH^*_{+\alpha+\beta}\end{aligned} \quad \text{Eqn 3.3}$$

In order to have the required symmetry for the Hamiltonian, $\hat{\sigma}_v\widehat{H}\hat{\sigma}_v^{-1} = \widehat{H}$, we must have $\hat{\sigma}_vH^r_{+\alpha+\alpha} = H^r_{+\alpha+\alpha}$, and $\hat{\sigma}_vH_{+\alpha+\beta} = H^*_{+\alpha+\beta}$. The two equalities point to the following $\hat{\sigma}_v$-eigenvalues for the real and imaginary parts of the matrix elements: $\left(\chi^{\sigma_v}_{Re}, \chi^{\sigma_v}_{Im}\right) = (1,0)$ and $(1,-1)$ for $H^r_{+\alpha+\alpha}$ and $H_{+\alpha+\beta}$, respectively. $\chi^{\sigma_v}_{Im} = 0$ indicates that the matrix element is real-valued.

A difference between the present work and ref. 55 is noted. We here show that it is unnecessary to transform the spin orbitals to $\hat{\sigma}_v$-eigenstates in deriving symmetry properties of the matrix elements in C_{3v} symmetry. $\hat{\sigma}_v$ converts each ket-bra dyad to its time-reversal counterpart (see the last paragraph in **Section 2.3.1**). According to the general block structure in Figure 2.4(b), the matrix element of a dyad and that of the time-reversal dyad are complex conjugates of each other. Therefore, to have the Hamiltonian invariant with respect to $\hat{\sigma}_v$, it is necessary to have $\hat{\sigma}_v H_{ij} = H_{ij}^*$, and resulting in the requirement of $\left(\chi_{Re}^{\sigma_v}, \chi_{Im}^{\sigma_v}\right) = (1,-1)$. This is the only constraint on the matrix element induced by $\hat{\sigma}_v$. $\left(\chi_{Re}^{\sigma_v}, \chi_{Im}^{\sigma_v}\right) = (1,0)$ is a special case of this general requirement for real-valued matrix elements. This rationale also applies in the derivation for the $(E\ +\ E)$, $(E\ +\ A)$, and $(A\ +\ A)$ inter-shell SOC below. Therefore, it is also unnecessary to construct $\hat{\sigma}_v$-eigenstates in those cases.

In D_3 symmetry, whose point group is isomorphic with C_{3v}, we need to consider the action of $\hat{C}_2^x$ on $\hat{H}$. With the $\hat{C}_2'$-transformations in Eqn 2.3 and Eqn 2.7, we have:

$$\begin{aligned}\hat{C}_2^x \hat{H} (\hat{C}_2^x)^{-1} = {} & (|+\alpha\rangle\langle+\alpha| + |-\beta\rangle\langle-\beta| - |-\alpha\rangle\langle-\alpha| \\ & - |+\beta\rangle\langle+\beta|)\hat{C}_2^x H_{+\alpha+\alpha}^r + (|-\beta\rangle\langle-\alpha| - |+\beta\rangle\langle+\alpha|)\hat{C}_2^x H_{+\alpha+\beta} \\ & + (|-\alpha\rangle\langle-\beta| - |+\alpha\rangle\langle+\beta|)\hat{C}_2^x H_{+\alpha+\beta}^*\end{aligned} \quad \text{Eqn 3.4}$$

In order to have $\hat{C}_2^x \hat{H} (\hat{C}_2^x)^{-1} = \hat{H}$, the matrix elements need to satisfy $\hat{C}_2^x H_{+\alpha+\alpha}^r = H_{+\alpha+\alpha}^r$ and $\hat{C}_2^x H_{+\alpha+\beta} = -H_{+\alpha+\beta}^*$. These equalities point to the following $\hat{C}_2'$-eigenvalues of the matrix elements: $\left(\chi_{Re}^{C_2'}, \chi_{Im}^{C_2'}\right) = (1,0)$ and $(-1,1)$ for $H_{+\alpha+\alpha}^r$ and $H_{+\alpha+\beta}$, respectively. Similarly to $\hat{\sigma}_v$ in C_{3v} symmetry, $\hat{C}_2'$ converts each ket-bra dyad to its time-reversal counterpart (again, the last paragraph in **Section 2.3.1**), but with an extra sign change for the dyads that involve one α and one β spin function, *i.e.*, those whose elements are in the *B* block. Correspondingly, the elements

in the A block must be converted to their complex conjugates by $\hat{C}_2'$, while those in the B block must be converted to the negative of their complex conjugates. These are the only constraints imposed by $\hat{C}_2'$ to the matrix elements. And it is unnecessary to construct $\hat{C}_2'$-eigenstates out of the spin orbitals to obtain the constraints. Similar arguments apply in the derivation for the $(E\ +\ E)$, $(E\ +\ A)$, and $(A\ +\ A)$ inter-shell SOC below.

In C_{3h} symmetry, the E orbitals are addressed by the prime or double-prime, depending on whether they are σ_h-even or -odd. Using p and q to express the generic superscript of prime and double-prime, the SO Hamiltonian reads

$$\begin{aligned}\widehat{H} = (&|+^p\alpha\rangle\langle+^p\alpha| + |-^p\beta\rangle\langle-^p\beta| - |-^p\alpha\rangle\langle-^p\alpha| - |+^p\beta\rangle\langle+^p\beta|)H^r_{+^p\alpha+^p\alpha} \\ &+ (|+^p\alpha\rangle\langle+^p\beta| - |-^p\alpha\rangle\langle-^p\beta|)H_{+^p\alpha+^p\beta} \\ &+ (|+^p\beta\rangle\langle+^p\alpha| - |-^p\beta\rangle\langle-^p\alpha|)H^*_{+^p\alpha+^p\beta}\end{aligned} \qquad \text{Eqn 3.5}$$

The same superscript for the spatial orbitals + and − determines that their phase flipping (if there are) cancel. With the $\hat{\sigma}_h$-transformations of spin functions in Eqn 2.8, we have:

$$\begin{aligned}\hat{\sigma}_h\widehat{H}\hat{\sigma}_h^{-1} = (&|+^p\alpha\rangle\langle+^p\alpha| + |-^p\beta\rangle\langle-^p\beta| - |-^p\alpha\rangle\langle-^p\alpha| \\ &- |+^p\beta\rangle\langle+^p\beta|)\hat{\sigma}_h H^r_{+^p\alpha+^p\alpha} \\ &+ (-|+^p\alpha\rangle\langle+^p\beta| + |-^p\alpha\rangle\langle-^p\beta|)\hat{\sigma}_h H_{+^p\alpha+^p\beta} \\ &+ (-|+^p\beta\rangle\langle+^p\alpha| + |-^p\beta\rangle\langle-^p\alpha|)\hat{\sigma}_h H^*_{+^p\alpha+^p\beta}\end{aligned} \qquad \text{Eqn 3.6}$$

To have $\hat{\sigma}_h\widehat{H}\hat{\sigma}_h^{-1} = \widehat{H}$, we need $\hat{\sigma}_h H^r_{+^p\alpha+^p\alpha} = H^r_{+^p\alpha+^p\alpha}$ and $\hat{\sigma}_h H_{+^p\alpha+^p\beta} = -H_{+^p\alpha+^p\beta}$. The matrix elements need to be σ_h-eigenfunctions with the eigenvalues $\chi^{\sigma_h} = 1$ and -1, respectively. It is interesting to note that even for this intra-shell SOC, the σ_h-eigenvalue of the matrix elements is not always 1, which is the case for the corresponding non-SOC intra-shell (and intra-term too) elements. The reason is related to the different σ_h-eigenvalues of $|\alpha\rangle$ and $|\beta\rangle$ (Eqn 2.8).

$\chi^{C_3} = e^{i\frac{2\pi}{3}}$ and $\chi^{\sigma_h} = -1$ for $H_{+_p\alpha+_p\beta}$ indicates that e''-type (e') modes are SO JT-active (-inactive) in first order expansion. This is because the linear monomial $\rho e^{i\phi}$ of a set of e'' coordinates has the specific χ^{C_3} and χ^{σ_h}, while any functions of e' coordinates must have $\chi^{\sigma_h} = 1$. On the contrary, when SOC is not considered, only e'-type modes are JT active. The JT-activity of e''-type modes is thus a purely relativistic effect. Please note that this relativistic JT-activity is in terms of the original E-type spatial orbitals. If we consider that SOC has split the E-type shell to the two sets of $E_{1/2}$- and $E_{3/2}$-type spinors, the e''-type modes is pJT-active in coupling the non-degenerate spinors (recalling that $|+\alpha\rangle$and $|+\beta\rangle$ transform as $E_{3/2}$- and $E_{1/2}$-type irreps, respectively).

D_{3h} is the composite of D_3 and C_{3h}. Correspondingly, the matrix elements need to adopt all four (three sets of) symmetry eigenvalues, $\left(\chi^{C_3}, \left(\chi^{C_2'}_{Re}, \chi^{C_2'}_{Im}\right), \chi^{\sigma_h}\right)$. Although the D_{3d} point group is isomorphic to D_{3h}, we cannot directly transplant the D_{3h} symmetry eigenvalues to D_{3d}. This is because the spin functions α and β are invariant under $\hat{I}$, but they gain phases under $\hat{\sigma}_h$. Under the action of $\hat{I}$,

$$\begin{aligned}\hat{I}\hat{H}\hat{I}^{-1} = \big(&|+_p\alpha\rangle\langle+_p\alpha| + |-_p\beta\rangle\langle-_p\beta| - |-_p\alpha\rangle\langle-_p\alpha| \\ &- |+_p\beta\rangle\langle+_p\beta|\big)\hat{I}H^r_{+_p\alpha+_p\alpha} \\ &+ \big(|+_p\alpha\rangle\langle+_p\beta| - |-_p\alpha\rangle\langle-_p\beta|\big)\hat{I}H_{+_p\alpha+_p\beta} \\ &+ \big(|+_p\beta\rangle\langle+_p\alpha| - |-_p\beta\rangle\langle-_p\alpha|\big)\hat{I}H^*_{+_p\alpha+_p\beta}\end{aligned} \qquad \text{Eqn 3.7}$$

Certainly, $\chi^I = 1$ for both $H^r_{+_p\alpha+_p\alpha}$ and $H_{+_p\alpha+_p\beta}$. Here, the subscript p has been used to represent the g and u symmetry of the E orbitals.

Our derivation for symmetry eigenvalues of all matrix elements in E-type intra-shell SOC problems in all six trigonal symmetries is finished. The eigenvalues are summarized in the E block

of Table 3.1. As discussed later, these eigenvalues guide us to look up appropriate expansion formulas for the matrix elements.

In **Section 2.3.3**, we show that only point group symmetry operations shall be considered in deriving expansion formulas of the SOC matrix elements. However, while the D_{3h} and D_{3d} point groups are isomorphic, with $\hat{\sigma}_h$ in the former being replaced by $\hat{I}$ in the latter, different symmetry eigenvalues are obtained for the two operators. Specifically, $\chi^{\sigma_h} = -1$ for $H_{+_p\alpha+_p\beta}$, but $\chi^{I} = 1$ for $H_{+_p\alpha+_p\beta}$. This seems inconsistent with our conclusion in **Section 2.3.3**: if only point group symmetries matter, the isomorphism between point groups shall strictly apply, and the matrix elements in isomorphic correspondence shall have the same eigenvalues for the corresponding symmetry elements. A further clarification is necessary.

The isomorphism between the matrix elements of the two point groups is applicable only when the two sets of ket-bra dyads transform as the corresponding irreps. For instance, in the E-type non-SO JT couplings in D_{3h} symmetry, the ket-bra dyad $(|+^p\rangle\langle+^p| + |-^p\rangle\langle-^p|)$ transforms as A_1', $(|+^p\rangle\langle+^p| - |-^p\rangle\langle-^p|)$ as A_2', $|+^p\rangle\langle-^p|$ and $|-^p\rangle\langle+^p|$ together as E'. In the corresponding D_{3d} problem, $(|+_p\rangle\langle+_p| + |-_p\rangle\langle-_p|)$ transforms as A_{1g}, $(|+_p\rangle\langle+_p| - |-_p\rangle\langle-_p|)$ transforms as A_{2g}, $|+_p\rangle\langle-_p|$ and $|-_p\rangle\langle+_p|$ together as E_g. In the isomorphic relation between the two point groups, A_1' corresponds to A_{1g}, A_2' to A_{2g}, and E' to E_g. These correspondences guarantee the isomorphism between the matrix elements of the two sets of dyads.

Now let's consider the dyads of the spin functions. $(|\alpha\rangle\langle\alpha| + |\beta\rangle\langle\beta|)$ transforms as A_1' in D_{3h} and A_{1g} in D_{3d}, $(|\alpha\rangle\langle\alpha| - |\beta\rangle\langle\beta|)$ as A_2' in D_{3h} and A_{2g} in D_{3d}. Good correspondences between the irreps of the two sets of dyads maintain so far. $|\alpha\rangle\langle\beta|$ and $|\beta\rangle\langle\alpha|$, however, transform as E'' in D_{3h} and E_g in D_{3d}. However, E_g corresponds to E', not E''. This inconsistence is carried to the dyads of spin orbitals, which are the direct products of the ket-bra dyads of the spatial orbitals

and the dyads of the spin functions. It is this inconsistence that eliminates the isomorphism between the $H_{+^p\alpha+^p\beta}$ and $H^r_{+_p\alpha+_p\beta}$ elements. The further underlying reason for this inconsistence is that the D^2_{3h} and D^2_{3d} double groups are not isomorphic, although their normal point groups are. The non-isomorphism arises from that the spin functions are invariant under $\hat{I}$ but gain the opposite phases $-i$ and i under $\hat{\sigma}_h$ (Eqn 2.8). The characters of the fundamental Fermion irreps composed of the spin functions are thus different: 2 in D^2_{3d} and 0 in D^2_{3h}. The different character tables of the $D^2_{3h}$and D^2_{3d} double groups can be seen in pages 260–261 in ref. 24. Similar non-trivial differences in symmetry eigenvalues of matrix elements between D_{3h} and D_{3d} symmetries also exist in the $(E\ +\ E)$-type and $(E\ +\ A)$-type inter-shell SOC below. The rationalization here also applies in those cases and is hence not repeated. We only need to consider symmetry operations in normal point groups in deriving symmetry properties of each matrix element. However, this conclusion does not mean the irrelevance of double group symmetry to SOC. Double group symmetry matters for this intrinsically spin-related interaction.

With all these understandings, we come back to the opposite symmetry eigenvalues of $H_{+\alpha+\beta}$ in C_{3v} and D_3: $\left(\chi^{\sigma_v}_{Re}, \chi^{\sigma_v}_{Im}\right) = (1,-1)$in the former and $(-1,1)$ in the latter. However, the C^2_{3v} and D^2_{3h} double groups are isomorphic and the spin ket-bra dyads transform as corresponding irreps in the two symmetries. Such an inconsistence should not occur. The inconsistence arises from the different transformations of the spin functions with respect to $\hat{\sigma}_v$ and $\hat{C}'_2$ (Eqn 2.6 *vs*. Eqn 2.7). And this difference can be removed. Replacing β by $-i\beta$, *i.e.*, rotating β by $-\pi$ about the C_3 axis and using the resultant spin function as the spin-down basis, the C'_2-transformation matrix is identical to the σ_v matrix in Eqn 2.6. Consequently, with such a new β, $H_{+\alpha+\beta}$ in D_3 has the same $\left(\chi^{\sigma_v}_{Re}, \chi^{\sigma_v}_{Im}\right) = (1,-1)$ as in C_{3v} symmetry. This phase multiplication of β does not change the $|\beta\rangle\langle\beta|$ dyad, as the phases in the bra and ket cancel. The symmetry eigenvalues of $H^r_{+\beta+\beta}$

(equivalently $H^r_{+\alpha+\alpha}$) are hence not affected by the phase, and the equivalence between the symmetry eigenvalues of $H^r_{+\alpha+\alpha}$in the two symmetries is maintained. Overall, the isomorphism of the SOC operators in C_{3v} and D_3 symmetries is regained with such a $-i$ phase multiplication of β. In short, the difference in the symmetry eigenvalues of $H_{+\alpha+\beta}$ in C_{3v} and D_3 symmetries is trivial and can be eliminated by a phase adjustment to the spin basis. Similar trivial differences in symmetry eigenvalues between C_{3v} and D_3 also exist in the $(E + E)$- and $(E + A)$-type SOC below. The rationalization will not be repeated.

Table 3.1:The eigenvalues of symmetry operators of the independent elements in trigonal and tetragonal vibronic Hamiltonian matrices. The σ_v- and C_2-eigenvalues are given for the real and imaginary parts of the matrix elements separately. The heading $(E + E)$ means the matrix elements underneath are relevant to the $(E + E)$ problems, *etc*. k and l stand for the 1 and 2 subscripts when σ_v or C_2' are relevant. p and q stand for the $'$ and $''$ superscripts when σ_h is relevant. Although p and q are placed as superscripts, they also stand for possible g and u subscripts when I is relevant.

		$\chi^{C_3\,a}$	$\chi^{C_4\,b}$	χ^{S_4}	$(\chi_{Re}^{\sigma_v}, \chi_{Im}^{\sigma_v})^{c}$	$\left(\chi_{Re}^{C_2'}, \chi_{Im}^{C_2'}\right)^{d}$	$\chi^{\sigma_h\,e}$	$\chi^{I\,f}$
E	$H^{r}_{+\alpha+\alpha}$	1	1	1	$(1,0)$	$(1,0)$	1	1
	$H_{+\alpha+\beta}$	$e^{i\frac{2\pi}{3}}$	i	$-i$	$(1,-1)$	$(-1,1)$	-1	1
$(E+E)^g$	$H_{+^p\alpha+^q\alpha}$	1	1	1	$\begin{pmatrix} \\ 1,-1 \\ \\ \end{pmatrix}$	$\begin{pmatrix} 1,-1 \end{pmatrix}$	$\begin{pmatrix} (-1)^{\delta_{pq}+1} \end{pmatrix}$	$\begin{pmatrix} \\ (-1)^{\delta_{pq}+1} \\ \\ \end{pmatrix}$
	$H_{+^p\alpha-^q\alpha}$	$e^{-i\frac{2\pi}{3}}$	-1	-1				
	$H_{+^p\alpha-^q\beta}$	1	$-i$	i		$\begin{pmatrix} \\ -1,1 \\ \\ \end{pmatrix}$	$\begin{pmatrix} \\ (-1)^{\delta_{pq}} \\ \\ \end{pmatrix}$	
	$H_{+^p\alpha+^q\beta}$	$e^{i\frac{2\pi}{3}}$	i	$-i$				
	$H_{-^p\alpha-^q\beta}$	$e^{i\frac{2\pi}{3}}$	i	$-i$				
	$H_{-^p\alpha+^q\beta}$	$e^{-i\frac{2\pi}{3}}$	$-i$	i				
$(E+A)^g$	$H_{+^p\alpha A_k^q\alpha}$	$e^{i\frac{2\pi}{3}}$	i	i	$\begin{pmatrix} \\ (-1)^{\delta_{k2}}, (-1)^{\delta_{k1}} \\ \\ \end{pmatrix}$	$\begin{pmatrix} (-1)^{\delta_{k2}}, (-1)^{\delta_{k1}} \\ (-1)^{\delta_{k1}}, (-1)^{\delta_{k2}} \end{pmatrix}$	$\begin{pmatrix} (-1)^{\delta_{pq}+1} \\ (-1)^{\delta_{pq}} \end{pmatrix}$	$\begin{pmatrix} \\ (-1)^{\delta_{pq}+1} \\ \\ \end{pmatrix}$
	$H_{+^p\alpha A_k^q\beta}$	$e^{-i\frac{2\pi}{3}}$	-1	1				
	$H_{-^p\alpha A_k^q\beta}$	1	1	-1				
$(A+A)^g$	$H^{i}_{A_k^p\alpha A_l^q\alpha}$	1	1	1	$\left(0,(-1)^{\delta_{kl}+1}\right)$	$\left(0,(-1)^{\delta_{kl}+1}\right)$	$(-1)^{\delta_{pq}+1}$	$\begin{pmatrix} \\ (-1)^{\delta_{pq}+1} \\ \\ \end{pmatrix}$
	$H_{A_k^p\alpha A_l^q\beta}$	$e^{i\frac{2\pi}{3}}$	i	$-i$	$\left((-1)^{\delta_{kl}+1}, (-1)^{\delta_{kl}}\right)$	$\left((-1)^{\delta_{kl}}, (-1)^{\delta_{kl}+1}\right)$	$(-1)^{\delta_{pq}}$	
$(E+B)^g$	$H_{+^p\alpha B_k^q\alpha}$		$-i$	$-i$	$\begin{pmatrix} \\ (-1)^{\delta_{k2}}, (-1)^{\delta_{k1}} \\ \\ \end{pmatrix}$	$\begin{pmatrix} (-1)^{\delta_{k2}}, (-1)^{\delta_{k1}} \\ (-1)^{\delta_{k1}}, (-1)^{\delta_{k2}} \end{pmatrix}$	$\begin{pmatrix} (-1)^{\delta_{pq}+1} \\ (-1)^{\delta_{pq}} \end{pmatrix}$	$\begin{pmatrix} \\ (-1)^{\delta_{pq}+1} \\ \\ \end{pmatrix}$
	$H_{+^p\alpha B_k^q\beta}$		1	-1				
	$H_{-^p\alpha B_k^q\beta}$		-1	1				
$(B+B)^g$	$H^{i}_{B_k^p\alpha B_l^q\alpha}$		1	1	$\left(0,(-1)^{\delta_{kl}+1}\right)$	$\left(0,(-1)^{\delta_{kl}+1}\right)$	$(-1)^{\delta_{pq}+1}$	$\begin{pmatrix} \\ (-1)^{\delta_{pq}+1} \\ \\ \end{pmatrix}$
	$H_{B_k^p\alpha B_l^q\beta}$		i	$-i$	$\left((-1)^{\delta_{kl}+1}, (-1)^{\delta_{kl}}\right)$	$\left((-1)^{\delta_{kl}}, (-1)^{\delta_{kl}+1}\right)$	$(-1)^{\delta_{pq}}$	
$(A+B)^g$	$H^{i}_{A_k^p\alpha B_l^q\alpha}$		-1	-1	$\left(0,(-1)^{\delta_{kl}+1}\right)$	$\left(0,(-1)^{\delta_{kl}+1}\right)$	$(-1)^{\delta_{pq}+1}$	$\begin{pmatrix} \\ (-1)^{\delta_{pq}+1} \\ \\ \end{pmatrix}$
	$H_{A_k^p\alpha B_l^q\beta}$		$-i$	i	$\left((-1)^{\delta_{kl}+1}, (-1)^{\delta_{kl}}\right)$	$\left((-1)^{\delta_{kl}}, (-1)^{\delta_{kl}+1}\right)$	$(-1)^{\delta_{pq}}$	

[a] Applicable for trigonal symmetries. [b] Applicable for tetragonal symmetries except S_4. [c] Applicable for C_{3v} and C_{4v} problems. $\chi_{Im}^{\sigma_v} = 0$ $(\chi_{Re}^{\sigma_v} = 0)$ means only the real (imaginary) part of the expansion formula is taken. [d] Applicable for D_3, D_{3h}, D_{3d}, D_4, D_{2d}, and D_{4h} problems. $\chi_{Im}^{C_2'} = 0$ $(\chi_{Re}^{C_2'} = 0)$ means only the real (imaginary) part of the expansion is taken. [e] Applicable for C_{3h} and D_{3h} problems. [f] Applicable for D_{3d}, C_{4h}, and D_{4h} problems. [g] The superscripts p and q represent the prime and double-prime in C_{3h} and D_{3h} symmetries. They also represent the g and u subscripts in D_{3d}, C_{4h}, and D_{4h} symmetries. For $(A + A)$-, $(E + E)$-, and $(B + B)$-type (only applicable for tetragonal symmetries) problems in C_3, C_{3v}, D_3, C_4, S_4, C_{4v}, D_4, and D_{2d} symmetries, they simply differentiate the two sets of orbitals that transform as the same irrep.

Section 3.1.2 ($E + E$)-Type Hamiltonian

This type of inter-shell SOC can be seen in many transition metal compounds. For instance, the d_{xz} and d_{yz} orbitals of the central metal form one set of E-type orbitals, and the $d_{x^2-y^2}$ and d_{xy} orbitals form another set. Superscripts p and q are used to differentiate the two sets. They also label the $'$ and $''$ σ_h-parities of the orbitals in D_{3h} symmetry, as well as the g and u I-parities in D_{3d} symmetry. The inter-shell SOC matrix takes the structure shown in Figure 3.2(a), which is consistent with the one shown in Figure 2.4(b), since the eight spinors are properly ordered. WET determines $H_{+^p\beta+^q\beta} = -H_{+^p\alpha+^q\alpha}$ and $H_{+^p\beta-^q\beta} = -H_{+^p\alpha-^q\alpha}$. Time-reversal symmetry determines $H_{+^p\beta-^q\beta} = H^*_{-^p\alpha+^q\alpha}$ and $H_{+^p\beta+^q\beta} = H^*_{-^p\alpha-^q\alpha}$. These four equalities together lead to $H_{-^p\alpha-^q\alpha} = -H^*_{+^p\alpha+^q\alpha}$ and $H_{-^p\alpha+^q\alpha} = -H^*_{+^p\alpha-^q\alpha}$. Therefore, only two independent elements remain in the A block and they are colored in blue and green in Figure 3.2(a). As discussed in **Section 2.3.2**, WET cannot be used to reduce the number of independent elements in the B block. There are hence in total six independent matrix elements.

(a)

	$+^p\alpha$	$-^p\alpha$	$+^q\alpha$	$-^q\alpha$	$-^p\beta$	$+^p\beta$	$-^q\beta$	$+^q\beta$
$+^p\alpha$	E_I intra-shell SOC		$H_{+^p\alpha+^q\alpha}$	$H_{+^p\alpha-^q\alpha}$	E_I intra-shell SOC		$H_{+^p\alpha-^q\beta}$	$H_{+^p\alpha+^q\beta}$
$-^p\alpha$			$-H^*_{+^p\alpha-^q\alpha}$	$-H^*_{+^p\alpha+^q\alpha}$			$H_{-^p\alpha-^q\beta}$	$H_{-^p\alpha+^q\beta}$
$+^q\alpha$			E_{II} intra-shell SOC		$-H_{+^p\alpha-^q\beta}$	$-H_{-^p\alpha-^q\beta}$	E_{II} intra-shell SOC	
$-^q\alpha$					$-H_{+^p\alpha+^q\beta}$	$-H_{-^p\alpha+^q\beta}$		
$-^p\beta$					E_I intra-shell SOC		$H^*_{+^p\alpha+^q\alpha}$	$H^*_{+^p\alpha-^q\alpha}$
$+^p\beta$							$-H_{+^p\alpha-^q\alpha}$	$-H_{+^p\alpha+^q\alpha}$
$-^q\beta$	complex conjugate						E_{II} intra-shell SOC	
$+^q\beta$								

(b)

	$X^q\alpha$	$Y^q\alpha$
$X^p\alpha$	$iIm(H_{+^p\alpha+^q\alpha}) + iIm(H_{+^p\alpha-^q\alpha})$	$-iRe(H_{+^p\alpha+^q\alpha}) + iRe(H_{+^p\alpha-^q\alpha})$
$Y^p\alpha$	$iRe(H_{+^p\alpha+^q\alpha}) + iRe(H_{+^p\alpha-^q\alpha})$	$iIm(H_{+^p\alpha+^q\alpha}) - iIm(H_{+^p\alpha-^q\alpha})$

(c)

	$X^q\beta$	$Y^q\beta$
$X^p\beta$	$-iIm(H_{+^p\alpha+^q\alpha}) - iIm(H_{+^p\alpha-^q\alpha})$	$iRe(H_{+^p\alpha+^q\alpha}) - iRe(H_{+^p\alpha-^q\alpha})$
$Y^p\beta$	$-iRe(H_{+^p\alpha+^q\alpha}) - iRe(H_{+^p\alpha-^q\alpha})$	$-iIm(H_{+^p\alpha+^q\alpha}) + iIm(H_{+^p\alpha-^q\alpha})$

(d)

	$X^q\beta$	$Y^q\beta$
$X^p\alpha$	$\frac{1}{2}(H_{+^p\alpha+^q\beta} + H_{-^p\alpha-^q\beta} + H_{+^p\alpha-^q\beta} + H_{-^p\alpha+^q\beta})$	$\frac{i}{2}(-H_{+^p\alpha+^q\beta} + H_{-^p\alpha-^q\beta} + H_{+^p\alpha-^q\beta} - H_{-^p\alpha+^q\beta})$
$Y^p\alpha$	$\frac{i}{2}(H_{+^p\alpha+^q\beta} - H_{-^p\alpha-^q\beta} + H_{+^p\alpha-^q\beta} - H_{-^p\alpha+^q\beta})$	$\frac{1}{2}(H_{+^p\alpha+^q\beta} + H_{-^p\alpha-^q\beta} - H_{+^p\alpha-^q\beta} - H_{-^p\alpha+^q\beta})$

(e)

	$X^p\beta$	$Y^p\beta$
$X^q\alpha$	$-\frac{1}{2}(H_{+^p\alpha+^q\beta} + H_{-^p\alpha-^q\beta} + H_{+^p\alpha-^q\beta} + H_{-^p\alpha+^q\beta})$	$-\frac{i}{2}(H_{+^p\alpha+^q\beta} - H_{-^p\alpha-^q\beta} + H_{+^p\alpha-^q\beta} - H_{-^p\alpha+^q\beta})$
$Y^q\alpha$	$-\frac{i}{2}(-H_{+^p\alpha+^q\beta} + H_{-^p\alpha-^q\beta} + H_{+^p\alpha-^q\beta} - H_{-^p\alpha+^q\beta})$	$-\frac{1}{2}(H_{+^p\alpha+^q\beta} + H_{-^p\alpha-^q\beta} - H_{+^p\alpha-^q\beta} - H_{-^p\alpha+^q\beta})$

Figure 3.2: (a) Structure of the inter-shell spin–orbit coupling matrix between two sets of E-type orbitals in the complex-valued bases. Only the inter-shell elements in the upper triangle of the matrix are given. The lower triangle is just the complex conjugate of the upper triangle. Matrix elements that are derived from one independent matrix element by time-reversal symmetry and WET are given in the same color. The blocks of the E-type intra-shell SOC matrix elements are indicated by text and they take the same structure as in Figure 3.1(a). Given in (b–d) are the blocks of the inter-shell SOC matrix in the real-valued bases. (b and c) are complex conjugates of each other. (d and e) are the negative of the transpose of each other.

With the six independent matrix elements shown in Figure 3.2(a), the inter-shell Hamiltonian reads

$$\begin{aligned}\widehat{H} = {} & (|+^{p}\alpha\rangle\langle+^{q}\alpha| - |+^{p}\beta\rangle\langle+^{q}\beta| + |-^{q}\beta\rangle\langle-^{p}\beta| - |-^{q}\alpha\rangle\langle-^{p}\alpha|)H_{+^{p}\alpha+^{q}\alpha} \\ & + h.c. + (|+^{p}\alpha\rangle\langle-^{q}\alpha| - |+^{p}\beta\rangle\langle-^{q}\beta| + |+^{q}\beta\rangle\langle-^{p}\beta| \\ & - |+^{q}\alpha\rangle\langle-^{p}\alpha|)\, H_{+^{p}\alpha-^{q}\alpha} \\ & + h.c. + (|+^{p}\alpha\rangle\langle-^{q}\beta| - |+^{q}\alpha\rangle\langle-^{p}\beta|)H_{+^{p}\alpha-^{q}\beta} \\ & + h.c. + (|+^{p}\alpha\rangle\langle+^{q}\beta| - |-^{q}\alpha\rangle\langle-^{p}\beta|)H_{+^{p}\alpha+^{q}\beta} \\ & + h.c. + (|-^{p}\alpha\rangle\langle-^{q}\beta| - |+^{q}\alpha\rangle\langle+^{p}\beta|)H_{-^{p}\alpha-^{q}\beta} \\ & + h.c. + (|-^{p}\alpha\rangle\langle+^{q}\beta| - |-^{q}\alpha\rangle\langle+^{p}\beta|)H_{-^{p}\alpha+^{q}\beta} + h.c.\end{aligned} \qquad \text{Eqn 3.8}$$

Here, each $h.c.$ stands for the hermitian conjugate of the operator component in front of it. $\hat{C}_3$ transforms the Hamiltonian as

$$\begin{aligned}\hat{C}_3\widehat{H}\hat{C}_3^{-1} = {} & (|+^{p}\alpha\rangle\langle+^{q}\alpha| - |+^{p}\beta\rangle\langle+^{q}\beta| + |-^{q}\beta\rangle\langle-^{p}\beta| \\ & - |-^{q}\alpha\rangle\langle-^{p}\alpha|)\hat{C}_3 H_{+^{p}\alpha+^{q}\alpha} \\ & + h.c. + e^{i\frac{2\pi}{3}}(|+^{p}\alpha\rangle\langle-^{q}\alpha| - |+^{p}\beta\rangle\langle-^{q}\beta| + |+^{q}\beta\rangle\langle-^{p}\beta| \\ & - |+^{q}\alpha\rangle\langle-^{p}\alpha|)\hat{C}_3 H_{+^{p}\alpha-^{q}\alpha} + h.c \\ & + (|+^{p}\alpha\rangle\langle-^{q}\beta| - |+^{q}\alpha\rangle\langle-^{p}\beta|)\hat{C}_3 H_{+^{p}\alpha-^{q}\beta} \\ & + h.c. + e^{-i\frac{2\pi}{3}}(|+^{p}\alpha\rangle\langle+^{q}\beta| - |-^{q}\alpha\rangle\langle-^{p}\beta|)\hat{C}_3 H_{+^{p}\alpha+^{q}\beta} \\ & + h.c. + e^{-i\frac{2\pi}{3}}(|-^{p}\alpha\rangle\langle-^{q}\beta| - |+^{q}\alpha\rangle\langle+^{p}\beta|)\hat{C}_3 H_{-^{p}\alpha-^{q}\beta} \\ & + h.c. + e^{i\frac{2\pi}{3}}(|-^{p}\alpha\rangle\langle+^{q}\beta| - |-^{q}\alpha\rangle\langle+^{p}\beta|)\hat{C}_3 H_{-^{p}\alpha+^{q}\beta} \\ & + h.c.\end{aligned} \qquad \text{Eqn 3.9}$$

Clearly, the C_3-eigenvalues of the six matrix elements are: $\chi^{C_3} = 1$ for $H_{+^p\alpha+^q\alpha}$ and $H_{+^p\alpha-^q\beta}$; $\chi^{C_3} = e^{-i\frac{2\pi}{3}}$ for $H_{+^p\alpha-^q\alpha}$ and $H_{-^p\alpha+^q\beta}$; $\chi^{C_3} = e^{i\frac{2\pi}{3}}$ for $H_{+^p\alpha+^q\beta}$ and $H_{-^p\alpha-^q\beta}$, so that $\hat{C}_3\hat{H}\hat{C}_3^{-1} = \hat{H}$.

In C_{3v} symmetry, under the action of $\hat{\sigma}_v$,

$$\begin{aligned}\hat{\sigma}_v\hat{H}\hat{\sigma}_v^{-1} = (&|-^p\beta\rangle\langle-^q\beta| - |-^p\alpha\rangle\langle-^q\alpha| + |+^q\alpha\rangle\langle+^p\alpha| \\ &- |+^q\beta\rangle\langle+^p\beta|)\hat{\sigma}_v H_{+^p\alpha+^q\alpha} \\ &+ h.c. + (|-^p\beta\rangle\langle+^q\beta| - |-^p\alpha\rangle\langle+^q\alpha| + |-^q\alpha\rangle\langle+^p\alpha| \\ &- |-^q\beta\rangle\langle+^p\beta|)\hat{\sigma}_v\, H_{+^p\alpha-^q\alpha} \\ &+ h.c. + (-|-^p\beta\rangle\langle+^q\alpha| + |-^q\beta\rangle\langle+^p\alpha|)\hat{\sigma}_v H_{+^p\alpha-^q\beta} \\ &+ h.c. + (-|-^p\beta\rangle\langle-^q\alpha| + |+^q\beta\rangle\langle+^p\alpha|)\hat{\sigma}_v H_{+^p\alpha+^q\beta} \\ &+ h.c. + (-|+^p\beta\rangle\langle+^q\alpha| - |-^q\beta\rangle\langle-^p\alpha|)\hat{\sigma}_v H_{-^p\alpha-^q\beta} \\ &+ h.c. + (-|+^p\beta\rangle\langle-^q\alpha| - |+^q\beta\rangle\langle-^p\alpha|)\hat{\sigma}_v H_{-^p\alpha+^q\beta} + h.c.\end{aligned} \qquad \text{Eqn 3.10}$$

Evidently, to have $\hat{\sigma}_v\hat{H}\hat{\sigma}_v^{-1} = \hat{H}$, we need $\hat{\sigma}_v H_{+^p\alpha+^q\alpha} = H^*_{+^p\alpha+^q\alpha}$; $\hat{\sigma}_v\, H_{+^p\alpha-^q\alpha} = H^*_{+^p\alpha-^q\alpha}$; $\hat{\sigma}_v H_{+^p\alpha-^q\beta} = H^*_{+^p\alpha-^q\beta}$; $\hat{\sigma}_v H_{+^p\alpha+^q\beta} = H^*_{+^p\alpha+^q\beta}$; $\hat{\sigma}_v H_{-^p\alpha-^q\beta} = H^*_{-^p\alpha-^q\beta}$; $\hat{\sigma}_v H_{-^p\alpha+^q\beta} = H^*_{-^p\alpha+^q\beta}$*. Therefore, all six independent matrix elements have $\left(\chi^{\sigma_v}_{Re}, \chi^{\sigma_v}_{Im}\right) = (1, -1)$.

In D_3 symmetry, under the action of $\hat{C}_2^x$,

$$\begin{aligned}\hat{C}_2^x\hat{H}(\hat{C}_2^x)^{-1} = {} & (|-^p\beta\rangle\langle-^q\beta| - |-^p\alpha\rangle\langle-^q\alpha| + |+^q\alpha\rangle\langle+^p\alpha| \\ & - |+^q\beta\rangle\langle+^p\beta|)\hat{C}_2^x H_{+^p\alpha+^q\alpha} \\ & + h.c. + (|-^p\beta\rangle\langle+^q\beta| - |-^p\alpha\rangle\langle+^q\alpha| + |-^q\alpha\rangle\langle+^p\alpha| \\ & - |-^q\beta\rangle\langle+^p\beta|)\hat{C}_2^x\, H_{+^p\alpha-^q\alpha} \\ & + h.c. + (|-^p\beta\rangle\langle+^q\alpha| + |-^q\beta\rangle\langle+^p\alpha|)\hat{C}_2^x H_{+^p\alpha-^q\beta} \\ & + h.c. + (|-^p\beta\rangle\langle-^q\alpha| + |+^q\beta\rangle\langle+^p\alpha|)\hat{C}_2^x H_{+^p\alpha+^q\beta} \\ & + h.c. + (|+^p\beta\rangle\langle+^q\alpha| - |-^q\beta\rangle\langle-^p\alpha|)\hat{C}_2^x H_{-^p\alpha-^q\beta} \\ & + h.c. + (|+^p\beta\rangle\langle-^q\alpha| - |+^q\beta\rangle\langle-^p\alpha|)\hat{C}_2^x H_{-^p\alpha+^q\beta} + h.c.\end{aligned}$$

Eqn 3.11

To have $\hat{C}_2^x\hat{H}(\hat{C}_2^x)^{-1} = \hat{H}$, we need $\hat{C}_2^x H_{+^p\alpha+^q\alpha} = H^*_{+^p\alpha+^q\alpha}$; $\hat{C}_2^x\, H_{+^p\alpha-^q\alpha} = H^*_{+^p\alpha-^q\alpha}$; $\hat{C}_2^x H_{+^p\alpha-^q\beta} = -H^*_{+^p\alpha-^q\beta}$; $\hat{C}_2^x H_{+^p\alpha+^q\beta} = -H^*_{+^p\alpha+^q\beta}$; $\hat{C}_2^x H_{-^p\alpha-^q\beta} = -H^*_{-^p\alpha-^q\beta}$; $\hat{C}_2^x H_{-^p\alpha+^q\beta} = -H^*_{-^p\alpha+^q\beta}$*. Therefore, $\left(\chi^{C_2'}_{Re}, \chi^{C_2'}_{Im}\right) = (1,-1)$ for $H_{+^p\alpha+^q\alpha}$ and $H_{+^p\alpha-^q\alpha}$, $(-1,1)$ for $H_{+^p\alpha-^q\beta}$, $H_{+^p\alpha+^q\beta}$, $H_{-^p\alpha-^q\beta}$ and $H_{-^p\alpha+^q\beta}$.

In the C_{3h} symmetry, the spatial orbitals are addressed by the prime and double-prime, which are symbolically represented by the superscripts p and q. Under the action of $\hat{\sigma}_h$,

$$
\begin{aligned}
\hat{\sigma}_h \hat{H} \hat{\sigma}_h^{-1} = (-1)^{\delta_{pq}+1}(&|+^p\alpha\rangle\langle+^q\alpha| - |+^p\beta\rangle\langle+^q\beta| + |-^q\beta\rangle\langle-^p\beta| \\
&- |-^q\alpha\rangle\langle-^p\alpha|)\hat{\sigma}_h H_{+^p\alpha+^q\alpha} \\
&+ h.c. + (-1)^{\delta_{pq}+1}(|+^p\alpha\rangle\langle-^q\alpha| - |+^p\beta\rangle\langle-^q\beta| \\
&+ |+^q\beta\rangle\langle-^p\beta| - |+^q\alpha\rangle\langle-^p\alpha|)\hat{\sigma}_h H_{+^p\alpha-^q\alpha} \\
&+ h.c. + (-1)^{\delta_{pq}}(|+^p\alpha\rangle\langle-^q\beta| - |+^q\alpha\rangle\langle-^p\beta|)\hat{\sigma}_h H_{+^p\alpha-^q\beta} \\
&+ h.c. + (-1)^{\delta_{pq}}(|+^p\alpha\rangle\langle+^q\beta| - |-^q\alpha\rangle\langle-^p\beta|)\hat{\sigma}_h H_{+^p\alpha+^q\beta} \\
&+ h.c. + (-1)^{\delta_{pq}}(|-^p\alpha\rangle\langle-^q\beta| - |+^q\alpha\rangle\langle+^p\beta|)\hat{\sigma}_h H_{-^p\alpha-^q\beta} \\
&+ h.c. + (-1)^{\delta_{pq}}(|-^p\alpha\rangle\langle+^q\beta| - |-^q\alpha\rangle\langle+^p\beta|)\hat{\sigma}_h H_{-^p\alpha+^q\beta} \\
&+ h.c.
\end{aligned}
\qquad \text{Eqn 3.12}
$$

The $(-1)^{\delta_{pq}+1}$ factor with the symbolic Kronecker delta arises from the product of the two E sets' $\hat{\sigma}_h$-parities. This factor becomes $(-1)^{\delta_{pq}}$ when the spin orbitals are different in bra and ket. Clearly, $\chi^{\sigma_h} = (-1)^{\sigma_{pq}+1}$ for $H_{+^p\alpha+^q\alpha}$ and $H_{+^p\alpha-^q\alpha}$ and $(-1)^{\delta_{pq}}$ for $H_{+^p\alpha-^q\beta}$, $H_{+^p\alpha+^q\beta}$, $H_{-^p\alpha-^q\beta}$, and $H_{-^p\alpha+^q\beta}$, to give a $\hat{\sigma}_h$-invariant Hamiltonian.

The matrix elements in D_{3h} symmetry must have all four symmetry eigenvalues, $\left(\chi^{C_3}, \left(\chi_{Re}^{C_2'}, \chi_{Im}^{C_2'}\right), \chi^{\sigma_h}\right)$. In D_{3d} symmetry, the orbitals are dressed by the g and u subscripts. The I-parities are still symbolically represented by the p and q superscripts, just for convenience, so that we can still use the Hamiltonian in Eqn 3.7 in the following derivation. Under the action of $\hat{I}$,

$$
\begin{aligned}
\hat{I}\hat{H}\hat{I}^{-1} = (-1)^{\delta_{pq}+1}&(|+^p\alpha\rangle\langle+^q\alpha| - |+^p\beta\rangle\langle+^q\beta| + |-^q\beta\rangle\langle-^p\beta| \\
&- |-^q\alpha\rangle\langle-^p\alpha|)\hat{I}H_{+^p\alpha+^q\alpha} \\
&+ h.c. + (-1)^{\delta_{pq}+1}(|+^p\alpha\rangle\langle-^q\alpha| - |+^p\beta\rangle\langle-^q\beta| \\
&+ |+^q\beta\rangle\langle-^p\beta| - |+^q\alpha\rangle\langle-^p\alpha|)\hat{I}H_{+^p\alpha-^q\alpha} \\
&+ h.c. + (-1)^{\delta_{pq}+1}(|+^p\alpha\rangle\langle-^q\beta| - |+^q\alpha\rangle\langle-^p\beta|)\hat{I}H_{+^p\alpha-^q\beta} \\
&+ h.c. + (-1)^{\delta_{pq}+1}(|+^p\alpha\rangle\langle+^q\beta| - |-^q\alpha\rangle\langle-^p\beta|)\hat{I}H_{+^p\alpha+^q\beta} \\
&+ h.c. + (-1)^{\delta_{pq}+1}(|-^p\alpha\rangle\langle-^q\beta| - |+^q\alpha\rangle\langle+^p\beta|)\hat{I}H_{-^p\alpha-^q\beta} \\
&+ h.c. + (-1)^{\delta_{pq}+1}(|-^p\alpha\rangle\langle+^q\beta| - |-^q\alpha\rangle\langle+^p\beta|)\hat{I}H_{-^p\alpha+^q\beta} \\
&+ h.c.
\end{aligned}
\qquad \text{Eqn 3.13}
$$

Evidently, only when $\chi^I = (-1)^{\delta_{pq}+1}$ for all the six matrix elements, the Hamiltonian is $\hat{I}$-invariant. All symmetry eigenvalues of the $(E + E)$-type SOC matrix elements have been derived and they are summarized in the $(E + E)$ block in Table 3.1.

Section 3.1.3 ($A + E$)-Type Hamiltonian

This is also a common type of inter-shell SOC in trigonal systems.[49] For instance, it can occur in transition metal compounds with E-type orbitals of d_{xz} and d_{yz} character and an A-type orbital of d_{z^2} character. Or similarly, but in main group compounds, between E-type orbitals of p_x and p_y character and an A-type orbital of p_z character.[54,55] $|A\alpha\rangle$ and $|A\beta\rangle$ transform as $E_{1/2}$-type irreps in any trigonal and tetragonal double groups except S_4^2. In the S_4^2 double group, they transform as the $E_{3/2}$ irrep. The SOC matrix in the complex-valued bases adopts the structure in Figure 3.3(a), which is consistent with the structure in Figure 2.4(b). WET determines $H_{+\beta A\beta} = -H_{+\alpha A\alpha}$. The time-reversal symmetry determines $H_{+\beta A\beta} = H^*_{-\alpha A\alpha}$. They together lead to

$H_{-\alpha A\alpha} = -H^*_{+\alpha A\alpha}$. There is thus only one independent matrix element in the *A* block of the SOC matrix, and three in the whole matrix.

Expressed using the three independent matrix elements in Figure 3.3(a), the Hamiltonian reads

$$\begin{aligned}\widehat{H} = (|+\alpha\rangle\langle A\alpha| - |A\alpha\rangle\langle -\alpha| + |A\beta\rangle\langle -\beta| - |+\beta\rangle\langle A\beta|)H_{+\alpha A\alpha} \\ + h.c. + (|+\alpha\rangle\langle A\beta| - |A\alpha\rangle\langle -\beta|)H_{+\alpha A\beta} \\ + h.c. + (|-\alpha\rangle\langle A\beta| - |A\alpha\rangle\langle +\beta|)H_{-\alpha A\beta} + h.c.\end{aligned} \quad \text{Eqn 3.14}$$

Under $\hat{C}_3$,

$$\begin{aligned}\hat{C}_3\widehat{H}\hat{C}_3^{-1} = e^{-i\frac{2\pi}{3}}(|+\alpha\rangle\langle A\alpha| - |A\alpha\rangle\langle -\alpha| + |A\beta\rangle\langle -\beta| \\ - |+\beta\rangle\langle A\beta|)\hat{C}_3H_{+\alpha A\alpha} + h.c \\ + e^{i\frac{2\pi}{3}}(|+\alpha\rangle\langle A\beta| - |A\alpha\rangle\langle -\beta|)\hat{C}_3H_{+\alpha A\beta} \\ + h.c. + (|-\alpha\rangle\langle A\beta| - |A\alpha\rangle\langle +\beta|)\hat{C}_3H_{-\alpha A\beta} + h.c.\end{aligned} \quad \text{Eqn 3.15}$$

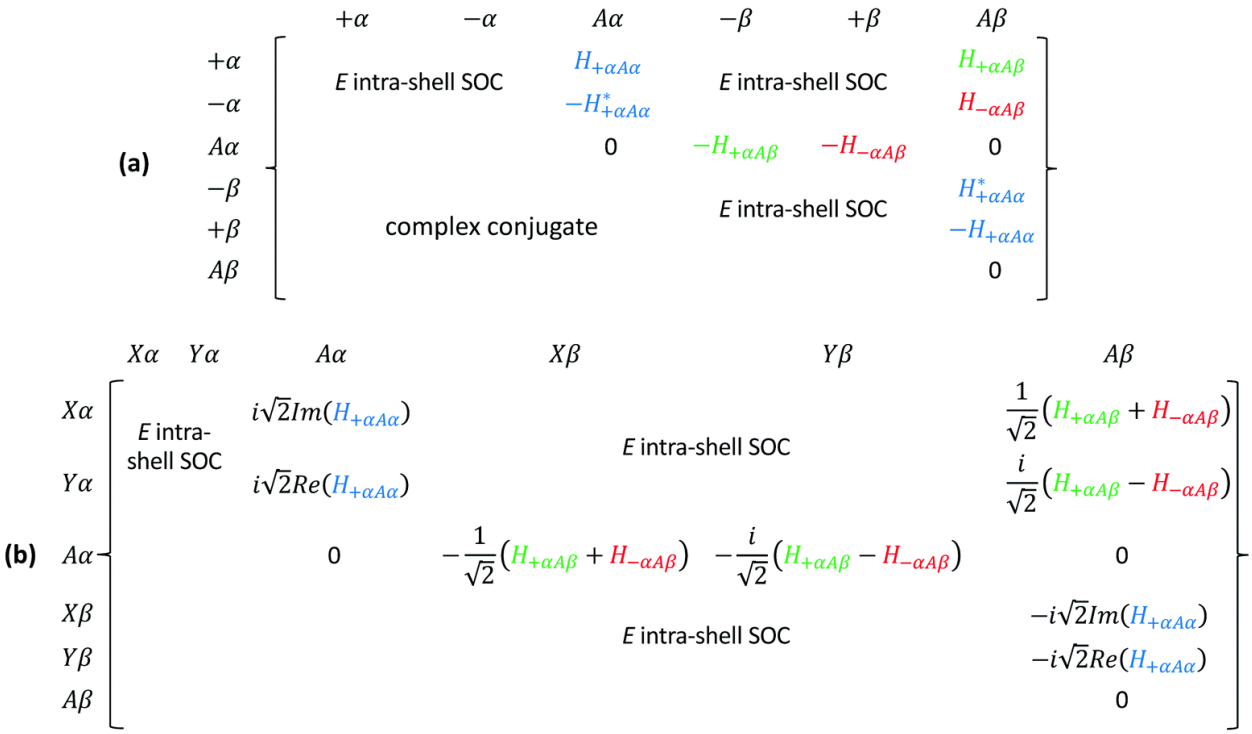

Figure 3.3: Structures of the inter-shell spin–orbit coupling matrix between a set of E-type orbitals and an A-type orbital in (a) the complex-valued and (b) the real-valued bases. Only the inter-shell elements in the upper triangle of the matrix are given. The lower triangle is just the complex conjugate of the upper triangle. Matrix elements that are derived from one independent matrix element by time-reversal symmetry and WET are given in the same color. The blocks of the E-type intra-shell SOC matrix elements are indicated by text and they take the same structure as in Figure 3.1(a).

Therefore, to have $\hat{C}_3\hat{H}\hat{C}_3^{-1} = \hat{H}$, we need to have $\chi^{C_3} = e^{i\frac{2\pi}{3}}$, $e^{-i\frac{2\pi}{3}}$, and 1 for $H_{+\alpha A\alpha}$, $H_{+\alpha A\beta}$, and $\hat{C}_3 H_{-\alpha A\beta}$, respectively.

In C_{3v} symmetry, the A-type orbital is dressed by a subscript 1 or 2, which is symbolically represented by k. The action of $\hat{\sigma}_v$ transforms the Hamiltonian to

$$\begin{aligned}\hat{\sigma}_v\hat{H}\hat{\sigma}_v^{-1} = (-1)^{\delta_{k2}}&(|-\beta\rangle\langle A_k\beta| - |A_k\beta\rangle\langle+\beta| + |A_k\alpha\rangle\langle+\alpha| \\ &- |-\alpha\rangle\langle A_k\alpha|)\hat{\sigma}_v H_{+\alpha A_k\alpha} \\ &+ h.c. + (-1)^{\delta_{k1}}(|-\beta\rangle\langle A_k\alpha| - |A_k\beta\rangle\langle+\alpha|)\hat{\sigma}_v H_{+\alpha A_k\beta} \\ &+ h.c. + (-1)^{\delta_{k1}}(|+\beta\rangle\langle A_k\alpha| - |A_k\beta\rangle\langle-\alpha|)\hat{\sigma}_v H_{-\alpha A_k\beta} \\ &+ h.c.\end{aligned} \quad \text{Eqn 3.16}$$

$\hat{\sigma}_v\hat{H}\hat{\sigma}_v^{-1} = \hat{H}$ requires $\hat{\sigma}_v H_{+\alpha A_k\alpha} = (-1)^{\delta_{k2}} H^*_{+\alpha A_k\alpha}$; $\hat{\sigma}_v H_{+\alpha A_k\beta} = (-1)^{\delta_{k2}} H^*_{+\alpha A_k\beta}$; $\hat{\sigma}_v H_{-\alpha A_k\beta} = H^*_{-\alpha A_k\beta}$. Therefore, $\left(\chi_{Re}^{\sigma_v}, \chi_{Im}^{\sigma_v}\right) = ((-1)^{\delta_{k2}}, (-1)^{\delta_{k1}})$ for all three matrix elements.

In D_3 symmetry,

$$\begin{aligned}\hat{C}_2^x\hat{H}(\hat{C}_2^x)^{-1} = (-1)^{\delta_{k2}}&(|-\beta\rangle\langle A_k\beta| - |A_k\beta\rangle\langle+\beta| + |A_k\alpha\rangle\langle+\alpha| \\ &- |-\alpha\rangle\langle A_k\alpha|)\hat{C}_2^x H_{+\alpha A_k\alpha} \\ &+ h.c. + (-1)^{\delta_{k2}}(|-\beta\rangle\langle A_k\alpha| - |A_k\beta\rangle\langle+\alpha|)\hat{C}_2^x H_{+\alpha A_k\beta} \\ &+ h.c. + (-1)^{\delta_{k2}}(|+\beta\rangle\langle A_k\alpha| - |A_k\beta\rangle\langle-\alpha|)\hat{C}_2^x H_{-\alpha A_k\beta} \\ &+ h.c.\end{aligned} \quad \text{Eqn 3.17}$$

$\hat{C}_2^x\hat{H}(\hat{C}_2^x)^{-1} = \hat{H}$ requires $\left(\chi_{Re}^{C_2'}, \chi_{Im}^{C_2'}\right) = ((-1)^{\delta_{k2}}, (-1)^{\delta_{k1}})$ for $H_{+\alpha A_k\alpha}$ and $((-1)^{\delta_{k1}}, (-1)^{\delta_{k2}})$ for $H_{+\alpha A_k\beta}$ and $H_{-\alpha A_k\beta}$.

In C_{3h} symmetry, the $(E + A)$-type SO Hamiltonian reads

$$\begin{aligned}\hat{H} = &(|+^p\alpha\rangle\langle A^q\alpha| - |A^q\alpha\rangle\langle-^p\alpha| + |A^q\beta\rangle\langle-^p\beta| - |+^p\beta\rangle\langle A^q\beta|)H_{+^p\alpha A^q\alpha} \\ &+ h.c. + (|+^p\alpha\rangle\langle A^q\beta| - |A^q\alpha\rangle\langle-^p\beta|)H_{+^p\alpha A^q\beta} + h.c.\end{aligned} \quad \text{Eqn 3.18}$$

p and q denote the $'$ and $''$ σ_h-parities. Under the action of $\hat{\sigma}_h$,

$$\begin{aligned}\hat{\sigma}_h\hat{H}\hat{\sigma}_h^{-1} = (-1)^{\delta_{pq}+1}&(|+^p\alpha\rangle\langle A^q\alpha| - |A^q\alpha\rangle\langle -^p\alpha| + |A^q\beta\rangle\langle -^p\beta| \\ &- |+^p\beta\rangle\langle A^q\beta|)\hat{\sigma}_h H_{+^p\alpha A^q\alpha} \\ &+ h.c. + (-1)^{\delta_{pq}}(|+^p\alpha\rangle\langle A^q\beta| - |A^q\alpha\rangle\langle -^p\beta|)\hat{\sigma}_h H_{+^p\alpha A^q\beta} \\ &+ h.c. + (-1)^{\delta_{pq}}(|-^p\alpha\rangle\langle A^q\beta| - |A^q\alpha\rangle\langle +^p\beta|)\hat{\sigma}_h H_{-^p\alpha A^q\beta} \\ &+ h.c.\end{aligned} \qquad \text{Eqn 3.19}$$

To have $\hat{\sigma}_h\hat{H}\hat{\sigma}_h^{-1} = \hat{H}$, we need $\chi^{\sigma_h} = (-1)^{\delta_{pq}+1}$ for $H_{+^p\alpha A^q\alpha}$ and $(-1)^{\delta_{pq}}$ for $H_{+^p\alpha A^q\beta}$ and $H_{-^p\alpha A^q\beta}$. The $(E + A)$-type Hamiltonians in D_{3h} symmetry simply adopt all four symmetry eigenvalues, $\left(\chi^{C_3}, \left(\chi_{Re}^{C_2'}, \chi_{Im}^{C_2'}\right), \chi^{\sigma_h}\right)$.

In D_{3d} symmetry, the $(E + A)$-type SO Hamiltonian reads

$$\begin{aligned}\hat{H} = &\left(|+_p\alpha\rangle\langle A_{kq}\alpha| - |A_{kq}\alpha\rangle\langle -_p\alpha| + |A_{kq}\beta\rangle\langle -_p\beta|\right. \\ &\left. - |+_p\beta\rangle\langle A_{kq}\beta|\right)H_{+\alpha A_{kq}\alpha} \\ &+ h.c. + \left(|+_p\alpha\rangle\langle A_{kq}\beta| - |A_{kq}\alpha\rangle\langle -_p\beta|\right)H_{+\alpha A_{kq}\beta} \\ &+ h.c. + \left(|-_p\alpha\rangle\langle A_{kq}\beta| - |A_{kq}\alpha\rangle\langle +_p\beta|\right)H_{-\alpha A_{kq}\beta} + h.c.\end{aligned} \qquad \text{Eqn 3.20}$$

p and q denote the g and u I-parities.

$$\begin{aligned}\hat{I}\hat{H}\hat{I}^{-1} = (-1)^{\delta_{pq}+1}&\left(|+_p\alpha\rangle\langle A_{kq}\alpha| - |A_{kq}\alpha\rangle\langle -_p\alpha| + |A_{kq}\beta\rangle\langle -_p\beta|\right. \\ &\left. - |+_p\beta\rangle\langle A_{kq}\beta|\right)\hat{I}H_{+_p\alpha A_{kq}\alpha} \\ &+ h.c. + (-1)^{\delta_{pq}+1}\left(|+_p\alpha\rangle\langle A_{kq}\beta|\right. \\ &\left. - |A_{kq}\alpha\rangle\langle -_p\beta|\right)\hat{I}H_{+_p\alpha A_{kq}\beta} \\ &+ h.c. + (-1)^{\delta_{pq}+1}\left(|-_p\alpha\rangle\langle A_{kq}\beta|\right. \\ &\left. - |A_{kq}\alpha\rangle\langle +_p\beta|\right)\hat{I}H_{-_p\alpha A_{kq}\beta} + h.c.\end{aligned} \qquad \text{Eqn 3.21}$$

To have $\hat{I}\hat{H}\hat{I}^{-1} = \hat{H}$, we need $\chi^I = (-1)^{\delta_{pq}+1}$ for all three matrix elements. All the symmetry eigenvalues derived in this section are summarized in the $E + A$ block of Table 3.1.

Section 3.1.4 ($A + A$)-Type Hamiltonian

SOC between two A-type orbitals is less common than the others. But it can occur, *e.g.*, in coupling the $f_{x^3-3xy^2}$ and $f_{y^3-3yx^2}$orbitals of an f-block atom at the trigonal center (exemplified in Figure 3.4(a)). This coupling is induced by the $\hat{z}^{(1)}_{eff,z}\hat{s}_z$ component in the dot product operator in Eqn 3.10. As mentioned in the end of **Section 2.3.2**, matrix elements of this type of coupling appear in the A block. At any undistorted trigonal structures, the $\hat{z}^{(1)}_{eff,x}\hat{s}_x$ and $\hat{z}^{(1)}_{eff,y}\hat{s}_y$ components cannot couple any A-type orbitals, because $\hat{z}^{(1)}_{eff,x}$and $\hat{z}^{(1)}_{eff,y}$belong to an E-type irrep, which is not contained by the direct product of two A-type irreps. However, this symmetry argument does not hold when the structure is distorted by JT/pJT interaction, which is our main concern. For instance, the two A-type orbitals shown in Figure 3.4(b) are composed of peripheral p orbitals in a D_{3h} framework. At the undistorted trigonal structure, the $\hat{z}^{(1)}_{eff,x}$ and $\hat{z}^{(1)}_{eff,y}$ matrix elements of the orbitals are zero due to cancellation of the contributions from the three peripheral atoms. As the structure is distorted along an e mode, the exact cancellation is alleviated, resulting in nonzero SOC. This type of coupling contributes elements in the B block. With all these considerations, we should not ignore the $(A + A)$-type SOC.

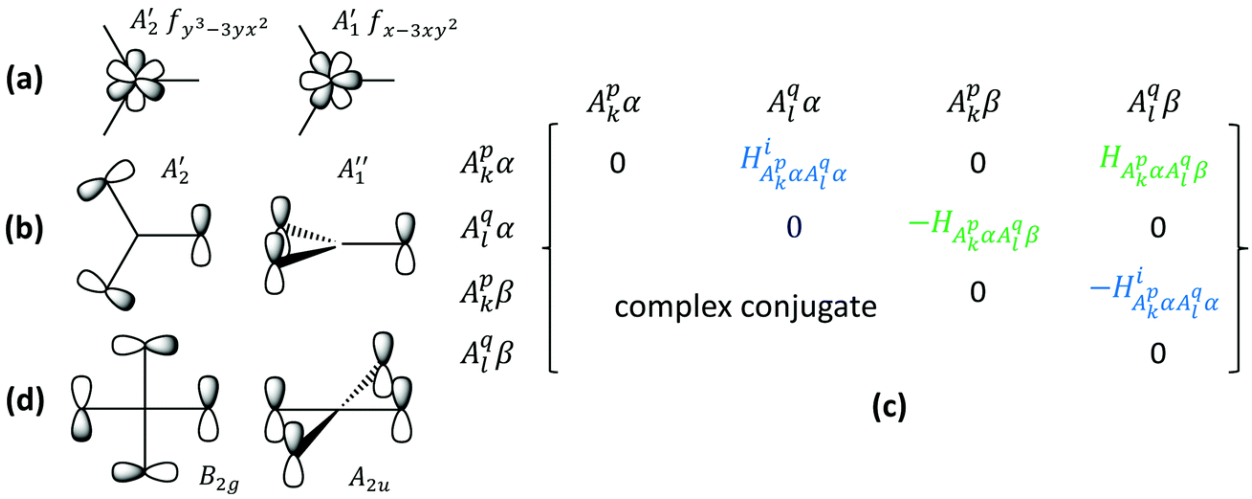

Figure 3.4: (a) $f_{x^3-3xy^2}$ and $f_{y^3-3yx^2}$orbitals at the center of a D_{3h} framework, with their irrep symbols; (b) two A-type orbitals that can have nonzero SOC along e' distortion from the D_{3h} structure; (c) structures of the inter-shell spin–orbit coupling matrix between two A-type orbitals. The lower triangle in (c) is just the complex conjugate of the upper triangle. Matrix elements that are derived from one independent matrix element by time-reversal symmetry and WET are given in the same color. The trivial zero A-type intra-shell SOC matrix elements are also given; (d) a B- and an A-type orbital that can have nonzero SOC along e_u distortion from the D_{4h} structure.

The $(A\ +\ A)$-type SOC matrix adopts the structure in Figure 3.4(c), with the A and B blocks each containing one element. k and l denote the 1 and 2 parities, and p and q the $'$and $''$ parities and g and u parities, whenever the parities are applicable. WET determines $H_{A_k^p\beta A_l^q\beta} = -H_{A_k^p\alpha A_l^q\alpha}$. The time-reversal symmetry determines $H_{A_k^p\beta A_l^q\beta} = (H_{A_k^p\alpha A_l^q\alpha})^*$. These two equalities determine $H_{A_k^p\alpha A_l^q\alpha}$ to be purely imaginary, which is denoted by the superscript i in Figure 3.4(c). The (A + A)-type SOC Hamiltonian reads

$$\hat{H} = \left(|A_k^p\alpha\rangle\langle A_l^q\alpha| + |A_l^q\beta\rangle\langle A_k^p\beta| - |A_l^q\alpha\rangle\langle A_k^p\alpha| - |A_k^p\beta|\rangle\langle A_l^q\beta|\right)H^i_{A_k^p\alpha A_l^q\alpha} + \left(|A_k^p\alpha\rangle\langle A_l^q\beta| - |A_l^q\alpha\rangle\langle A_k^p\beta|\right)H_{A_k^p\alpha A_l^q\beta} + h.c. \quad \text{Eqn 3.22}$$

Under the action of $\hat{C}_3$, the Hamiltonian becomes

$$\begin{aligned}\hat{C}_3\hat{H}\hat{C}_3^{-1} = &\left(\left|A_k^p\alpha\right\rangle\left\langle A_l^q\alpha\right| + \left|A_l^q\beta\right\rangle\left\langle A_k^p\beta\right| - \left|A_l^q\alpha\right\rangle\left\langle A_k^p\alpha\right|\right.\\ &\left. - \left|A_k^p\beta\right|\right\rangle\left\langle A_l^q\beta\right|\Big)\hat{C}_3 H^i_{A_k^p\alpha A_l^q\alpha}\\ &+ e^{-i\frac{2\pi}{3}}\left(\left|A_k^p\alpha\right\rangle\left\langle A_l^q\beta\right| - \left|A_l^q\alpha\right\rangle\left\langle A_k^p\beta\right|\right)\hat{C}_3 H_{A_k^p\alpha A_l^q\beta} + h.c.\end{aligned} \qquad \text{Eqn 3.23}$$

To have $\hat{C}_3\hat{H}\hat{C}_3^{-1} = \hat{H}$, we need $\chi^{C_3} = 1$ and $e^{i\frac{2\pi}{3}}$ for $H^i_{A_k^p\alpha A_l^q\alpha}$and $H_{A_k^p\alpha A_l^q\beta}$, respectively.

In C_{3v} symmetry, $\hat{\sigma}_v$ transforms the Hamiltonian to

$$\begin{aligned}\hat{\sigma}_v\hat{H}\hat{\sigma}_v^{-1} = &(-1)^{\delta_{kl}+1}\left(\left|A_k^p\beta\right\rangle\left\langle A_l^q\beta\right| + \left|A_l^q\alpha\right\rangle\left\langle A_k^p\alpha\right| - \left|A_l^q\beta\right\rangle\left\langle A_k^p\beta\right|\right.\\ &\left. - \left|A_k^p\alpha\right|\right\rangle\left\langle A_l^q\alpha\right|\Big)\hat{\sigma}_v H^i_{A_k^p\alpha A_l^q\alpha}\\ &+ (-1)^{\delta_{kl}}\left(\left|A_k^p\beta\right\rangle\left\langle A_l^q\alpha\right| - \left|A_l^q\beta\right\rangle\left\langle A_k^p\alpha\right|\right)\hat{\sigma}_v H_{A_k^p\alpha A_l^q\beta} + h.c.\end{aligned} \qquad \text{Eqn 3.24}$$

In order to have $\hat{\sigma}_v\hat{H}\hat{\sigma}_v^{-1} = \hat{H}$, the matrix elements need to satisfy $\hat{\sigma}_v H^i_{A_k^p\alpha A_l^q\alpha} = (-1)^{\delta_{kl}+1}H^i_{A_k^p\alpha A_l^q\alpha}$and $\hat{\sigma}_v H_{A_k^p\alpha A_l^q\beta} = (-1)^{\delta_{kl}+1}H^*_{A_k^p\alpha A_l^q\beta}$, *i.e.*, $\left(\chi^{\sigma_v}_{Re}, \chi^{\sigma_v}_{Im}\right) = (0, (-1)^{\delta_{kl}+1})$ and $((-1)^{\delta_{kl}+1}, (-1)^{\delta_{kl}})$ for the two elements, respectively. Similar to the $\chi_{Im} = 0$ cases above, $\chi_{Re} = 0$ arises from that the element is purely imaginary.

In D_3 symmetry, $\hat{C}_2^x$ transforms the Hamiltonian to

$$\begin{aligned}\hat{C}_2^x\hat{H}(\hat{C}_2^x)^{-1} = &(-1)^{\delta_{kl}+1}\left(\left|A_k^p\beta\right\rangle\left\langle A_l^q\beta\right| + \left|A_l^q\alpha\right\rangle\left\langle A_k^p\alpha\right| - \left|A_l^q\beta\right\rangle\left\langle A_k^p\beta\right|\right.\\ &\left. - \left|A_k^p\alpha\right|\right\rangle\left\langle A_l^q\alpha\right|\Big)\hat{C}_2^x H^i_{A_k^p\alpha A_l^q\alpha}\\ &+ (-1)^{\delta_{kl}+1}\left(\left|A_k^p\beta\right\rangle\left\langle A_l^q\alpha\right| - \left|A_l^q\beta\right\rangle\left\langle A_k^p\alpha\right|\right)\hat{C}_2^x H_{A_k^p\alpha A_l^q\beta}\\ &+ h.c.\end{aligned} \qquad \text{Eqn 3.25}$$

In order to have $\hat{C}_2^x \hat{H} (\hat{C}_2^x)^{-1} = \hat{H}$, we need $\hat{C}_2^x H^i_{A_k^p \alpha A_l^q \alpha} = (-1)^{\delta_{kl}+1} H^i_{A_k^p \alpha A_l^q \alpha}$ and $\hat{C}_2^x H_{A_k^p \alpha A_l^q \beta} = (-1)^{\delta_{kl}} H^*_{A_k^p \alpha A_l^q \beta}$, *i.e.*, $\left(\chi^{C_2'}_{Re}, \chi^{C_2'}_{Im}\right) = (0, (-1)^{\delta_{kl}+1})$ and $((-1)^{\delta_{kl}}, (-1)^{\delta_{kl}+1})$ for the two elements, respectively.

In C_{3h} symmetry, $\hat{\sigma}_h$ transforms $\hat{H}$ to

$$\begin{aligned} \hat{\sigma}_h \hat{H} \hat{\sigma}_h^{-1} = (-1)^{\delta_{pq}+1} \big(& \left|A_k^p \alpha\right\rangle\left\langle A_l^q \alpha\right| + \left|A_l^q \beta\right\rangle\left\langle A_k^p \beta\right| - \left|A_l^q \alpha\right\rangle\left\langle A_k^p \alpha\right| \\ & - \left|A_k^p \beta\right|\rangle\left\langle A_l^q \beta\right| \big) \hat{\sigma}_h H^i_{A_k^p \alpha A_l^q \alpha} \\ & + (-1)^{\delta_{pq}} \big(\left|A_k^p \alpha\right\rangle\left\langle A_l^q \beta\right| - \left|A_l^q \alpha\right\rangle\left\langle A_k^p \beta\right| \big) \hat{\sigma}_h H_{A_k^p \alpha A_l^q \beta} + h.c. \end{aligned} \qquad \text{Eqn 3.26}$$

In order to have $\hat{\sigma}_h \hat{H} \hat{\sigma}_h^{-1} = \hat{H}$, we need $\hat{\sigma}_h H^i_{A_k^p \alpha A_l^q \alpha} = (-1)^{\delta_{pq}+1} H_{A_k^p \alpha A_l^q \alpha}$ and $\hat{\sigma}_h H_{A_k^p \alpha A_l^q \beta} = (-1)^{\delta_{pq}} H_{A_k^p \alpha A_l^q \beta}$, *i.e.*, $\chi^{\sigma_h} = (-1)^{\delta_{pq}+1}$ and $(-1)^{\delta_{pq}}$ for the two elements, respectively.

Matrix elements in D_{3h} symmetry need to be characterized by all four (three sets of) symmetry eigenvalues. In D_{3d} symmetry, $\hat{I}$ transforms the Hamiltonian to

$$\begin{aligned} \hat{I} \hat{H} \hat{I}^{-1} = (-1)^{\delta_{pq}+1} \big(& \left|A_k^p \alpha\right\rangle\left\langle A_l^q \alpha\right| + \left|A_l^q \beta\right\rangle\left\langle A_k^p \beta\right| - \left|A_l^q \alpha\right\rangle\left\langle A_k^p \alpha\right| \\ & - \left|A_k^p \beta\right|\rangle\left\langle A_l^q \beta\right| \big) \hat{I} H^i_{A_k^p \alpha A_l^q \alpha} \\ & + (-1)^{\delta_{pq}+1} \big(\left|A_k^p \alpha\right\rangle\left\langle A_l^q \beta\right| - \left|A_l^q \alpha\right\rangle\left\langle A_k^p \beta\right| \big) \hat{I} H_{A_k^p \alpha A_l^q \beta} + h.c. \end{aligned} \qquad \text{Eqn 3.27}$$

Evidently, we need $\chi^I = (-1)^{\delta_{pq}+1}$ for both elements. All symmetry eigenvalues of the $(A + A)$-type SOC matrix elements have been derived and they are summarized in the $(A + A)$ block in Table 3.1.

Section 3.1.5 The table of symmetry eigenvalues

Table 3.1 is the central contribution of this work. This table allows us to identify symmetry eigenvalues of matrix elements of all bimodal SO JT/pJT problems in trigonal symmetries. When E-type orbitals are involved, the symmetry eigenvalues are for the elements in the complex-valued E components. In practice, quantum chemistry calculations generate data for real-valued E components. To facilitate the use of our expansion formulas in actual simulations, the structures of the SOC matrices in the real-valued E orbitals representations are also given in Figure 3.1–Figure 3.3. The matrices in the complex-valued spinors are more relevant to systems with strong SO interaction, since the spinors are symmetry-adapted for the relevant double groups. The matrices in the real-valued spin orbitals are more relevant to systems with weak to intermediate SO interaction, since the real-valued spatial orbitals are adapted for the relevant point groups.

Section 3.2 Hamiltonian structures and symmetry eigenvalues for tetragonal systems

Symmetry-wise, the spatial orbitals in tetragonal and trigonal symmetries **ONLY** differ in their C_n-eigenvalues. Consequently, the results derived above for trigonal problems, which are obtained without explicit consideration of C_3-eigenvalues, are directly applicable to tetragonal problems. These results include the matrix structures in Figure 3.1–Figure 3.3, the σ_v-eigenvalues, the C_2-eigenvalues, and the I-eigenvalues. In short, the only additional derivation for tetragonal SOC problems is to obtain C_4- and S_4-eigenvalues of the relevant independent matrix elements.

The orbitals with $\chi^{C_4} = 1, -1, (i, -i)$ transform as A-, B-, and E-type irreps in tetragonal symmetries, respectively. Given the extra B-type irrep, there are the following additional types of SOC in tetragonal symmetries: B intra-shell coupling, $(A + B)$, $(B + B)$, and $(B + E)$ inter-shell coupling. $|B\alpha\rangle$ and $|B\beta\rangle$ transform as $E_{3/2}$-type irreps in any tetragonal double groups

except S_4^2, in which as the $E_{1/2}$ irrep. With the real-valued $\chi^{C_4} = -1$, B-type orbitals can always be taken real-valued, just like A-type orbitals. Therefore, the B-type intra-shell SOC is null. The $(B + E)$ inter-shell coupling adopts the same matrix form as the $(A + E)$ coupling in Figure *3.3*, only with the A orbital label being replaced by B. An example of the $(B + E)$ coupling is between a dxy orbital (or $d_{x^2-y^2}$ orbital) and a (d_{xz}, d_{yz}) set of orbitals at a tetragonal center. The $(A + B)$ and $(B + B)$ couplings adopt the same matrix form as the $(A + A)$ coupling in Figure *3.4*(c), only with one and both A orbital labels being replaced by B, respectively. The $(B + B)$ inter-shell coupling is commonly seen between a $d_{x^2-y^2}$ orbital and a d_{xy} orbital at a tetragonal center. A- and B-type orbitals that can be SO coupled through e-type distortion are exemplified in Figure 3.4(d).

The C_4-eigenvalues of the tetragonal matrix elements are derived in a similar way as for the C_3-eigenvalues above. Skipping the details, the resultant C_4-eigenvalues are all summarized in Table 3.1. It is not accidental that the χ^{C_4}s of the $(E + A)$ and $(E + B)$ tetragonal problems differ by a sign change, and so do those of the $(A + A)$ and $(A + B)$ tetragonal problems. This is related to the $\chi^{C_4} = 1$ and -1 for A- and B-type orbitals, respectively. Also, the $(A + A)$ and $(B + B)$ type problems share the same χ^{C_4}s, since the sign changes of the two B-type orbitals cancel. We note again that the same set of σ_v-, C_2-, and I-eigenvalues are shared by the same type of trigonal and tetragonal problems. The $(E + A)$ and $(E + B)$ tetragonal problems share the same set of σ_v-, C_2-, and I-eigenvalues, since the two types of problems only differ in χ^{C_4}s of their independent matrix elements. For the same reason, the $(A + A)$, $(A + B)$ and $(B + B)$ tetragonal problems share the same set of σ_v-, C_2-, and I-eigenvalues.

Summarized in Table 3.1 are also S_4-eigenvalues, which are relevant for problems in S_4 symmetry. The C_4^2 and S_4^2 double groups are isomorphic. However, the C_4- and S_4-eigenvalues

are not all identical. Those for the B block elements have opposite signs. The fundamental reason for this difference is that the α and β spin functions transform as the $E_{1/2}$ irrep in the C_4^2 double group, while as the $E_{3/2}$irrep in the S_4^2 double group. This is because the $\hat{\sigma}_h$ hidden in the $\hat{S}_4$ operator brings an extra rotation of π to the spin functions. Consequently, the action of $\hat{S}_4$ on the $|\alpha\rangle\langle\beta|$dyad results in an extra -1 factor compared to the action of $\hat{C}_4$. All derivation work in this study has been finished. Again, Table 3.1 is our central contribution.

Chapter 4 Expansion formulas and comparisons with previous results

All bimodal expansion formulas that feature the symmetry eigenvalues summarized in Table 3.1, except $\left(\chi_{Re}^{\sigma_v,C_2'}, \chi_{Im}^{\sigma_v,C_2'}\right) = (0, \pm 1)$, have been derived before in the context of non-SO pJT/JT interactions in trigonal[57,61] and tetragonal[59] symmetries. The trigonal formulas are summarized in Table. A. I–Table. A. VI in **Appendix**, and the tetragonal formulas in Table. A. VII–Table. A. XV in **Appendix**. Given the symmetry eigenvalues in Table 3.1, one can easily look up symmetry-adapted expansions for a specific SO JT/pJT problem. Here we use three examples to show how to obtain expansion formulas for specific SO pJT/JT problems, and compare our formulas with those obtained in previous studies. Please note that we can organize the formalisms in a set of tables, and this is a result of the root-branch approach. The expansion formulas previously derived for non-SO pJT/JT problems can be re-used for SO pJT/JT problems, and this is a result of the modularized approach.

Section 4.1 $(\boldsymbol{E + A_1})\otimes(\boldsymbol{e + a_1})$ in $\boldsymbol{C_{3v}}$ symmetry

This specific SO pJT problem is considered because the expansions of its matrix elements were derived in ref. 55. Comparison with those results confirms the correctness of our general formalism.

In Figure 3.3 we see that there are three independent matrix elements for this problem: $H_{+\alpha A_1\alpha}$, $H_{+\alpha A_1\beta}$, and $H_{-\alpha A_1\beta}$. From Table 3.1, we see that $\left(\chi^{C_3}, \left(\chi_{Re}^{\sigma_v}, \chi_{Im}^{\sigma_v}\right)\right) = \left(e^{i\frac{2\pi}{3}}, (1,-1)\right)$, $\left(e^{-i\frac{2\pi}{3}}, (1,-1)\right)$, and $(1,(1,-1))$ for the three elements in order. $\chi^{C_3} = e^{i\frac{2\pi}{3}}$ of $H_{+\alpha A_1\alpha}$ directs us to Table. A. II (**Appendix**), whose $(e\ +\ a)$-row gives the root expansion:

$$H_{+\alpha A\alpha} = \rho^{|3n-1|+2K}[b_{I_1,2K}^{r,3n-1} z^{I_1} \cos((3n-1)\phi) - b_{I_2,2K}^{i,3m} z^{I_2} \sin((3n-1)\phi) + i(b_{I_1,2K}^{r,3m} z^{I_1} \sin((3n-1)\phi) + b_{I_2,2K}^{i,3m} z^{I_2} \cos((3n-1)\phi))] \quad \text{Eqn 4.1}$$

Throughout this work, all summation (power) indices that are in the absolute value symbol take all integer values, while the others only take nonnegative integer values. Also, Einstein's convention of summing over duplicate indices is followed. In the expansion formula, the subscript 1 of the a_1 orbital has been dropped because this is the expansion in the lowest (in correspondence to "root") C_3 symmetry among all trigonal symmetries. $\chi^{C_3} = e^{i\frac{2\pi}{3}}$ also directs us to Table. A. IV (**Appendix**), and the $(e\ +\ a_1)\ -\ (1,-1)$ entry there is "$b^r\ nz$", *i.e.*, only the terms with the b^r coefficients in Eqn 4.1 shall be nonzero. Therefore, the final expansion for $H_{+\alpha A_1\alpha}$ is obtained:

$$H_{+\alpha A_1\alpha} = b_{I_1,2K}^{r,3n-1} z^{I_1} \rho^{|3n-1|+2K} e^{i(3n-1)\phi} \quad \text{Eqn 4.2}$$

The symmetry eigenvalues of $H_{+\alpha A_1\beta}$ are identical to those of $H_{+\alpha A_1\alpha}$ except for the χ^{C_3} takes the complex conjugate. Therefore, the $H_{+\alpha A_1\beta}$ expansion is the complex conjugate of the $H_{+\alpha A_1\alpha}$ expansion:

$$H_{+\alpha A_1\beta} = c_{I_1,2K}^{r,3n-1} z^{I_1} \rho^{|3n-1|+2K} e^{-i(3n-1)\phi} \quad \text{Eqn 4.3}$$

Please note that the expansion formulas of $H_{+\alpha A_1\alpha}$ and $H_{+\alpha A_1\beta}$ are connected by taking complex conjugate. The coefficients in the two expansions are not correlated. That is why we use c^r to label the coefficients in the $H_{+\alpha A_1\beta}$ expansion.

The $\chi^{C_3} = 1$ of $H_{-\alpha A_1\beta}$directs us to Table. A. I (**Appendix**), whose $(e\ +\ a)$ row gives the root expansion

$$H_{-\alpha A_1 \beta} = \rho^{|3m|+2K}[a^{r,3m}_{I_1,2K} z^{I_1} \cos(3m\phi) - a^{i,3m}_{I_2,2K} z^{I_2} \sin(3m\phi) + i\left(a^{r,3m}_{I_1,2K} z^{I_1} \sin(3m\phi) + a^{i,3m}_{I_2,2K} z^{I_2} \cos(3m\phi)\right)] \quad \text{Eqn 4.4}$$

The $\chi^{C_3} = 1$ also directs us to Table. A. III (**Appendix**). Applying the "$a^r\ nz$" constraint in the $(e\ +\ a_1) - (1, -1)$ entry there to the root formula, we have the final expansion

$$H_{-\alpha A_1 \beta} = a^{r,3m}_{I_1,2K} z^{I_1} \rho^{|3m|+2K} e^{i3m\phi} \quad \text{Eqn 4.5}$$

Figure 3.3 (b) shows that the three complex-valued independent matrix elements become four real-valued independent matrix elements in the real basis set. They take the form of the following expansion formulas:

$$H_{X\alpha A_1 \alpha} = i\sqrt{2} Im\left(H_{+\alpha A_1 \alpha}\right) = i b^{r,3n-1}_{I_1,2K} z^{I_1} \rho^{|3n-1|+2K} \sin(3n-1)\phi\ ;$$

$$H_{Y\alpha A_1 \alpha} = i\sqrt{2} Re\left(H_{+\alpha A_1 \alpha}\right) = i b^{r,3n-1}_{I_1,2K} z^{I_1} \rho^{|3n-1|+2K} \cos(3n-1)\phi\ ;$$

$$H_{X\alpha A_1 \beta} = \frac{1}{\sqrt{2}}\left(H_{+\alpha A_1 \beta} + H_{-\alpha A_1 \beta}\right) = c^{r,3n-1}_{I_1,2K} z^{I_1} \rho^{|3n-1|+2K} e^{-i(3n-1)\phi} + a^{r,3m}_{I_1,2K} z^{I_1} \rho^{|3m|+2K} e^{i3m\phi}; \quad \text{Eqn 4.6}$$

$$H_{Y\alpha A_1 \beta} = \frac{i}{\sqrt{2}}\left(H_{+\alpha A_1 \beta} - H_{-\alpha A_1 \beta}\right) = i c^{r,3n-1}_{I_1,2K} z^{I_1} \rho^{|3n-1|+2K} e^{-i(3n-1)\phi} - i a^{r,3m}_{I_1,2K} z^{I_1} \rho^{|3m|+2K} e^{i3m\phi}.$$

The common factors $\sqrt{2}$ and $\frac{1}{\sqrt{2}}$ have been absorbed in the coefficients b^r, a^r ,and c^r. Up to 4th order, the term-by-term expansions are

$$H_{X\alpha A_1\alpha} = -ib_{0,0}^{r,-1}y + ib_{0,0}^{r,2}2xy - ib_{1,0}^{r,-1}zy - ib_{0,2}^{r,-1}(x^2+y^2)y$$
$$+ ib_{1,0}^{r,2}z2xy - ib_{2,0}^{r,-1}z^2y - ib_{0,0}^{r,-4}4xy(x^2-y^2)$$
$$+ ib_{0,2}^{r,2}(x^2+y^2)2xy - ib_{1,2}^{r,-1}z(x^2+y^2)y + ib_{2,0}^{r,2}z^2 2xy$$
$$- ib_{3,0}^{r,-1}z^3y$$

$$H_{Y\alpha A_1\alpha} = ib_{0,0}^{r,-1}x + ib_{0,0}^{r,2}(x^2-y^2) + ib_{1,0}^{r,-1}zx + ib_{0,2}^{r,-1}(x^2+y^2)x$$
$$+ ib_{1,0}^{r,2}z(x^2-y^2) + ib_{2,0}^{r,-1}z^2x + ib_{0,0}^{r,-4}(x^4+y^4-6x^2y^2)$$
$$+ ib_{0,2}^{r,2}(x^4-y^4) + ib_{1,2}^{r,-1}z(x^2+y^2)x + ib_{2,0}^{r,2}z^2(x^2-y^2)$$
$$+ ib_{3,0}^{r,-1}z^3x$$

$$H_{X\alpha A_1\beta} = a_{0,0}^{r,0} + a_{1,0}^{r,0}z + c_{0,0}^{r,-1}(x-iy) + a_{0,2}^{r,0}(x^2+y^2) + a_{2,0}^{r,0}z^2$$
$$+ c_{0,0}^{r,2}(x^2-y^2-i2xy) + c_{1,0}^{r,-1}z(x-iy)$$
$$+ a_{0,0}^{r,-3}(x^3-3xy^2-i3x^2y+iy^3)$$
$$+ a_{0,0}^{r,3}(x^3-3xy^2+i3x^2y-iy^3) + a_{1,2}^{r,0}z(x^2+y^2)$$
$$+ a_{3,0}^{r,0}z^3 + c_{0,2}^{r,-1}(x^2+y^2)(x-iy) + c_{1,0}^{r,2}z(x^2-y^2+i2xy)$$
$$+ c_{2,0}^{r,-1}z^2(x-iy) + a_{0,4}^{r,0}(x^2+y^2)^2$$
$$+ a_{1,0}^{r,-3}z(x^3-3xy^2-i3x^2y+iy^3)$$
$$+ a_{1,0}^{r,3}z(x^3-3xy^2+i3x^2y-iy^3) + a_{2,2}^{r,0}z^2(x^2+y^2)$$
$$+ a_{4,0}^{r,0}z^4 + c_{0,0}^{r,-4}\left(x^4+y^4-6x^2y^2-i4xy(x^2-y^2)\right)$$
$$+ c_{0,2}^{r,2}(x^2+y^2)(x^2-y^2+i2xy)$$
$$+ c_{1,2}^{r,-1}z(x^2+y^2)(x-iy) + c_{2,0}^{r,2}z^2(x^2-y^2+i2xy)$$
$$+ c_{3,0}^{r,-1}z^3(x-iy)$$

Eqn 4.7

Replacing c^r by ic^r and a^r by ia^r in the $H_{X\alpha A_1\beta}$ expansion, we obtain the $H_{Y\alpha A_1\beta}$ expansion. The three expansions in Eqn 4.7 are identical to those given in ref. 55 except for some trivial phase differences. The correctness of our general formalism is confirmed.

Section 4.2 $(E' + A_2'')\otimes(e' + a_2'')$ problem in D_{3h} symmetry

Another example is the $(E' + A_2'')\otimes(e' + a_2'')$ SO pJT problem in D_{3h} symmetry, whose expansion formulas were derived in ref. 54 under the assumption that the E' and A_2'' orbitals arise from one set of p orbitals that are located at the D_{3h} center. From Table 3.1, we immediately obtain the symmetry eigenvalues of the three independent matrix elements: $\left(\chi^{C_3}, \left(\chi_{Re}^{C_2'}, \chi_{Im}^{C_2'}\right), \chi^{\sigma_h}\right) = (e^{i\frac{2\pi}{3}}, (-1,1), -1)$ for $H_{+'\alpha A_2''\alpha}$, $(e^{-i\frac{2\pi}{3}}, (1,-1), 1)$ for $H_{+'\alpha A_2''\beta}$, and $= (1, (1,-1), 1)$ for $H_{-'\alpha A_2''\beta}$. Guided by these eigenvalues and consulting the root formulas table and constraints tables, we obtain the general expansion formulas of the elements:

$$H_{+'\alpha A_2''\alpha} = b_{2I_1+1,2K}^{r,3n-1} z^{2I_1+1} \rho^{|3n-1|+2K} e^{i(3n-1)\phi};$$
$$H_{+'\alpha A_2''\beta} = c_{2I_1,2K}^{r,3n-1} z^{2I_1} \rho^{|3n-1|+2K} e^{-i(3n-1)\phi}; \quad \text{Eqn 4.8}$$
$$H_{-'\alpha A_2''\beta} = a_{2I_1,2K}^{r,3m} z^{2I_1} \rho^{|3m|+2K} e^{i3m\phi}.$$

They differ from the counterparts in Eqn 4.2 and Eqn 4.3 and Eqn 4.4 in the selections of the z powers. We can hence obtain $H_{X'\alpha A_2''\alpha}$ and $H_{X'\alpha A_2''\beta}$ expansions up to 4th order by taking only the terms with odd powers of z in the $H_{X\alpha A_1\alpha}$ and $H_{Y\alpha A_1\beta}$ expansions in Eqn 4.7, respectively:

$$H_{X'\alpha A_2''\alpha} = -ib_{1,0}^{r,-1} zy + ib_{1,0}^{r,2} z2xy - ib_{1,2}^{r,-1} z(x^2+y^2)y - ib_{3,0}^{r,-1} z^3 y; \quad \text{Eqn 4.9}$$
$$H_{Y'\alpha A_2''\alpha} = ib_{1,0}^{r,-1} zx + ib_{1,0}^{r,2} z(x^2-y^2) + ib_{1,2}^{r,-1} z(x^2+y^2)x + ib_{3,0}^{r,-1} z^3 x.$$

They are identical to the expansions given in eqn (39b) and (39c) in ref. 54, except for a trivial sign difference in $H_{Y'\alpha A_2''\alpha}$.

Similarly, we obtain the $H_{X'\alpha A_2''\beta}$ expansion up to 4th order by taking the terms with even powers of z in the $H_{X\alpha A_1\beta}$ expansion in Eqn 4.7:

$$\begin{aligned} H_{X'\alpha A_2''\beta} = {} & a_{0,0}^{r,0} + c_{0,0}^{r,-1}(x - iy) + a_{0,2}^{r,0}(x^2 + y^2) + a_{2,0}^{r,0}z^2 \\ & + c_{0,0}^{r,2}(x^2 - y^2 - i2xy) + (a_{0,0}^{r,-3} + a_{0,0}^{r,3})(x^3 - 3xy^2) \\ & + a_{0,0}^{r,-3} + a_{0,0}^{r,3})i(3x^2y - y^3) + c_{0,2}^{r,-1}(x^2 + y^2)(x - iy) \\ & + c_{2,0}^{r,-1}z^2(x - iy) + a_{0,4}^{r,0}(x^2 + y^2)^2 + a_{2,2}^{r,0}z^2(x^2 + y^2) \\ & + a_{4,0}^{r,0}z^4 + c_{0,0}^{r,-4}\left(x^4 + y^4 - 6x^2y^2 - i4xy(x^2 - y^2)\right) \\ & + c_{0,2}^{r,2}(x^2 + y^2)(x^2 - y^2 + i2xy) \\ & + c_{2,0}^{r,2}z^2(x^2 - y^2 + i2xy) \end{aligned} \qquad \text{Eqn 4.10}$$

Discrepancy is seen between this expansion and the one given in eqn (39e) in ref. 54, which lacks the term corresponding to the $i(3x^2y - y^3)$monomial. The assumption there that all three orbitals arise from a common set of p orbitals imposes higher symmetry to the $(E' + A_2'')$ problem, and naturally keeps fewer terms in the expansions. Specifically, this assumption excludes all terms with the $i \sin 3m\phi$ angular factor in the $H_{X'\alpha A_2''\beta}$expansion. Under this assumption, the $H_{X'\alpha A_2''\beta}$ expansion takes a form of $iH_{X'Y'} - H_{X'X'} - H_{A_2''A_2''}$ (see eqn (14b), (14e) and (21e) in ref. 54), where the real-valued H_{IJ} stands for the electrostatic, non-SO coupling between states I and J. The component that is $\hat{C}_3$-invariant terms from $H_{A_2''A_2''}$ and $H_{X'X'}$, both of which contain terms with $\cos 3m\phi$ but not those with $i \sin 3m\phi$.

We are not criticizing the work of ref. 54. As mentioned in **Chapter 1**, this excellent work motivated us to derive the present formalism. The authors of ref. 54 have clearly discussed the

approximation nature of the formulas therein and the limits of their use. The comparison here is only to highlight the capacity of the present formalism. It provides both the terms that are included and not included by the three-p-approximation.

Section 4.3 $(\boldsymbol{E_u + A_{2u}})\otimes(\boldsymbol{e_u + b_{1g} + b_{2g}})$ problem in $\boldsymbol{D_{4h}}$ symmetry

First order expansion formulas of this SO pJT problem are given in ref.75 in the context of studying Ng^+F_4 cations (Ng: a noble gas atom). We take this problem as an example to show how to obtain trimodal expansions from the presented bimodal formalism. First, we identify the three independent matrix elements and their symmetry eigenvalues $\left(\chi^{C_4}, \left(\chi_{Re}^{C_2'}, \chi_{Im}^{C_2'}\right), \chi^{I}\right)$ in Table 3.1: $H_{+_u\alpha A_{2u}\alpha}$, $(i,(-1,1),1)$; $H_{+_u\alpha A_{2u}\beta}$, $(-1,(1,-1),1)$; $H_{-_u\alpha A_{2u}\beta}$, $(1,(1,-1),1)$. Second, we recognize that there are four types of products of monomials of the two b coordinates, $w_1^{2I_1+1}w_2^{2I_2+1}$, $w_1^{2I_1+1}w_2^{2I_2}$, $w_1^{2I_1}w_2^{2I_2+1}$, and $w_1^{2I_1}w_2^{2I_2}$, which transform as a_{2g}, b_{1g}, b_{2g}, and a_{1g} coordinates, respectively. w_1 and w_2 are used to label the actual b_{1g} and b_{2g} coordinates. Third, using the symmetry eigenvalues and from Table. A. VII–Table. A. XV(**Appendix**), we extract the $(e_u + a_{2g})$, $(e_u + b_{1g})$, $(e_u + b_{2g})$, and $(e_u + a_{1g})$ expansion formulas for the three matrix elements. We call these the intermediate expansions.

The $(e_u + b_g) - (i,1)$ and $(e_u + a_g) - (i,1)$entries in Table. A. XV (**Appendix**) are both "na" (not applicable) and therefore, the intermediate expansions for $H_{+_u\alpha A_{2u}\alpha}$ are null and so is the $(e_u + b_{1g} + b_{2g})$ expansion. This is consistent with the null $H_{w_1V_1}$ element in eqn (21) of ref.75. The $(e_u + a_{2g})$ intermediate expansion for $H_{+_u\alpha A_{2u}\beta}$ is

$$b_{2I,2K}^{r,4k+2} z^{2I} \rho^{|4k+2|+2K} e^{i(4k+2)\phi} + i b_{2I+1,2K}^{r,4k+2} z^{2I+1} \rho^{|4k+2|+2K} e^{i(4k+2)\phi} \qquad \text{Eqn 4.11}$$

where z is used to label the symbolic a_{2g} coordinate. The other three intermediate expansions for this matrix element and all four intermediate expansions for $H_{-_u\alpha A_{2u}\beta}$ are not shown. The fourth step is to replace the symbolic coordinates by the corresponding products of the two b coordinates. For instance, in Eqn 4.11, z is replaced by $w_1^{2I_1+1}w_2^{2I_2+1}$, and after some simple algebraic manipulation, the expansion becomes

$$b_{2I_1,2I_2,2K}^{r,4k+2}w_1^{2I_1}w_2^{2I_2}\rho^{|4k+2|+2K}e^{i(4k+2)\phi} + ib_{2I_1+1,2I_2+1,2K}^{r,4k+2}w_1^{2I_1+1}w_2^{2I_2+1}\rho^{|4k+2|+2K}e^{i(4k+2)\phi} \quad \text{Eqn 4.12}$$

The other three intermediate expansions for $H_{+_u\alpha A_{2u}\beta}$ become

$$b_{2I_1+1,2I_2,2K}^{r,4k}w_1^{2I_1+1}w_2^{2I_2}\rho^{|4k|+2K}e^{i4k\phi} + b_{2I_1,4I_2,2K}^{r,4k+2}w_1^{2I_1}w_2^{4I_2}\rho^{|4k+2|+2K}e^{i(4k+2)\phi};$$

$$b_{4I_1,2I_2,2K}^{r,4k+2}w_1^{4I_1}w_2^{2I_2}\rho^{|4k+2|+2K}e^{i(4k+2)\phi} + ib_{2I_1,2I_2+1,2K}^{r,4k}w_1^{2I_1}w_2^{2I_2+1}\rho^{|4k|+2K}e^{i4k\phi}; \quad \text{Eqn 4.13}$$

$$b_{2I_1,2I_2,2K}^{r,4k+2}w_1^{2I_1}w_2^{2I_2}\rho^{|4k+2|+2K}e^{i(4k+2)\phi}.$$

The analogue expansions for $H_{-_u\alpha A_{2u}\beta}$ are not shown.

The fifth and final step is to sum all the four expansions corresponding to the four types of b monomial products. Combining duplicate terms, the final expansion formulas are

$$\begin{aligned} H_{+_u\alpha A_{2u}\beta} = {} & b_{2I_1,2I_2,2K}^{r,4k+2}w_1^{2I_1}w_2^{2I_2}\rho^{|4k+2|+2K}e^{i(4k+2)\phi} \\ & + b_{2I_1+1,2I_2,2K}^{r,4k}w_1^{2I_1+1}w_2^{2I_2}\rho^{|4k|+2K}e^{i4k\phi} \\ & + ib_{2I_1+1,2I_2+1,2K}^{r,4k+2}w_1^{2I_1+1}w_2^{2I_2+1}\rho^{|4k+2|+2K}e^{i(4k+2)\phi} \\ & + ib_{2I_1,2I_2+1,2K}^{r,4k}w_1^{2I_1}w_2^{2I_2+1}\rho^{|4k|+2K}e^{i4k\phi} \end{aligned} \quad \text{Eqn 4.14}$$

$$
\begin{aligned}
H_{-_u\alpha A_{2u}\beta} = {} & a^{r,4k}_{2I_1,2I_2,2K} w_1^{2I_1} w_2^{2I_2} \rho^{|4k|+2K} e^{i4k\phi} \\
& + a^{r,4k+2}_{2I_1+1,2I_2,2K} w_1^{2I_1+1} w_2^{2I_2} \rho^{|4k+2|+2K} e^{i(4k+2)\phi} \\
& + i a^{r,4k+2}_{2I_1+1,2I_2+1,2K} w_1^{2I_1+1} w_2^{2I_2+1} \rho^{|4k|+2K} e^{i4k\phi} \\
& + i a^{r,4k+2}_{2I_1+1,2I_2,2K} w_1^{2I_1+1} w_2^{2I_2} \rho^{|4k+2|+2K} e^{i(4k+2)\phi} \\
& + i a^{r,4k+2}_{2I_1,2I_2,2K} w_1^{2I_1} w_2^{2I_2+1} \rho^{|4k+2|+2K} e^{i(4k+2)\phi}
\end{aligned}
\qquad \text{Eqn 4.15}
$$

Keeping up to the linear terms, $H_{+_u\alpha A_{2u}\beta} = b^{r,0}_{1,0,0} w_1 + i b^{r,0}_{0,1,0} w_2$ and $H_{-_u\alpha A_{2u}\beta} = a^{r,0}_{0,0,0}$, which are consistent with $H_{w_1 V_2} = -\sqrt{2}(\gamma q_1 - i\delta q_2)$ and $H_{U_2 V_2} = \sqrt{2}\beta$ in eqn (21) of ref. 75, respectively.

Expansion formulas involving more vibrational modes can be obtained in a similar fashion. For non-degenerate modes (a- and b-type modes), we can always combine their monomials to have symbolic single mode coordinates. For problems with more e-type modes, we can always decompose single e mode's monomials to products of multiple e modes' monomials. For example, to obtain the $(b_{1g} + b_{2g} + e_{2u})$ expansions for the two matrix elements above, we simply need to replace $\rho^{|4k|+2K} e^{i4k\phi}$ by $\rho_1^{|4k-m|+2K_1} \rho_2^{|m|+2K_2} e^{i[(4k-m)\phi_1 + m\phi_2]}$ and $\rho^{|4k+2|+2K} e^{i(4k+2)\phi}$ by $\rho_1^{|4k+2-m|+2K_1} \rho_2^{|m|+2K_2} e^{i[(4k+2-m)\phi_1 + m\phi_2]}$, and then to add the extra summation indices to the coefficient labels. Depending on the parities of the matrix elements and the modes, further constraints on the summation indices may be applicable.

Chapter 5 Conclusion

In this work, we present a general formalism for all bimodal spin–orbit (pseudo-)Jahn–Teller problems in trigonal and tetragonal symmetries. The formalism gives us expansion formulas of spin–orbit matrix elements in symmetry-adapted vibrational coordinates up to arbitrary order. The derivation is based on the fundamental symmetry requirements of the spin–orbit vibronic Hamiltonian operator and does not rely on a specific form of the operator. The root-branch approach and the modularized approach facilitate the derivation so much that thousands of problems in the two classes of symmetries are covered in this work. The formalism is presented as four generic matrices, one table of symmetry eigenvalues, two tables of root expansion formulas, and ten tables of constraints. We can identify independent matrix elements and look up their expansion formulas using the tables. With the generic matrix structures, we can easily construct the total spin–orbit vibronic Hamiltonian operator from the independent matrix elements. With all these features, the formalism is programmable. The correctness, completeness, and conciseness of the formalism is demonstrated by comparisons with formulas derived in earlier studies. Given the ubiquity of trigonal and tetragonal spin–orbit (pseudo-)Jahn–Teller problems, especially for heavy element compounds of the symmetries, the applicability of the presented formalism is broad.

The derivation in this work also lays a solid foundation for future derivation for the spin–orbit (pseudo-)Jahn–Teller formalism for general axial symmetries with arbitrary n-fold principal axes. The generic matrix structures and the σ_v-, C_2-, and I-eigenvalues are transferable. We will still need to derive C_n- and S_n-eigenvalues, and some extra root expansion formulas and the constraints onto them. Since spin–orbit and non-spin–orbit (pseudo-)Jahn–Teller formalisms only differ in symmetry eigenvalues of independent matrix elements, we can combine the two

formalisms into one. It will be an interesting future study to derive the unified formalism for spin–orbit and non-spin–orbit (pseudo-)Jahn–Teller problems in arbitrary axial symmetries.

Reference

[1] H. A. Jahn and E. Teller, *Proc. R. Soc. London, Ser. A*, 1937, **161**, 220–235.

[2] R. Englman *Jahn–Teller Effect in Molecules and Crystals*, John Wiley and Sons, Ltd, London, 1972.

[3] I. B. Bersuker and V. Z. Polinger, *Vibronic Interactions in Molecules and Crystals* , Springer-Verlag, 1989.

[4] I. B. Bersuker *The Jahn–Teller Effect*, Cambridge University Press, Cambridge, UK, 2006.

[5] U. Öpik and M. H. L. Pryce, Proc. *R. Soc. London, Ser. A*, 1957, **238**, 425 —447.

[6] T. A. Barckholtz and T. A. Miller, Int. *Rev. Phys. Chem.*, 1998, **17**, 435 —524

[7] J. B. Goodenough *Annu. Rev. Mater. Sci.*, 1998, **28**, 1 —27

[8] I. B. Bersuker *Chem. Rev.*, 2001, **101**, 1067 —1114

[9] B. E. Applegate, T. A. Barckholtz and T. A. Miller, Chem. *Soc. Rev.*, 2003, **32**, 38 —49

[10] H. Köppel *Conical intersections: electronic structure, dynamics and spectroscopy*, W. Domcke, D. R. Yarkony and H. Köppel, World Scientific, New Jersey, 2004, pp. 429–472

[11] M. A. Halcrow *Chem. Soc. Rev.*, 2013, **42**, 1784 —1795

[12] I. B. Bersuker *Chem. Rev.*, 2013, **113**, 1351 —1390

[13] I. B. Bersuker *Adv. Chem. Phys.*, 2016, **160**, 159 —208

[14] T. Mondal *Phys. Chem. Chem. Phys.*, 2018, **20**, 9401 —9410.

[15] C. M. Marian *Spin–Orbit Coupling in Molecules*, K. B. Lipkowitz and D. B. Boyd, Wiley-VCH, New York, 2001, pp. 99–204

[16] D. G. Fedorov, S. Koseki, M. W. Schmidt and M. S. Gordon, *Int. Rev. Phys. Chem.*, 2003, **22**, 551 —592

[17] P. Pyykkö *Annu. Rev. Phys. Chem.*, 2012, **63**, 45 —64

[18] T. Zeng, D. G. Fedorov, M. W. Schmidt and M. Klobukowski, *J. Chem. Phys.*, 2011, **134**, 214108

[19] T. Zeng, D. G. Fedorov and M. Klobukowski, J. *Chem. Phys.*, 2009, **131**, 124109

[20] T. Zeng, D. G. Fedorov and M. Klobukowski, J. *Chem. Phys.*, 2010, **132**, 074102

[21] T. Zeng, D. G. Fedorov and M. Klobukowski, J. *Chem. Phys.*, 2010, **133**, 114107

[22] T. Zeng, D. G. Fedorov and M. Klobukowski, J. *Chem. Phys.*, 2011, **134**, 024108

[23] L. Alvarez-Thon, J. David, R. Arratia-Pérez and K. Seppelt, *Phys. Rev. A: At., Mol., Opt. Phys.*, 2008, **77**, 034502.

[24] K. Balasubramanian *Relativistic Effects in Chemistry Part A*, John Wiley and Sons, Inc., New York, 1997.

[25] K. Balasubramanian and D. Majumdar *J. Chem. Phys.*, 2001, **115**, 8795.

[26] A. Pérez-Villa, J. David, P. Fuentealba and A. Restrepo, *Chem. Phys. Lett.*, 2011, **507**, 57 —62.

[27] A. V. Marenich and J. E. Boggs, J. *Phys. Chem. A*, 2004, **108**, 10594 —10601

[28] M. S. Schuurman, D. E. Weinberg and D. R. Yarkony, J. *Chem. Phys.*, 2007, **127**, 104309

[29] B. Molina, J. R. Soto and A. Calles, *Eur. Phys. J. D*, 2009, **51**, 225 —231

[30] L. V. Poluyanov and W. Domcke, *Jahn–Teller Effect: Fundamentals and Implications for Physics and Chemistry*, H. Köppel, D. R. Yarkony and H. Barentzen, Springer, New York, 2009, pp. 77–97

[31] D. Opalka, M. Segado, L. V. Poluyanov and W. Domcke, *Phys. Rev. A: At., Mol., Opt. Phys.*, 2010, **81**, 042501

[32] P. Mondal, D. Opalka, L. V. Poluyanov and W. Domcke, *Chem. Phys.*, 2011, **387**, 56 —65

[33] P. Mondal, D. Opalka, L. V. Poluyanov and W. Domcke, *J. Chem. Phys.*, 2012, **136**, 084308

[34] L. V. Poluyanov and W. Domcke, Conical *intersections: theory, computation and experiment*, W. Domcke, D. R. Yarkony and H. Köppel, World Scientific, New Jersey, 2011, pp. 117–154

[35] D. Opalka, L. V. Poluyanov and W. Domcke, *J. Chem. Phys.*, 2011, **135**, 104108

[36] S. Matsika and D. R. Yarkony, *Adv. Chem. Phys.*, 2003, **124**, 557 —583.

[37] L. V. Poluyanov and W. Domcke, *Chem. Phys.*, 2010, **374**, 86 —93

[38] T. Zeng, D. G. Fedorov, M. W. Schmidt and M. Klobukowski, *J. Chem. Theory Comput.*, 2011, **7**, 2864 —2875.

[39] T. Zeng, D. G. Fedorov, M. W. Schmidt and M. Klobukowski, *J. Chem. Theory Comput.*, 2012, **8**, 3061 —3071.

[40] T. J. Penfold, E. Gindensperger, C. Daniel and C. M. Marian, *Chem. Rev.*, 2018, **118**, 6975 —7025.

[41] W. Moffitt and W. Thorson, *Phys. Rev.*, 1957, **108**, 1251 —1255.

[42] L. V. Poluyanov and W. Domcke, *J. Chem. Phys.*, 2008, **129**, 224102.

[43] L. V. Poluyanov and W. Domcke, *Chem. Phys.*, 2012, **407**, 1 —8.

[44] W. Domcke, S. Mishra and L. V. Poluyanov, *Chem. Phys.*, 2006, **322**, 405 —410.

[45] A. Viel and W. Eisfeld, *J. Chem. Phys.*, 2004, **120**, 4603 —4613.

[46] W. Eisfeld and A. Viel, *J. Chem. Phys.*, 2005, **122**, 204317.

[47] S. Mahapatra, W. Eisfeld and H. Köppel, *Chem. Phys. Lett.*, 2007, **441**, 7 —15.

[48] S. Bhattacharyya, D. Opalka, L. V. Poluyanov and W. Domcke, *J. Phys.: Conf. Ser.*, 2013, **428**, 012015

[49] S. Bhattacharyya, D. Opalka, L. V. Poluyanov and W. Domcke, *J. Phys. Chem. A*, 2014, **118**, 11962 —11970.

[50] W. Eisfeld, O. Vieuxmaire and A. Viel, *J. Chem. Phys.*, 2014, **140**, 224109.

[51] T. Codd, M.-W. Chen, M. Roudjane, J. F. Stanton and T. A. Miller, *J. Chem. Phys.*, 2015, **142**, 184305.

[52] T. Mondal *Phys. Chem. Chem. Phys.*, 2018, **20**, 9401 —9410.

[53] H. K. Tran, J. F. Stanton and T. A. Miller, *J. Mol. Spectrosc.*, 2018, **343**, 102 —115.

[54] W. Domcke, D. Opalka and L. V. Poluyanov, J. *Chem. Phys.*, 2016, **144**, 124101.

[55] T. Weike and W. Eisfeld, J. *Chem. Phys.*, 2016, **144**, 104108.

[56] A. D. Liehr *J. Phys. Chem.*, 1963, **67**, 389 —471.

[57] T. Zeng and I. Seidu, *Phys. Chem. Chem. Phys.*, 2017, **19**, 11098 —11110.

[58] T. Zeng, R. J. Hickman, A. Kadri and I. Seidu, *J. Chem. Theory Comput.*, 2017, **13**, 5004 —5018.

[59] R. J. Hickman, R. A. Lang and T. Zeng, Phys. *Chem. Chem. Phys.*, 2018, **20**, 12312 — 12322.

[60] R. A. Lang, A. Japahuge and T. Zeng, *Chem. Phys.*, 2018, **515**, 36 —45.

[61] I. Seidu, P. Goel, X.-G. Wang, B. Chen, X.-B. Wang and T. Zeng, *Phys. Chem. Chem. Phys.*, 2019, **21**, 8679 —8690

[62] M. Douglas and N. M. Kroll, *Ann. Phys.*, 1974, **82**, 89 —155.

[63] B. A. Hess *Phys. Rev. A: At., Mol., Opt. Phys.*, 1986, **33**, 3742 —3748.

[64] M. Barysz and A. J. Sadlej, *J. Chem. Phys.*, 2002, **116**, 2696 —2704.

[65] T. Nakajima and K. Hirao, *Chem. Phys. Lett.*, 1999, **302**, 383 —391.

[66] M. Barysz *J. Chem. Phys.*, 2000, **113**, 4003.

[67] D. G. Fedorov and M. S. Gordon, *J. Chem. Phys.*, 2000, **112**, 5611 —5623.

[68] C. M. Marian and U. Wahlgren, *Chem. Phys. Lett.*, 1996, **251**, 357 —364.

[69] F. Neese *J. Chem. Phys.*, 2005, **122**, 034107.

[70] A. Berning, M. Schweizer, H.-J. Werner, P. J. Knowles and P. Palmieri, *Mol. Phys.*, 2000, **98**, 1823 —1833.

[71] T. Zeng *J. Chem. Phys.*, 2017, **146**, 144103.

[72] D. G. Fedorov and M. S. Gordon, in *Symmetry in Spin–Orbit Coupling*, ed. M. R. Hoffmann and K.G. Dyall, American Chemical Society, Washington, 2002, vol. ACS Symposium Series 828, pp. 276–297.

[73] C. A. Mead *J. Chem. Phys.*, 1979, **70**, 2276 —2283.

[74] H. A. Kramers *Proc. Acad. Amesterdam*, 1930, **33**, 959.

[75] V. I. Osherov, M. V. Osherov and L. V. Poluyanov, *Mol. Phys.*, 2018, **116**, 1358 —1363.

Appendix

Appendix 1 Expansion formulas in trigonal symmetries

All bimodal expansion formulas that feature the symmetry eigenvalues χ^{C_3}, $\left(\chi_{Re}^{\sigma_v}, \chi_{Im}^{\sigma_v}\right)$, $\left(\chi_{Re}^{C_2'}, \chi_{Im}^{C_2'}\right)$, χ^{σ_h} ,and χ^{I} are summarized in Table. A. I to Table. A. VI. In these tables z is used to represent coordinates of a-type vibrations and the polar coordinates ρ and φ for e-type vibrations. For coordinates of vibrational modes of the same type of irreducible representations (irreps), subscripts (1) and (2) are used to differentiate them. *Please do not mistake the parenthesized (1) and (2) for the subscripts 1 and 2 of A-type irreps. The latter de- note whether the A-type irreps are symmetric or antisymmetric with respect to $\hat{\sigma}_v$ in C_{3v} symmetry, and with respect to C_2' in D_3, D_{3h},and D_{3d} symmetries.*

Tables A. I and A.II give the bimodal expansions that are $\hat{C}_3$-eigenfunctions, with $\chi^{C_3} = 1$and $e^{i\frac{2\pi}{3}}$, respectively. Those are called the root expansions, as they satisfy the symmetry requirements of C_3, symmetry, the *lowest* symmetry in all trigonal symmetries. Expansions with $\chi^{C_3} = e^{-i\frac{2\pi}{3}}$ are simply complex conjugates of those with $\chi^{C_3} = e^{i\frac{2\pi}{3}}$. They are hence not given. Please note that in all expansion throughout this work, the summation indices that appear in the absolute value symbol take all integer values, while the other indices only take nonnegative integer values.

Tables A.III and A.IV summarize the constraints that need to be applied to the root expansions, so that the resultant *branch* expansions feature ($\left(\chi_{Re}^{\sigma_v}, \chi_{Im}^{\sigma_v}\right)$ or $\left(\chi_{Re}^{C_2'}, \chi_{Im}^{C_2'}\right)$. Similarly, Tables A. V and A.VI summarize the constraints that give the *branch* expansions that feature χ^{σ_h} or χ^{I}.

Table. A. I. Expansion formulas for $\hat{C}_3$-eigenfunctions of the bimodal vibrational coordinates with eigenvalue 1.

Modes	Expansion formulas
$(a+a)$	$a^{r}_{I_1,I_2} z^{I_1}_{(1)} z^{I_2}_{(2)} + i a^{i}_{I_3,I_4} z^{I_3}_{(1)} z^{I_4}_{(2)}$
$(e+a)$	$a^{3m}_{I,2K} z^{I} \rho^{\lvert 3m\rvert+2K} e^{i3m\phi} = \rho^{\lvert 3m\rvert+2K} \left[a^{r,3m}_{I_1,2K} z^{I_1} \cos(3m\phi) - a^{i,3m}_{I_2,2K} z^{I_2} \sin(3m\phi) \right.$ $\left. + i \left(a^{r,3m}_{I_1,2K} z^{I_1} \sin(3m\phi) + a^{i,3m}_{I_2,2K} z^{I_2} \cos(3m\phi) \right) \right]$
$(e+e)$	$a^{m,3n}_{2K_1,2K_2} \rho^{\lvert m\rvert+2K_1}_{(1)} \rho^{\lvert 3n-m\rvert+2K_2}_{(2)} e^{i(m\phi_{(1)}+(3n-m)\phi_{(2)})} = \rho^{\lvert m\rvert+2K_1}_{(1)} \rho^{\lvert 3n-m\rvert+2K_2}_{(2)}$ $\left[(a^{r,m,3n}_{2K_1,2K_2} \cos(m\phi_{(1)} + (3n-m)\phi_{(2)}) - a^{i,m,3n}_{2K_1,2K_2} \sin(m\phi_{(1)} + (3n-m)\phi_{(2)})) \right.$ $\left. + i(a^{r,m,3n}_{2K_1,2K_2} \sin(m\phi_{(1)} + (3n-m)\phi_{(2)}) + a^{i,m,3n}_{2K_1,2K_2} \cos(m\phi_{(1)} + (3n-m)\phi_{(2)})) \right]$

Table. A. II. Expansion formulas for $\hat{C}_3$-eigenfunctions of the bimodal vibrational coordinates with eigenvalue $e^{i\frac{2\pi}{3}}$.

Modes	Expansion formulas
$(a+a)$	not applicable (na)
$(e+a)$	$b^{3n-1}_{I,2K} z^{I} \rho^{\lvert 3n-1\rvert+2K} e^{i(3n-1)\phi} = \rho^{\lvert 3n-1\rvert+2K} \left[b^{r,3n-1}_{I_1,2K} z^{I_1} \cos((3n-1)\phi) - b^{i,3n-1}_{I_2,2K} z^{I_2} \sin((3n-1)\phi) \right.$ $\left. + i \left(b^{r,3n-1}_{I_1,2K} z^{I_1} \sin((3n-1)\phi) + b^{i,3n-1}_{I_2,2K} z^{I_2} \cos((3n-1)\phi) \right) \right]$
$(e+e)$	$b^{m,3n-1}_{2K_1,2K_2} \rho^{\lvert m\rvert+2K_1}_{(1)} \rho^{\lvert 3n-1-m\rvert+2K_2}_{(2)} e^{i(m\phi_{(1)}+(3n-1-m)\phi_{(2)})} = \rho^{\lvert m\rvert+2K_1}_{(1)} \rho^{\lvert 3n-1-m\rvert+2K_2}_{(2)}$ $\left[b^{r,m,3n-1}_{2K_1,2K_2} \cos(m\phi_{(1)} + (3n-1-m)\phi_{(2)}) - b^{i,m,3n-1}_{2K_1,2K_2} \sin(m\phi_{(1)} + (3n-1-m)\phi_{(2)}) \right.$ $\left. + i \left(b^{r,m,3n-1}_{2K_1,2K_2} \sin(m\phi_{(1)} + (3n-1-m)\phi_{(2)}) + b^{i,m,3n-1}_{2K_1,2K_2} \cos(m\phi_{(1)} + (3n-1-m)\phi_{(2)}) \right) \right]$

Table. A. III. Constraints on expansions in Table. A. I to give the appropriate $\chi_{Re}^{\sigma_v,C_2'}$ and $\chi_{Im}^{\sigma_v,C_2'}$. When $\chi_{Im}^{\sigma_v,C_2'} = 0$, only the real part of the corresponding entry in Table. A. I should be considered. When $\chi_{Re}^{\sigma_v,C_2'} = 0$, only the imaginary part of the corresponding entry in Table. A. I should be considered.

Modes	$1,(1,0)$	$1,(-1,0)$	$1,(1,-1)$	$1,(0,1)$	$1,(0,-1)$
(a_1+a_1)	nr[†]	na	na	nr	na
(a_1+a_2)[‡]	I_2 even[¶]	I_2 odd	I_2 even, I_4 odd	I_4 even	I_4 odd
(a_2+a_2)	I_1, I_2 ee or oo[§]	I_1, I_2 eo or oe[£]	I_1, I_2 ee or oo, I_3, I_4 eo or oe	I_3, I_4 ee or oo	I_3, I_4 eo or oe
$(e+a_1)$	cos nz[#]	sin nz	a^r nz	cos nz	sin nz
$(e+a_2)$	I_1 even, I_2 odd	I_1 odd, I_2 even	I_1 even, I_2 odd	I_1 odd, I_2 even	I_1 even, I_2 odd
$(e+e)$	cos nz	sin nz	a^r nz	cos nz	sin nz

[†] "nr" means "no restriction". [‡]For two modes whose irreps only differ in subscripts, (1)-subscripted coordinates in Table. A. I are for the first (a_1 here) and (2)- for the second ($a_2$here) mode. [¶] I_2 needs to be even. [§] I_1 and I_2need to be both even or both odd. [£] When I_1 is even, I_2 must be odd, and vice versa. [#] Only the terms associated with cosine factors are nonzero.

Table. A. IV. Constraints on expansions in Table. A. II to give the appropriate $\chi_{Re}^{\sigma_v,C_2'}$ and $\chi_{Im}^{\sigma_v,C_2'}$.

Modes	$e^{i\frac{2\pi}{3}},(1,-1)$	$e^{i\frac{2\pi}{3}},(-1,1)$
$(e+a_1)$	b^r nz	b^i nz
$(e+a_2)$	I_1 even, I_2 odd	I_1 odd, I_2 even
$(e+e)$	b^r nz	b^i nz

Table. A. V. Constraints on expansions in Table. A. I to give the appropriate ($\chi^{C_3}=1, \chi^{\sigma_h, I}$). The modes here are given for σ_h. The $'$ and $''$ can be correspondingly replaced by the g and u subscripts for the D_{3d} symmetry.

Vibrational Modes	$(1,1)$	$(1,-1)$
$(a'+a')$	nr	na
$(a'+a'')^{\dagger}$	I_2, I_4 even	I_2, I_4 odd
$(a''+a'')$	I_1, I_2 ee or oo I_3, I_4 ee or oo	I_1, I_2 eo or oe I_3, I_4 eo or oe
$(e'+a')$	nr	na
$(e''+a')$	$3m$ even	$3m$ odd
$(e'+a'')$	I even	I odd
$(e''+a'')$	$3m, I$ ee or oo	$3m, I$ eo or oe
$(e'+e')$	nr	na
$(e''+e')$	m even	m odd
$(e''+e'')$	$3n$ even	$3n$ odd

† For two modes whose irreps only differ in subscripts, (1)-subscripted coordinates in Table. A. I are for the first (a' here) and (2)- for the second (a'' here) mode. This rule applies in all constraints tables.

Table. A. VI. Constraints on expansions in Table. A. II to give the appropriate ($\chi^{C_3} = e^{i\frac{2\pi}{3}}, \chi^{\sigma_h, I}$). The modes here are given for σ_h. The $'$ and $''$ can be correspondingly replaced by the g and u subscripts for the D_{3d} symmetry.

Vibrational Modes	$(e^{i\frac{2\pi}{3}}, 1)$	$(e^{i\frac{2\pi}{3}}, -1)$
$(e' + a')$	nr	na
$(e'' + a')$	$3n$ odd	$3n$ even
$(e' + a'')$	I even	I odd
$(e'' + a'')$	$3n$ even,I odd $3n$ odd, I even	$3n$ even,I even $3n$ odd, I odd
$(e' + e')$	nr	na
$(e'' + e')$	m even	m odd
$(e'' + e'')$	$3n$ odd	$3n$ even

Appendix 2 Expansion formulas in tetragonal symmetries

All bimodal expansion formulas that feature the symmetry eigenvalues χ^{C_4}, $\left(\chi_{Re}^{\sigma_v}, \chi_{Im}^{\sigma_v}\right)$, $\left(\chi_{Re}^{C_2'}, \chi_{Im}^{C_2'}\right)$, χ^{σ_h} ,and χ^{I} are summarized in Table. A. I to Table. A. VI. In these tables z is used to represent coordinates of a-type vibrations, w for b-type vibrations, and the polar coordinates ρ and ϕ for e-type vibrations. For coordinates of vibrational modes of the same type of irreducible representations (irreps), subscripts (1) and (2) are used to differentiate them. *Please do not mistake the parenthesized (1) and (2) for the subscripts 1 and 2 of A-type irreps. The latter de- note whether the A- and B- type irreps are symmetric or antisymmetric with respect to* $\hat{\sigma}_v$ *in* C_{4v} *symmetry, and with respect to* C_2' *in* $D_{2\mathrm{d}}$, D_4,*and* D_{4h} *symmetries.*

Tables A. VII and A.IX give the bimodal expansions that that are $\hat{C}_4$-eigenfunctions, with $\chi^{C_4} = 1, -1$, and i, respectively. Those are called the root expansions, as they satisfy the symmetry requirements of C_4 symmetry, the *lowest* symmetry in all tetragonal symmetries. Expansions with $\chi^{C_4} = -i$ are simply complex conjugates of those with $\chi^{C_4} = i$. They are hence not given. Please note that in all expansion throughout this work, the summation indices that appear in the absolute value symbol take all integer values, while the other indices only take nonnegative integer values. Please note that C_4 and S_4 are isomorphic point groups. The C_4 -eigenvalues are also S_4 -eigenvalues and the root expansion formulas are also applicable for S_4 symmetry.

Tables A.X and A.XII summarize the constraints that need to be applied to the root expansions, so that the resultant *branch* expansions feature ($\left(\chi_{Re}^{\sigma_v}, \chi_{Im}^{\sigma_v}\right)$ or $\left(\chi_{Re}^{C_2'}, \chi_{Im}^{C_2'}\right)$. Similarly, Tables A. XIII and A.XV summarize the constraints that give the *branch* expansions that feature χ^{I}.

Table. A. VII. Expansion formulas for $\hat{C}_4$-eigenfunctions of the bimodal vibrational coordinates with eigenvalue 1.

Modes	Expansion formulas
$(a+a)$	$a^r_{I_1,I_2} z^{I_1}_{(1)} z^{I_2}_{(2)} + i a^i_{I_3,I_4} z^{I_3}_{(1)} z^{I_4}_{(2)}$
$(a+b)$	$a^r_{I_1,2J} z^{I_1} w^{2J} + i a^i_{I_2,2J} z^{I_2} w^{2J}$
$(b+b)$	$a^r_{2J_1+1,2J_2+1} w^{2J_1+1}_{(1)} w^{2J_2+1}_{(2)} + i a^i_{2J_1+1,2J_2+1} w^{2J_1+1}_{(1)} w^{2J_2+1}_{(2)}$ $+a^r_{2J_1,2J_2} w^{2J_1}_{(1)} w^{2J_2}_{(2)} + i a^i_{2J_1,2J_2} w^{2J_1}_{(1)} w^{2J_2}_{(2)}$
$(e+a)$	$a^{4m}_{I,2K} z^I \rho^{\lvert 4m\rvert+2K} e^{i4m\phi} = \rho^{\lvert 4m\rvert+2K} [a^{r,4m}_{I_1,2K} z^{I_1} \cos(4m\phi) - a^{i,4m}_{I_2,2K} z^{I_2} \sin(4m\phi)$ $+i a^{r,4m}_{I_1,2K} z^{I_1} \sin(4m\phi) + i a^{i,4m}_{I_2,2K} z^{I_2} \cos(4m\phi)]$
$(e+b)$	$a^{2m}_{2I,2K} w^{mod(m,2)+2I} \rho^{\lvert 2m\rvert+2K} e^{i2m\phi} = w^{mod(m,2)+2I} \rho^{\lvert 2m\rvert+2K} \left[a^{r,2m}_{2I,2K} \cos(2m\phi)\right.$ $\left.-a^{i,2m}_{2I,2K} \sin(2m\phi) + i a^{r,2m}_{2I,2K} \sin(2m\phi) + i a^{i,2m}_{2I,2K} \cos(2m\phi)\right]$
$(e+e)$	$a^{m_1,4n}_{2K_1,2K_2} \rho^{\lvert m_1\rvert+2K_1}_{(1)} \rho^{\lvert 4n-m_1\rvert+2K_2}_{(2)} e^{i(m_1\phi_{(1)}+(4n-m_1)\phi_{(2)})} = \rho^{\lvert m_1\rvert+2K_1}_{(1)} \rho^{\lvert 4n-m_1\rvert+2K_2}_{(2)}$ $\left[(a^{r,m_1,4n}_{2K_1,2K_2} \cos(m_1\phi_{(1)} + (4n-m_1)\phi_{(2)}) - a^{i,m_1,4n}_{2K_1,2K_2} \sin(m_1\phi_{(1)} + (4n-m_1)\phi_{(2)}))\right.$ $\left.+i(a^{r,m_1,4n}_{2K_1,2K_2} \sin(m_1\phi_{(1)} + (4n-m_1)\phi_{(2)}) + a^{i,m_1,4n}_{2K_1,2K_2} \cos(m_1\phi_{(1)} + (4n-m_1)\phi_{(2)}))\right]$

Table. A. VIII. Expansion formulas for $\hat{C}_4$-eigenfunctions of the bimodal vibrational coordinates with eigenvalue -1.

Modes	Expansion formulas
$(a+a)$	na
$(a+b)$	$b^r_{I_1,2J+1} z^{I_1} w^{2J+1} + i b^i_{I_2,2J+1} z^{I_2} w^{2J+1}$
$(b+b)$	$b^r_{2J_1+1,2J_2} w^{2J_1+1}_{(1)} w^{2J_2}_{(2)} + i b^i_{2J_1+1,2J_2} w^{2J_1+1}_{(1)} w^{2J_2}_{(2)} + b^r_{2J_1,2J_2+1} w^{2J_1}_{(1)} w^{2J_2+1}_{(2)} + i b^i_{2J_1,2J_2+1} w^{2J_1}_{(1)} w^{2J_2+1}_{(2)}$
$(e+a)$	$b^{4n+2}_{I,2K} z^I \rho^{\lvert 4n+2\rvert+2K} e^{i(4n+2)\phi} = \rho^{\lvert 4n+2\rvert+2K} \left[b^{r,4n+2}_{I_1,2K} z^{I_1} \cos((4n+2)\phi) - b^{i,4n+2}_{I_2,2K} z^{I_2} \sin((4n+2)\phi)\right.$ $\left.+i b^{r,4n+2}_{I_1,2K} z^{I_1} \sin((4n+2)\phi) + i b^{i,4n+2}_{I_2,2K} z^{I_2} \cos((4n+2)\phi)\right]$
$(e+b)$	$b^{2m}_{2I,2K} w^{mod(m,2)+2I+1} \rho^{\lvert 2m\rvert+2K} e^{i2m\phi} = w^{mod(m,2)+2I+1} \rho^{\lvert 2m\rvert+2K} \left[b^{r,2m}_{2I,2K} \cos(2m\phi) - b^{i,2m}_{2I,2K} \sin(2m\phi)\right.$ $\left.+i b^{r,2m}_{2I,2K} \sin(2m\phi) + i b^{i,2m}_{2I,2K} \cos(2m\phi)\right]$
$(e+e)$	$b^{m_1,4n+2}_{2K_1,2K_2} \rho^{\lvert m_1\rvert+2K_1}_{(1)} \rho^{\lvert 4n+2-m_1\rvert+2K_2}_{(2)} e^{i(m_1\phi_{(1)}+(4n+2-m_1)\phi_{(2)})} = \rho^{\lvert m_1\rvert+2K_1}_{(1)} \rho^{\lvert 4n+2-m_1\rvert+2K_2}_{(2)}$ $\left[(b^{r,m_1,4n+2}_{2K_1,2K_2} \cos(m_1\phi_{(1)} + (4n+2-m_1)\phi_{(2)}) - b^{i,m_1,4n+2}_{2K_1,2K_2} \sin(m_1\phi_{(1)} + (4n+2-m_1)\phi_{(2)}))\right.$ $\left.+i(b^{r,m_1,4n+2}_{2K_1,2K_2} \sin(m_1\phi_{(1)} + (4n+2-m_1)\phi_{(2)}) + b^{i,m_1,4n+2}_{2K_1,2K_2} \cos(m_1\phi_{(1)} + (4n+2-m_1)\phi_{(2)}))\right]$

Table. A. IX. Expansion formulas for $\hat{C}_4$-eigenfunctions of the bimodal vibrational coordinates with eigenvalue i.

Modes	Expansion formulas
$(\gamma+\gamma)^{\dagger}$	na
$(e+a)$	$c_{I,2K}^{4n+1} z^I \rho^{\lvert 4n-1\rvert+2K} e^{i(4n-1)\phi} = \rho^{\lvert 4n-1\rvert+2K}\left[c_{I_1,2K}^{r,4n-1} z^{I_1}\cos((4n-1)\phi) - c_{I_2,2K}^{i,4n-1} z^{I_2}\sin((4n-1)\phi)\right]$ $+i\rho^{\lvert 4n-1\rvert+2K}\left[c_{I_1,2K}^{r,4n-1} z^{I_1}\sin((4n-1)\phi) + c_{I_2,2K}^{i,4n-1} z^{I_2}\cos((4n-1)\phi)\right]$
$(e+b)$	$c_{2I,2K}^{2n-1} w^{mod(n,2)+2I}\rho^{\lvert 2n-1\rvert+2K} e^{i(2n-1)\phi}$ $= w^{mod(n,2)+2I}\rho^{\lvert 2n-1\rvert+2K}\left[c_{2I,2K}^{r,2n-1}\cos((2n-1)\phi) - c_{2I,2K}^{i,2n-1}\sin((2n-1)\phi)\right]$ $+iw^{mod(n,2)+2I}\rho^{\lvert 2n-1\rvert+2K}\left[c_{2I,2K}^{r,2n-1}\sin((2n-1)\phi) + c_{2I,2K}^{i,2n-1}\cos((2n-1)\phi)\right]$
$(e+e)$	$c_{2K_1,2K_2}^{m_1,4n-1}\rho_{(1)}^{\lvert m_1\rvert+2K_1}\rho_{(2)}^{\lvert 4n-1-m_1\rvert+2K_2} e^{i(m_1\phi_{(1)}+(4n-1-m_1)\phi_{(2)})} = \rho_{(1)}^{\lvert m_1\rvert+2K_1}\rho_{(2)}^{\lvert 4n-1-m_1\rvert+2K_2}$ $\left[(c_{2K_1,2K_2}^{r,m_1,4n-1}\cos(m_1\phi_{(1)}+(4n-1-m_1)\phi_{(2)}) - c_{2K_1,2K_2}^{i,m_1,4n-1}\sin(m_1\phi_{(1)}+(4n-1-m_1)\phi_{(2)})\right.$ $\left.+i(c_{2K_1,2K_2}^{r,m_1,4n-1}\sin(m_1\phi_{(1)}+(4n-1-m_1)\phi_{(2)}) + c_{2K_1,2K_2}^{i,m_1,4n-1}\cos(m_1\phi_{(1)}+(4n-1-m_1)\phi_{(2)}))\right]$

† Including $(a+a)$, $(b+b)$, and $(a+b)$.

Table. A. X. Constraints on expansions in Table. A. VII to give the appropriate $\chi_{Re}^{\sigma_v,C_2'}$ and $\chi_{Im}^{\sigma_v,C_2'}$. When $\chi_{Im}^{\sigma_v,C_2'} = 0$ ($\chi_{Re}^{\sigma_v,C_2'} = 0$), only the real (imaginary) part of the corresponding entry in Table. A. VII should be considered.

Modes	$(1,(1,0))$	$(1,(-1,0))$	$(1,(1,-1))$	$(1,(0,1))$	$(1,(0,-1))$
(a_1+a_1)	nr[†]	na	na	nr	na
(a_1+a_2)[‡]	I_2 even[¶]	I_2 odd	I_2 even, I_4 odd	I_4 even	I_4 odd
(a_2+a_2)	I_1, I_2 ee or oo[§]	I_1, I_2 eo or oe[£]	I_1, I_2 ee or oo, I_3, I_4 eo or oe	I_3, I_4 ee or oo	I_3, I_4 eo or oe
$(a_1+b_1),(a_1+b_2)$	nr	na	na	nr	na
$(a_2+b_1),(a_2+b_2)$	I_1 even	I_1 odd	I_1 even, I_2 odd	I_2 even	I_2 odd
$(b_1+b_1),(b_2+b_2)$	nr	na	na	nr	na
(b_1+b_2)	a_{ee} nz[$]	a_{oo} nz[$]	a_{ee}^r, a_{oo}^i nz	a_{ee} nz	a_{oo} nz
$(e+a_1),(e+b_1),$	cos nz[#]	sin nz	a^r nz	cos nz	sin nz
$(e+a_2)$	I_1 even, I_2 odd	I_1 odd, I_2 even	I_1 even, I_2 odd	I_1 odd, I_2 even	I_1 even, I_2 odd
$(e+b_2)$	cos nz if m even, sin nz if m odd	sin nz if m even, cos nz if m odd	a^r nz if m even, a^i nz if m odd	cos nz if m even, sin nz if m odd	sin nz if m even, cos nz if m odd
$(e+e)$	cos nz	sin nz	a^r nz	cos nz	sin nz

[†] "nr" means "no restriction". [‡]For two modes whose irreps only differ in subscripts, (1)-subscripted coordinates in Table. A. VII are for the first (a_1 here) and (2)- for the second (a_2 here) mode. [¶] I_2 needs to be even. [§] I_1 and I_2need to be both even or both odd. [£] When I_1 is even, I_2 must be odd, and vice versa. [$] a_{ee} means $a_{2J_1,2J_2}$. a_{oo} means $a_{2J_1+1,2J_2+1}$. "nz" means only these coefficients are nonzero. [#] Only the terms associated with cosine factors are nonzero.

Table. A. XI. Constraints on expansions in Table. A. VIII to give the appropriate $\chi_{Re}^{\sigma_v,C_2'}$ and $\chi_{Im}^{\sigma_v,C_2'}$. When $\chi_{Im}^{\sigma_v,C_2'} = 0$ ($\chi_{Re}^{\sigma_v,C_2'} = 0$), only the real (imaginary) part of the corresponding entry in Table. A. VIII should be considered.

Modes	$(-1,(1,0))$	$(-1,(-1,0))$	$(-1,(1,-1))$	$(-1,(0,1))$	$(-1,(0,-1))$
(a_1+b_1)	nr	na	na	nr	na
(a_1+b_2)	na	nr	na	na	nr
(a_2+b_1)	I_1 even	I_1 odd	I_1 even, I_2 odd	I_2 even	I_2 odd
(a_2+b_2)	I_1 odd	I_1 even	I_1 odd, I_2 even	I_2 odd	I_2 even
(b_1+b_1)	nr	na	na	nr	na
(b_1+b_2)	b_{oe} nz	b_{eo} nz	b_{oe}^r, b_{eo}^i nz	b_{oe} nz	b_{eo} nz
(b_2+b_2)	na	nr	na	na	nr
$(e+a_1),(e+b_1)$	cos nz	sin nz	b^r nz	cos nz	sin nz
$(e+a_2)$	I_1 even, I_2 odd	I_1 odd, I_2 even	I_1 even, I_2 odd	I_1 odd, I_2 even	I_1 even, I_2 odd
$(e+b_2)$	cos nz if m odd, sin nz if m even	sin nz if m odd, cos nz if m even	b^r nz if m odd, b^i nz if m even	sin nz if m odd, cos nz if m even	cos nz if m odd, sin nz if m even
$(e+e)$	cos nz	sin nz	b^r nz	cos nz	sin nz

Table. A. XII. Constraints on expansions in Table. A. IX to give the appropriate $\chi_{Re}^{\sigma_v}$ and $\chi_{Im}^{\sigma_v}$.

Modes	$(i,(1,-1))$	$(i,(-1,1))$
$(e+a_1)$, $(e+b_1)$	c^r nz	c^i nz
$(e+a_2)$	I_1 even, I_2 odd	I_1 odd, I_2 even
$(e+b_2)$	c^r (c^i) nz if n even (odd)	c^r (c^i) nz if n odd (even)
$(e+e)$	c^r nz	c^i nz

Table. A. XIII. Constraints on expansions in Table. A. VII to give the appropriate ($\chi^{C_4} = 1, \chi^I$).

Vibrational Modes	$(1,1)$	$(1,-1)$
$(a_g + a_g)$	nr	na
$(a_g + a_u)$	I_2 even	I_2 odd
$(a_u + a_u)$	I_1, I_2 ee or oo I_3, I_4 ee or oo	I_1, I_2 eo or oe I_3, I_4 eo or oe
$(a_g + b_g)$, $(a_g + b_u)$	nr	na
$(a_u + b_g)$, $(a_u + b_u)$	I_1 even	I_1 odd
$(b_g + b_g)$, $(b_u + b_u)$	nr	na
$(b_g + b_u)$	a_{ee} nz	a_{oo} nz
$(e_g + a_g)$, $(e_u + a_g)$	nr	na
$(e_g + a_u)$, $(e_u + a_u)$	I even	I odd
$(e_g + b_g)$, $(e_u + b_g)$	nr	na
$(e_g + b_u)$, $(e_u + b_u)$	m even	m odd
$(e_g + e_g)$, $(e_u + e_u)$	nr	na
$(e_g + e_u)$	m_1 even	m_1 odd

Table. A. XIV. Constraints on expansions in Table. A. VIII to give the appropriate ($\chi^{C_4} = -1, \chi^{I}$).

Vibrational Modes	$(-1,1)$	$(-1,-1)$
$(a_g + b_g)$	nr	na
$(a_g + b_u)$	na	nr
$(a_u + b_g)$	I_1 even	I_1 odd
$(a_u + b_u)$	I_1 odd	I_1 even
$(b_g + b_g)$	nr	na
$(b_g + b_u)$	b_{oe} nz	b_{eo} nz
$(b_u + b_u)$	na	nr
$(e_u + a_g)$, $(e_g + a_g)$	nr	na
$(e_u + a_u)$, $(e_g + a_u)$	I even	I odd
$(e_u + b_g)$, $(e_g + b_g)$	nr	na
$(e_u + b_u)$, $(e_g + b_u)$	m odd	m even
$(e_u + e_u)$	nr	na
$(e_u + e_g)$	m_1 even	m_1 odd
$(e_g + e_g)$	nr	na

Table. A. XV. Constraints on expansions in Table. A. IX to give the appropriate ($\chi^{C_4} = i, \chi^{I}$).

Vibrational Modes	$(i, 1)$	$(i, -1)$
$(e_g + a_g)$	nr	na
$(e_g + a_u)$	I even	I odd
$(e_u + a_g)$	na	nr
$(e_u + a_u)$	I odd	I even
$(e_g + b_g)$	nr	na
$(e_g + b_u)$	n even	n odd
$(e_u + b_g)$	na	nr
$(e_u + b_u)$	n odd	n even
$(e_g + e_g)$	nr	na
$(e_g + e_u)$	m_1 odd	m_1 even
$(e_u + e_u)$	na	nr